Green Energy and Technology

Bhajan Lal
Omar Nashed

Chemical Additives for Gas Hydrates

Springer

Green Energy and Technology

Climate change, environmental impact and the limited natural resources urge scientific research and novel technical solutions. The monograph series Green Energy and Technology serves as a publishing platform for scientific and technological approaches to "green"—i.e. environmentally friendly and sustainable—technologies. While a focus lies on energy and power supply, it also covers "green" solutions in industrial engineering and engineering design. Green Energy and Technology addresses researchers, advanced students, technical consultants as well as decision makers in industries and politics. Hence, the level of presentation spans from instructional to highly technical. **Indexed in Scopus**.

More information about this series at http://www.springer.com/series/8059

Bhajan Lal · Omar Nashed

Chemical Additives for Gas Hydrates

Springer

Bhajan Lal
Department of Chemical Engineering
Universiti Teknologi PETRONAS
Seri Iskandar, Perak, Malaysia

Omar Nashed
Department of Chemical Engineering
Universiti Teknologi PETRONAS
Seri Iskandar, Perak, Malaysia

ISSN 1865-3529 ISSN 1865-3537 (electronic)
Green Energy and Technology
ISBN 978-3-030-30749-3 ISBN 978-3-030-30750-9 (eBook)
https://doi.org/10.1007/978-3-030-30750-9

This Springer imprint is published by the registered company Springer Nature Switzerland AG
The registered company address is: Gewerbestrasse 11, 6330 Cham, Switzerland

Preface

Over the past couple of centuries, the increasing energy demand for global economic progression is primarily fulfilled by fossil fuels. Gas hydrate formation can be boon and nuisance for oil and gas industry which further provide opportunities and challenge to academicians and researchers. In both cases, chemical industry uses different types of additive to address the challenge or explore gas hydrate formation potential. This book is the result of an updated extensive survey of the state-of-the-art information on use of additive on gas hydrate applications by the author. This book is intended to provide a guideline for the academicians, researchers, and stakeholders on the chemical additives for different gas hydrate applications such as flow assurance, natural gas storage, and transportation. Since gas hydrates have been identified, several approaches have been used to manage it. However, in most cases, the chemical method is more practicable to gas hydrate inhibition and formation. This book consists of four chapters discussing different aspects of gas hydrates.

Chapter 1 presents a brief introduction on the definition, structure, and formation of gas hydrates, as well as issues and potential applications related to it.

Chapter 2 focuses on the chemical inhibition of gas hydrates. The conventional and recently investigated inhibitors were discussed, along with their function and mechanism. It is observed that the trend over the past decade has focused on finding alternative inhibitors that could minimize the cost and environmental concern.

Chapter 3 briefly discusses the mechanical promotion of gas hydrates. However, our focus was on chemical hydrate promoters that can be used for different potential applications. Thermodynamic promoters were discussed according to their mechanism. Additionally, the kinetic promoters were presented and discussed.

Chapter 4 summarizes the thermodynamic and kinetic models used for gas hydrate applications. A literature review has been done on the applied models. This chapter aims to help the researchers to identify the appropriate model for each class of chemicals.

It is a great pleasure to thank Springer for providing this opportunity to share this book with the scientific community. This book could not have been completed without the support and contribution of the authors involved. In the end, we would like to seek your cooperation to share your thoughts and feedback in order to improve our future work.

Seri Iskandar, Malaysia

Bhajan Lal
Omar Nashed

Contents

Contributors

Cornelius Borecho Bavoh Chemical Engineering Department, Universiti Teknologi PETRONAS, Bandar Seri Iskandar, Perak Darul Ridzuan, Malaysia;
CO2 Research Center (CO2RES), Institute of Contaminant Management for Oil & Gas, Universiti Teknologi PETRONAS, Bandar Seri Iskandar, Perak, Malaysia

Abdulhalim Shah Bin Maulud CO2 Research Center (CO2RES), Institute of Contaminant Management for Oil & Gas, Universiti Teknologi PETRONAS, Bandar Seri Iskandar, Perak, Malaysia;
Chemical Engineering Department, Universiti Teknologi PETRONAS, Bandar Seri Iskandar, Perak Darul Ridzuan, Malaysia

Mohamad Azmi Bustam Chemical Engineering Department, Universiti Teknologi PETRONAS, Bandar Seri Iskandar, Perak Darul Ridzuan, Malaysia;
Centre of Research in Ionic Liquids (CORIL), Universiti Teknologi PETRONAS, Bandar Seri Iskandar, Perak, Malaysia

Lau Kok Keong Chemical Engineering Department, Universiti Teknologi PETRONAS, Bandar Seri Iskandar, Perak Darul Ridzuan, Malaysia;
CO2 Research Center (CO2RES), Institute of Contaminant Management for Oil & Gas, Universiti Teknologi PETRONAS, Bandar Seri Iskandar, Perak, Malaysia

Muhammad Saad Khan Texas A&M University at Qatar, Doha, Qatar

Bhajan Lal Chemical Engineering Department, Universiti Teknologi PETRONAS, Bandar Seri Iskandar, Perak Darul Ridzuan, Malaysia;
CO2 Research Center (CO2RES), Institute of Contaminant Management for Oil & Gas, Universiti Teknologi PETRONAS, Bandar Seri Iskandar, Perak, Malaysia

Omar Nashed Chemical Engineering Department, Universiti Teknologi PETRONAS, Bandar Seri Iskandar, Perak Darul Ridzuan, Malaysia;
CO2 Research Center (CO2RES), Institute of Contaminant Management for Oil & Gas, Universiti Teknologi PETRONAS, Bandar Seri Iskandar, Perak, Malaysia

Behzad Partoon CO2 Research Center (CO2RES), Institute of Contaminant Management for Oil & Gas, Universiti Teknologi PETRONAS, Bandar Seri Iskandar, Perak, Malaysia

Khalik M. Sabil School of Energy, Institute of Petroleum Engineering, Geoscience, Infrastructure and Society, Heriot-Watt University Malaysia, Putrajaya, Malaysia

S. Jai Krishna Sahith Mechanical Engineering Department, Universiti Teknologi PETRONAS, Bandar Seri Iskandar, Perak Darul Ridzuan, Malaysia

Azmi Mohd Shariff Chemical Engineering Department, Universiti Teknologi PETRONAS, Bandar Seri Iskandar, Perak Darul Ridzuan, Malaysia;
CO2 Research Center (CO2RES), Institute of Contaminant Management for Oil & Gas, Universiti Teknologi PETRONAS, Bandar Seri Iskandar, Perak, Malaysia

Chapter 1
Introduction to Gas Hydrates

Cornelius Borecho Bavoh, Bhajan Lal and Lau Kok Keong

1.1 History of Gas Hydrate

According to Sloan and Koh [1], the research and development of clathrate hydrate, from its discovery to present times, can be classified into three phases. The first phase began in 1778, when Joseph Priestley observed the formation of the SO_2 hydrate under laboratory conditions. However, Joseph Priestley did not call it hydrate until 30 years later, in 1811, when Sir Humphrey Davy observed a similar phenomenon in his laboratory with chlorine and water, thus naming it gas hydrates. Since then, hydrates have become an area of interest with regard to scientific laboratory research. The second phase began with the discovery by E. G. Hammershmidt in 1934, suggesting that gas hydrates were the cause of oil and gas pipeline blockages, rather than ice [2]. This began research on the prevention of gas hydrate formation and plugs in oil and gas pipelines. Research on gas hydrate inhibitors increased due to natural gas production and operations higher pressures and lower temperatures conditions.

In the 1960s, a group of Soviet geologists realized the existence of natural gas hydrates in larger quantities in subsea sediments in the tropical, Antarctic Ocean and below the permafrost zones [3]. This discovery commenced the third phase of hydrate research in order to understand natural gas hydrate deposition and develop its production technologies. Interestingly, it has been established that natural gas hydrates possess the potential to become a future energy source to replace fossil fuels [3]. Research has shown that the estimated amounts of natural gas hydrate reserves sit at about 1.5×10^{16} m^3 which doubles that of fossil fuels [3]. Active research on natural gas production from natural gas hydrate reservoir sources is still ongoing, as a means to develop natural gas production techniques. However, other applications of gas hydrates such as sea water desalination [4], gas storage and transportation [5–7], and mixed gas separation through hydrates for CO_2 sequestration [8–15] have been introduced and are still under active research until now. It is hoped that such technologies can be commercialized. Based on the recent rise in climate change issues related to CO_2 emissions, hydrate-based CO_2 methods to capture and store are on the rise.

B. Lal and O. Nashed, *Chemical Additives for Gas Hydrates*, Green Energy and Technology, https://doi.org/10.1007/978-3-030-30750-9_1

1.2 Introducing Gas Hydrates

Gas hydrates are ice-like non-stoichiometric compounds which are formed by trapping of gas (guest) molecules into hydrogen-bonded water molecules (host) [1, 16, 17]. They usually form under high-pressure and low-temperature conditions, with the host and guest molecules bonding together via van der Waals forces. A typical gas hydrate structure contains about 85% water molecules, with the water molecules bonded together by hydrogen bonds to form cages which trap the guest molecules [1]. The guest molecule could be liquid or gas. However, the majority of applied and reported guests are typically gases. Some common guest molecules are methane, ethane, propane, carbon dioxide, natural gas, etc. They have similar properties as ice, but differentiate massively in terms of mechanical strength, heat capacity, and thermal conductivity [18, 19]. On the other hand, Tetra-n-butylammonium bromide (TBAB), Tetrahydrofuran (THF), Cyclopentane are the most common liquid gas hydrate formers.

1.2.1 Gas Hydrate Structure

Generally, three common types of gas hydrate structures are reported. They are the cubic structure I (sI), the cubic structure II (sII), and the hexagonal structure H (sH) (see Fig. 1.1) [20–22]. The type of gas hydrate structures which is formed is highly influenced by the shape, type, and size of the guest molecule. The shape and size of the hydrate cavities in the cages determine the difference in their structure, while the type and size of the gas molecules accommodated by the water display the type of hydrate formed [19, 23, 24]. Mostly, subsea pipeline flow streams contain methane, propane, and ethane. Therefore, sI and sII are the common hydrate structures formed in oil and gas pipelines [19].

A certain amount of water molecules are required to form each hydrate structure as shown in Fig. 1.1. Generally, all hydrate structures contain small pentagonal dodecahedron (5^{12}) cavities as illustrated in Fig. 1.1. Each pentagonal dodecahedron cavity is made up of 12 pentagonal faces. Considering Fig. 1.1, sI consists of a small pentagonal dodecahedral cage (5^{12}) and a large tetrakaidecahedral cage ($5^{12}6^2$). The sI small cage has 12 pentagonal faces, and the large cage has 12 pentagonal and 2 hexagonal faces, containing a total of 46 water molecules. The sI cage consists of two small and six large cavities. The sII consists of a small pentagonal dodecahedral cage (5^{12}) and a large hexacaidecahedral cage ($5^{12}6^4$). The sII small cage has 12 pentagonal faces, and the large cage has 12 pentagonal and 4 hexagonal faces, consisting of 136 water molecules. The sI cage consists of 16 small and 8 large cavities. The sH has three sizes: the small pentagonal dodecahedral cage (5^{12}), the medium irregular dodecahedral cage ($4^3 5^6 6^3$), and the large icosahedral cage ($5^{12}6^8$). The sH small cage has 12 pentagonal faces, and medium, 3 square, 6 pentagonal, and 3 hexagonal faces. The large 12 pentagonal and 8 hexagonal faces on the cage consist of 34 water molecules [1, 19]. The sH cage consists of three small cavities, two medium cavities,

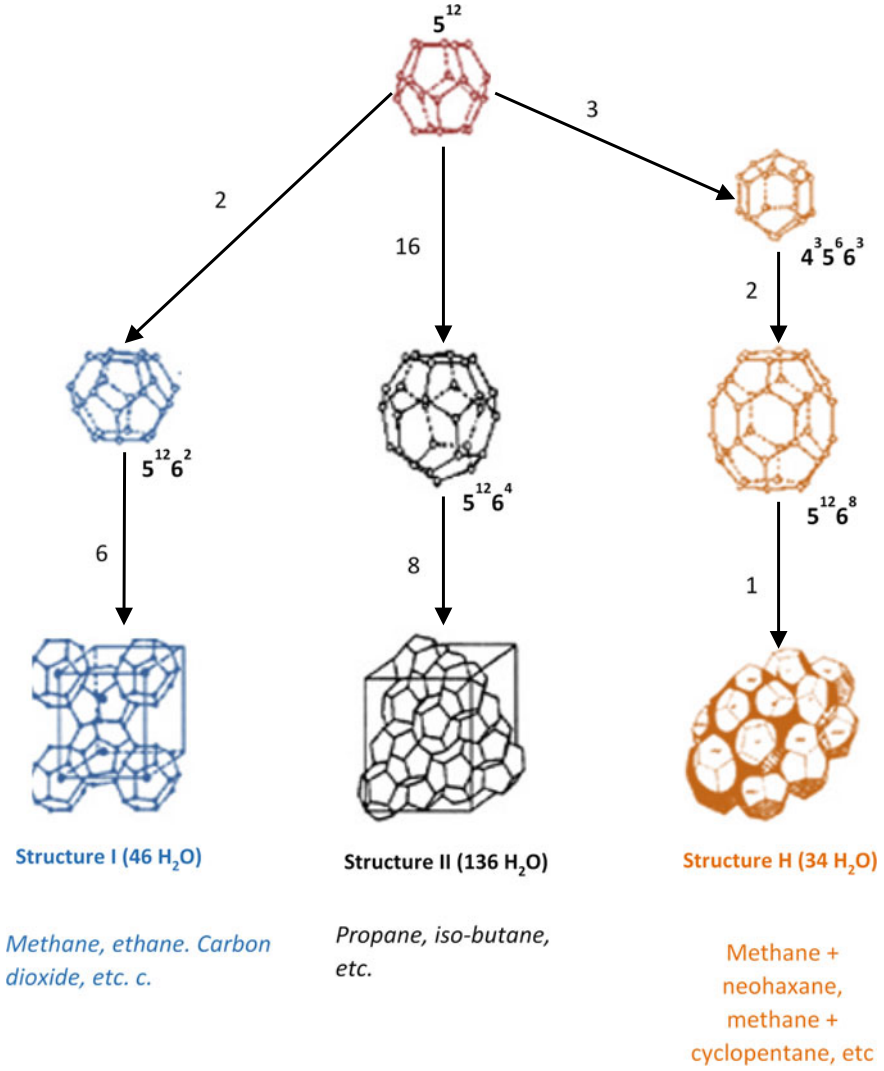

Fig. 1.1 Details of common gas hydrate structures

and a large cavity. Mostly, the small cavity accommodates one guest molecule, and the larger cavity has two guest molecules with the appropriate size and shape. For the sH hydrate to form, two guest molecules must be present. The gas hydrate cage occupancy by the guest molecules depends on the pressure and temperature.

Interestingly, only small gas molecules <10 Å may probably fill the hydrogen-bonded water cavities. Guest molecules such as carbon dioxide, methane, and ethane have molecular diameters in the range of 4.2–6 A, hence, they usually form sI hydrates. Other gases with molecular diameters less than 4.2 A form sII hydrate structures, for example nitrogen and hydrogen. Generally, the 5^{12} cages in the sII

hydrates per volume are 3 times the size of the sI, hence explaining the reason why some smaller molecules such as N_2 form sII hydrates and are very stable in such structures [1]. On the other hand, guest molecules with diameters of 6–7 A, such as propane or isobutane, form sII. However, some guest molecules are reported to form more than one hydrate structure. For example, cyclopentane (c-C_3H_6) forms either sI or sII hydrates [1]. Nevertheless, guest molecules ranging from 7 to 9.8 A such as cycloheptane or neohexene form sH hydrate structures when they are mixed with smaller gas molecules such as CH_4 and N_2.

Under the thermodynamic conditions found in oil and gas pipelines, a single guest molecule may occupy one hydrate lattice cavity. However, in some cases, multiple cage occupancies could take place if there are much smaller sized guest molecules in relatively large cavities. Not all hydrate cavities can be occupied with the guest, that is to say, there is no "perfect" gas hydrate crystal. It has been reported that guest molecules such as argon, oxygen, nitrogen, and hydrogen molecules could have multiple cage occupancies.

Generally, the ideal molar gas-to-water ratio for sI, sII, and sH is 1:5 3/4, 1:5 2/3, and 1:5 2/3, respectively. Thus, water molecules are almost always more than the stoichiometric composition with the ideal molar gas–water ratio and full occupancy. This can be simplified as 1:6, considering the inaccuracy in the cage occupancy. This can be fairly observed in the sI hydrate of methane or xenon, which has a hydration number of about 6. The guest-to-cavity ratio is also a major factor accounting for the non-stoichiometry of the cavity filling. Therefore, a perfect non-stoichiometric hydration occurs as the diameter ratio attains unity. No strong forces or chemical bonds exist between the host and the guest molecules; instead, a weak van der Waals force bonds the hydrated structures together. However, the London dispersion forces are the most dominant among the molecules with temporal dipoles. This is much more evident in the presence of the hydrates, which are formed between non-polar natural gas molecules and water. For instance, the total bond energy of the interaction between the water and the methane in simple methane hydrates consists of about 87% London dispersion forces [25].

For every hydrate structure, the thermodynamic (macroscopic) properties are very critical. Therefore, hydrate structural changes adversely affect its thermodynamic conditions. For example, the addition of propane to methane changes the methane hydrate structure from sI to sII. This consequently changes the phase behaviour of methane to suit the new structural stability. When this happens, propane molecules aid to stabilize the large cavity ($5^{12}6^4$) of the structure for two hydrates. This results in a huge drop in the hydrate equilibrium pressure [25]. Interestingly, a mixed hydrate between methane and ethane is expected to form the sI structure, since both of them are sI hydrate formers. However, a transition in their phase behaviour mostly occurs at certain ethane concentrations (below 0.25–0.28 mol fraction of ethane in the mixture), resulting in sII hydrates [25]. This structural transformation is attributed to an unfavourable partitioning condition between the large and the small cavities in the sI hydrate (2:6, respectively).

It has been reported that sI and sII hydrates can coexist during methane hydrate formation. It is believed that there is a rapid CH_4 diffusion on the interface of both these hydrate structures [26]. Apart from the structural transformation and coexistence, the variation in sI and sII polyhedral cages also coexists with different non-stoichiometric ratios. Similar observations were confirmed via molecular dynamic simulations by Jacobson et al. [27]. The enthalpy of the dissociation (H_d) of the hydrate is another example of microscopic properties which disrupt the macroscopic behaviour of the hydrate formation. The enthalpy of dissociation (H_d) is not only associated with the density of the hydrogen bonds, but also associated with the hydrate cavities' cage occupancy. When both large and small cages are filled, H_d decreases, compared in cases where only the large cages are filled. This suggests that an increased hydrate cage occupancy guarantees easier hydrate structure disassociation with less heat. An increase in pressure and guest concentrations could increase the hydrate cage's occupancy. It is important to note that H_d might remain constant with increased hydrate stability with lower dissociation pressure and/or higher dissociation temperatures. This is because the hydrate's lattice stability is dependent on the hydrate's dissociation time with pressure reduction. Therefore, hydrate remediation would be efficient with reduced hydrate lattice stability. Hence, a good understanding of the gas hydrate's lattice stability is very important for hydrate risk management in oil and gas flow assurance fields.

1.2.2 Hydrates Verse Ice

It is believed that gas hydrates have very high amounts of water in their structures. Hydrate structures contain about 85% of water, which makes them relatively comparable to ice in properties. Gas hydrate hydrogen bonds are longer than ice by 1% [25]. Much more details of the differences between hydrates and ice can be found in the book by Sloan [1]. However, the major variations in hydrates and ice are in their mechanical and thermal properties. Ice has less mechanical strength than that of hydrates. According to Durham et al. [28], methane hydrate structures are about 20 times stronger than ice. It was summarized that this is because the rate of water diffusion in hydrates is two orders of magnitude lower than that of ice. In addition, the thermal conductivity of sII and sI hydrates (~0.5 W m^{-1} K^{-1}) is significantly smaller than that of ice Ih (~2.2 W m^{-1} K^{-1}) [29]. Similarly, hydrates have a higher heat capacity (~2100 J kg^{-1} K^{-1}), which is much more than ice Ih (~1700 J kg^{-1} K^{-1}) [30].

1.2.3 Gas Hydrate Formation

The basic requirements necessary for hydrate formation are lower temperature, high pressure, the presence of guest molecules, and the desired amounts of water molecules. The formation process is not chemical, but physical in nature, and no chemical bonds exist between the guest and the water molecules. It must be stated that the guest molecule rotates freely within the cavities of the water molecules. Gas hydrate formation is a crystallization process, which consists of nucleation and crystal growth processes, followed by a massive accumulation process as described in the following subsections.

1.2.4 Gas Hydrate Nucleation Process

Gas hydrate nucleation is a microscopic phenomenon, which consists of a tiny number of molecules. This process refers to the formation and growth of hydrate nuclei into a critical size for further growth. Hydrate nucleation is characterized by induction time determination (the time elapsed during which the nucleation processes take place, which includes the formation of gas–water clusters and their growth into stable nuclei with a critical size) [1]. It is a stochastic and time-dependent process and can last from seconds to hours or days, depending on the mixing conditions, composition, apparatus, etc. The stochastic nature of hydrate formation is a result of the degree of metastability (the ability of a non-equilibrium state to persist for a long period of time) that exists in the formation process.

Hydrate nucleation is usually known as a primary nucleation, because the nucleation takes place from freshwater and guest systems. Thus, there is no hydrate formation history or particles in the system. During hydrate nucleation, water molecules group around the guest molecules to form incomplete or complete crystal embryos. These embryos continuously form and shrink due to local mass, pressure, and temperature changes. The mechanism makes the nucleation hydrate a free energy-dependent and statistically random process. When the hydrate nuclei achieve a critical size, the free energy barrier is overcome, and next stage in nucleation is initiated for further growth. During the nucleation process, stage factors such as energy barrier, driving force, critical size, and nucleation rates are very important.

The hydrate formation nucleation and the metastability of gas hydrates can be well understood by observing the pressure and temperature plots in Fig. 1.2. In Fig. 1.2, AB represents the hydrate equilibrium curve, and CD is the so-called thermodynamic spinodal curve that defines the metastable limit. In the metastable region of Fig. 1.2, the system does not have enough energy to overcome the entropy/enthalpy barrier for the creation of critical-sized nuclei. Hence, in this area, crystallization might be aided by the addition of a seed nucleus/crystal, but not without. At point *P*, which acts as the formation process, the system is said to be in a superheated state by the amount of *PR*; therefore, hydrate nucleation is impossible. Hydrate nucleation begins rapidly and

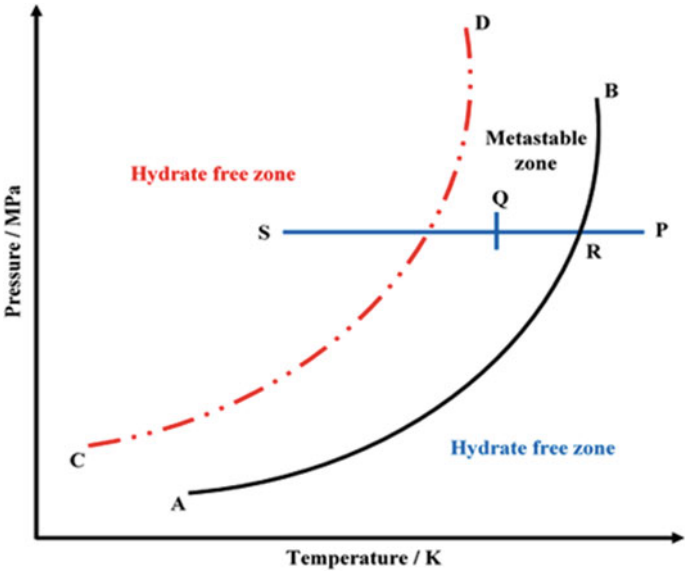

Fig. 1.2 Hydrate formation as function of subcooling, AB—equilibrium line and CD—spinodal line

crystallizes to the left of the line CD, due to the high driving force. However, between the hydrate equilibrium curve (AB) and the thermodynamic spinodal curve (CD), at point Q, a metastable zone is reached, which is characterized by the possibility to form hydrate nuclei or not to form nuclei. When hydrate nucleation is complete, the cages formed are unstable and can either dissipate or grow to hydrate unit cells, or drive the agglomerations of unit cells, thus forming metastable nuclei.

1.2.5 Gas Hydrate Nucleation Mechanism

The solubility of gases in liquid water can give a better understanding of why certain gases form more stable hydrates than others [1]. Previous studies have shown that gas hydrate nucleation takes place at the vapour–liquid interface [1]. To better understand hydrate nucleation processes, the extended model of labile cluster nucleation hypothesis by Christiansen and Sloan [31] becomes important. Their model is based on the fact that water clusters around dissolved gas molecules which may grow to achieve a critical radius, as shown schematically in Fig. 1.3. When a critical size cluster agglomeration is reached, nucleation is said to be complete, which allows hydrate growth to begin.

Generally, gas hydrate nucleation processes can be divided into two types: homogeneous (HON) or heterogeneous (HEN) processes. Homogeneous hydrate nucleation processes take place in systems without impurities. It normally consists of two

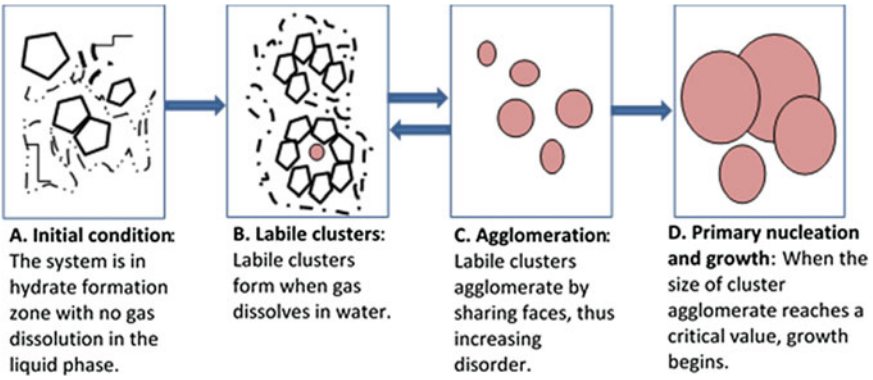

Fig. 1.3 Schematic model of the labile cluster nucleation hypothesis

phases: the solute and the nuclei/growing crystal [32]. In real life, it is unusual to observe a HON nucleation process. Gas hydrate nucleation occurs at the gas–liquid interface, which mostly consists of impurities. Also, foreign surfaces such as the reactor/pipe walls might also play an important role in the process. Hence, gas hydrate nucleation processes in real life are generally heterogeneous (HEN). The initial stage of any hydrate study or application is the nucleation stage and thus must be critically considered. However, hydrate nucleation studies are very difficult because it takes place at the molecular level, and are thus considered probabilistic.

The hydrate nucleation phenomenon is controlled by the energy barrier and critical size. Initially, the hydrate embryos form via the battling between the volume excess free energy and the surface excess free energy. Through this process, the surface excess free energy allows solute molecules to participate in the clustering of the subcritical embryos. On the other hand, the volume excess free energy allows solute molecules to fuse into the bulk of the critical-sized hydrate nuclei. Eventually, the existing free energy barrier and critical size of the forming hydrate nuclei develop stable particles with respect to Gibbs free energy, which then drives the hydrate growth progression and hence forms the setting for describing various hydrate nucleation phenomena.

Another important factor worth considering is the driving force. Expressing the hydrate nucleation process of individually clustered embryos or nuclei mechanisms is different from that of the hydrate nucleation driving force at a given pressure and temperature. The clustering embryos are useful to determine the distance from point Q in the metastable area, to the spinodal curve and the label region as shown in Fig. 1.2. At the spinodal point, nucleation assumes a likely occurrence and the chance of nucleation increases with increasing distance from the spinodal curve in the label region. With a sufficient degree of supercooling, and distance in the label region, nucleation becomes spontaneous. Thus, the driving force defines the ability of nucleation and its ability to become spontaneous.

The size of the system can influence the total excess energy needed in a system at any given temperature. Therefore, considering an experimental apparatus with a certain width, the "apparent metastable region", Q', would be somewhat system size and geometry dependent. Ke et al. [25] reported that their hydrate reactor with a diameter of 120 mm demonstrated a fast hydrate nucleation with less subcooling, as compared to reactors with the same diameters, such as 90, 60, and 20 mm. This suggests that decreasing reactor diameter would result in an increase in the degree of subcooling to achieve the required hydrate nucleation. The variation in hydrate nucleation with system size and geometry might be related to the different metastable limits in the reactors itself. However, sample size or amount of water is also system size dependent. However, factors such as system cooling rate, stirring speed, and type were not considered in their discussion. But, their factors also have very serious effects on the hydrate nucleation process.

1.2.6 Factors That Enhance Hydrate Nucleation Process

In addition to the condition necessary for hydrate formation, other factors such as agitation cause interfacial gas + liquid + crystal structures to be dispersed within the liquid, giving the appearance of a bulk nucleation from the surface, which affects the resulting hydrate formation. The presence of nucleation sites (such as impurities like sand) and free water may enhance hydrate nucleation or formation. These factors only enhance hydrate formation but are not ultimately necessary for hydrate formation.

1.2.7 Gas Hydrate Growth Process

Following hydrate nucleation, hydrate growth takes place. The hydrate crystal growth process depicts the growth of stable hydrate nuclei into solid hydrates. The growth of a hydrate is dependent on the interfacial area, pressure, temperature, agitation, water history, and the degree of supercooling. From Fig. 1.4, the sudden pressure drop caused by the consumption of gas molecules to form hydrate structure depicts hydrate growth and the constant pressure in the system, showing the completion of the formation of hydrates [1]. During hydrate growth, the mass transport of the gas to the hydrate's surface is of major importance and may dominate the process. In addition, the exothermic heat of hydrate formation can also control hydrate growth.

1.3 Gas Hydrate Issues

Oil and gas are mostly transported via pipelines from the wellheads to the production site. When these pipelines are operated under thermodynamic (temperature and

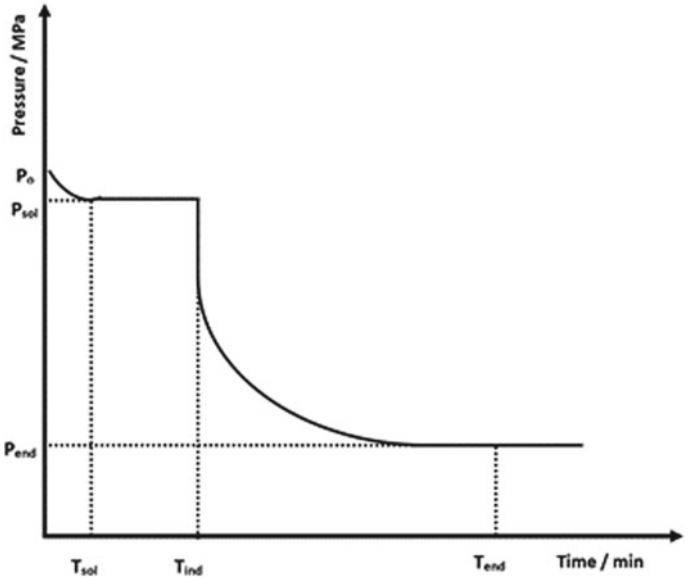

Fig. 1.4 Schematic representation of the pressure-time plot during kinetic hydrate formation experiment

pressure) conditions which favour hydrate formation, gas hydrate may form in them and may plug the pipelines in severe cases [19].

Gas hydrates form and plug transmission pipelines, resulting in uneconomical operation, conditions, and production stoppages, as well as loss of lives in severe cases. At times, production facilities and drilling operations may also experience hydrate plug issues, especially in deep-sea operations. According to Li et al. [33], the cost of preventing or removing hydrate blocks from pipelines is estimated to over US$200 M annually. Hydrate formation does affect the industry not only economically, but environmentally as well, and can lead to loss of human lives and reduction or stoppages in production. As petroleum activities move into deeper offshore areas, where temperature and pressure conditions are favourable for hydrate formation, especially in the Gulf of Mexico, the Caspian Sea, the North Sea, and permafrost regions like Alaska, the gas hydrates continue to be a major problem that must be mitigated for safe operations to take place.

In view of this, the oil and gas industries have continuously attempted to develop and modify technologies to mitigate hydrate formation.

The available methods for gas hydrate mitigation are water removal, heating, depressurization, and chemical injection [34–36]. Even though these are the available methods, some are not practical in real-world situations, especially with respect to water removal. Some are also expensive, leading to their difficulty in application. Therefore, injection of chemical inhibitors is most commonly applied in the industry [36].

Water removal is the best mitigation method for gas hydrates because once water is completely taken out of the flow stream, no hydrate will form. However, this is only true ideally. It is not practical to completely remove water from the hydrocarbon flow stream. The heating method focuses on the mechanism of using electric heaters to keep the pipeline temperatures in the non-hydrate formation region (i.e. increasing temperature). It is mostly used to keep pipeline temperatures higher during shutdown periods and can also be applied to melt hydrates when the pipeline is plugged [34]. The electric heating method is comparatively more expensive. Moreover, depressurizing pipelines in order to lower the pressure below the hydrate formation pressure is not a suitable method for industrial processes, since it may decrease the energy density to a point that is not economical. So, this method is mostly used to dissociate hydrates after gas hydrates are already formed, and there is a necessity to carry out hydrate plug removal during long shutdowns. The process is very slow and can last for longer periods [34].

Chemical inhibition consists of different inhibition techniques. The first group of chemical inhibitors that are used are thermodynamic inhibitors (THIs), such as alcohols (mainly methanol and glycol). They have been in use for several years. These primarily inhibit gas hydrate formation by depressing the freezing point. The major limitation of thermodynamic inhibition is the large amounts of methanol or glycol required (often more than 20 wt% of the aqueous phase) [32, 33]. In addition, alcohols can cause safety problems since they are highly flammable liquids. It is worth noting that these chemicals are also not environmentally friendly and biogradable. Due to these challenges, new chemical inhibitors were introduced in the 1990s, also known as low-dosage hydrate inhibitors (LDHIs). There are two types of LDHIs, which are anti-agglomerates and kinetic hydrate inhibitors (KHIs). The latter mainly inhibits hydrates by delaying the hydrate nucleation time and is mostly polymers (PVP), while the former allows hydrates to form, but prevents them from agglomeration. One advantage of LDHIs is that they are used at low concentrations (<2 wt%) and have been successfully used in the industry over several years. However, as the oil and gas offshore activities move deeper, these inhibitions face challenges at high subcooling temperatures. Therefore, there is a need for the development of new inhibitors. Recently, ionic liquids (ILs) have been introduced as a dual functional gas hydrate inhibitor (i.e. they have the ability to delay hydrate formation and growth and also shift the equilibrium hydrate curve to low-temperature and/or high-pressure regions) [24, 35, 37–45]. Most recently, natural amino acids and biomolecules have been proposed as novel gas hydrate inhibitors [46–48]. However, less inhibition impact has been observed as compared to the conventional hydrate inhibitors. Research on these novel inhibitors is still at the early stages and is ongoing to discover a less expensive, environmentally friendly, and effective gas hydrate inhibition impact. Chapter 2 gives much more details and the state-of-the-art depictions with regard to the performance associated with recent novel inhibitors (ionic liquids, amino acids, and biomolecules).

1.4 Potential Application of Gas Hydrates

Gas hydrate is a potential technology prospect for the future with several important applications in energy, water, and environment research domains. Some known and established applications of gas hydrates are natural gas production, energy storage, gas separation, cold energy storage, CO_2 sequestration, energy transport, and desalination applications. These applications generally require gas hydrate formation across various systems to have an efficient and fast hydrate formation, with low energy applications and effective separation factors.

1.4.1 Hydrate as Energy Source

There are large amounts of methane gas hydrates forming as solids in sediments and sedimentary rocks within 2000 m of the earth's crust in the permafrost and deep-water regions [49]. Interestingly, it has been established that natural gas hydrate is the next potential future energy source that will replace fossil fuels. Research has shown that the estimated amount of natural gas hydrate reserves (about 1.5×1016 m^3) in the world doubles that of fossil fuel [3]. The estimated amount of natural gas hydrates varies considerably. However, a realistic estimate is that 1016 m^3 of methane exists in hydrate form. The reserves of methane hydrate pose to be more than the conventional natural gas reserves and support the recent commitment to economically produce methane hydrates. Since its discovery, the subject of in situ gas hydrates immediately attracted the attention of a wide range of researchers because of its huge quintiles and energy potentials, its possible climate impact, and the drilling and production problems associated with in situ hydrates. Recently, there has been lots of research works to carry out drilling and produce natural gas hydrates, with countries such as the USA, Japan, China, India, making some great progress in that regard.

1.4.2 The Capture and Sequestration of Carbon Dioxide

The effects of industrial emission of CO_2 and its impact on the environment leading to global warming as claimed in the literature have gained importance in recent years. The main sources of carbon dioxide emissions in the atmosphere are manufacturing industries including cement, iron, and steel making. Thermal power generation and petrochemical industries also contribute massively to the emission of CO_2 in the atmosphere [50]. CO_2 capture and sequestration are now key areas of active research across many industrialized countries in a bid to conquer global warming. Moreover, the basis of CO_2 is to capture CO_2 not only as a polluting greenhouse gas, but also as an important raw material. Currently, available techniques for CO_2 capture and

separation are handled using chemical solvents, adsorption, chemisorptions, absorption, and chemical bonding through mineralization. However, due to the amount of chemicals used, environmental concerns, and cost, the application of these CO_2 capture methods is limited. Therefore, the development of new less energy-intensive processes is of major research interest. The gas hydrate crystallization techniques have certain advantages, as the major chemical needed for CO_2 hydrate formation is water, thus providing cheaper and greener chemical applications, as water is very common and is known as a potential chemical for life. Interestingly, the use of gas hydrate promoters can lower the energy demands for hydrate formation [11]. After separation, the capture of carbon dioxide must be sequestered. Similar to hydrate inhibition, there are two types of gas hydrate promoters. Thermodynamic promoters such as THF [51] and acetone [52] are used to shift the behaviour of the hydrate phase boundary. In addition, kinetic hydrate promoters are used to enhance the hydrate formation kinetics. A well-known kinetic promoter is SDS [53]. On the other hand, QAS such as TBAB [54] is known as semi-clathrate hydrate and is also known to be a thermodynamic promoter. Due to the ineffectiveness and environmental concerns, nanoparticles [55] and amino acids [48] have been introduced as a source of good kinetic hydrate promoters comparable to SDS. Chapter 3 deals with much more current developments in the field of hydrate promoters which are available across the literature works.

1.4.3 Natural Gas Storage and Transportation

Gas hydrate can also be employed for the transportation and storage of natural gases [56]. This is possible because of the high gas storage capacity of hydrates. It is believed that 1 m^3 gas hydrate can store about 180 m^3 of gas, which provides a high gas concentration storage [57]. Natural gas hydrate (NGH) is regarded as an important technique among several methods for transporting gas from production fields to the place of use, which includes pipeline natural gas (PNG), liquefied natural gas (LNG), compressed natural gas (CNG), gas to liquid (GTL), gas to commodity (GTC), and gas to wire (GTW), i.e. electricity. Storage and transportation of natural gases in the form of gas hydrates have an economic advantage mainly because of the lower investment in infrastructure and equipment [56]. The key to NGH storage and transportation is to overcome longer induction times and accelerate the hydrate formation. A great deal of research has been done to increase the hydrate formation rate via hydrate promoters, including adding surfactants, stirring, bubbling to the solution [50]. However, the economic aspect remaining is the separation factor in determining the optimal process efficiency. The review of hydrate-based application in gas storage and transportation was presented by Veluswamy et al. [56].

1.4.4 Cool Storage Application

The increasing demand of electric power for residential air conditioning and the depletion of the ozone layers by chlorofluorocarbons (CFCs) have brought about an emphasis on using alternative cool storage systems which shift this demand to off-peak periods and eliminate the need for using conventional refrigerants such as chlorofluorocarbons (CFCs) and hydrofluorocarbons (HFCs) [58]. CO_2 hydrate is an alternative way for the refrigeration process in the form of clathrate hydrate slurries which acts as a two-phase (solid–liquid) refrigerant. These two-phase refrigerants have a high latent heat of fusion (sometimes also known as phase change materials), which are much more energy efficient than the single-phase refrigerants. CO_2 hydrate slurries are promising systems in the field of cold distribution and storage as phase change materials due to the fact that the melting temperatures of some of these clathrate hydrates are consistent with the temperature needed in applications, such as air conditioning. Instead of using mechanical methods, the heat of dissociation of CO_2 hydrates can be generated by direct gas injection into an aqueous solution as in the case of ice slurries. The heat of dissociation of these slurries has been found to be suitable for its application in refrigeration [59].

1.4.5 Desalination

Most countries have clean water challenges though they have lots of sea water which contains salts. In addition, the oil and gas industry generates large volumes of produced water. The quantities of water are constantly increasing because mature fields have much larger water-to-oil ratio than new fields in production. The produced water is usually saline (30–300 g/L of total dissolved solids). This high salinity restricts their disposal options on shore and also becomes an obstacle to recycling or reuse of the water. Since hydrates are formed between water and gas, both sea and produced water can be treated using hydrate-based promoters.

In this process, the pure water molecules, now in solid form (hydrate), can be recovered by melting and separation which leads to desalination. This method has been long studied in the past using methane hydrate or carbon dioxide hydrate. For different technical and economic reasons, no real industrial solutions emerged at that time using such gas host molecules. Recent advancements in the research of clathrate promoters have opened the door to more adequate, robust, and cheaper solutions, as opposed to methane or carbon dioxide, for a type of application such as desalination. Linga's laboratory plays a vital role in the desalination studies in recent times, with a patent in which they developed a new experimental method for desalination studies [60, 61]. Similarly, active research on the effects of hydrate promoters is still ongoing to fully implement this technology.

1.5 Gas Hydrate Testing Method

This section deals with recent gas hydrate apparatus and techniques used by researchers to test hydrate inhibitors and promoters, thermodynamically and kinetically.

1.5.1 Apparatus

In order to successfully apply gas hydrate-based technologies, a good understanding and evaluation of the formation of kinetics and phase behaviour in gas hydrate promoters and inhibitors are very useful. Generally, authors/researchers employ various forms of techniques to achieve the required hydrate kinetics and phase behaviour. Further details on the apparatus and techniques used for hydrate studies are provided in Sloan's book [1]. However, in recent times, various simulations and experimental apparatus and techniques have been adopted. A high-pressure reactor [62–64], mostly called autoclaves, is the most employed experimental apparatus. However, there have been instances where nuclear magnetic resonance (NMR) microscopy [65], in situ powder X-ray diffraction [22, 46], and ultrasonic equipment have been employed to study the phase behaviour and kinetics of hydrate formation. However, rocking cell and differential scanning calorimetry (HP DSC) [36, 37, 66, 67] are mostly used for hydrate phase behaviour, and the rest are mostly employed for hydrate kinetics, and molecular and structural studies. In addition, some studies have also been conducted using high-pressure flow loops to evaluate the kinetics of hydrate formation [68, 69]. Another technique that has been used for kinetic studies is the high-pressure automated lag time apparatus (HP-ALTA). This technique offers a wide range to run lots of experiments in a short time [70].

1.5.2 Hydrate Kinetic Measurement

Generally, gas hydrate kinetic studies are based on their applications. However, the methods of measuring hydrate kinetic are similar but the interpretation is solely reserved for the kind of hydrate application under study. The kinetic measurements are based on their formation and disassociation path. Sloan's book gives details on how these quantities are measured; however in this book, we would consider recent hydrate kinetic measurements used by the authors. Kinetic indicators are hydrate nucleation time and rate, growth rate, total gas uptake/consumption, hydrate dissociation rate, hydrate conversion ratio, hydrate preservative ability, etc. Herein, the recent methods used to measure the aforementioned hydrate kinetic indicators are briefly discussed. There are generally two methods for testing hydrate nucleation processes. The first is the nucleation at constant temperature and degree of subcooling,

and the second method involves nucleation during which constant cooling experiments take place. The latter evaluates the subcooling at which hydrate nucleation will happen. The former determines the hydrate nucleation rate and induction time at a specific driving force. Because the subcooling point is less probabilistic at constant cooling, some researchers prefer to use the second method. Generally, at constant subcooling and temperature induction, time measurement is very stochastic and not preferred by some authors. However, it is worth noting that the subcooling point method is also stochastic in application, since the nucleation time/rate are all dependent on the degree of subcooling. On the other hand, for constant temperature mode, a fixed subcooling is applied in the system. Hence, the nucleation time/rate depends on a function of a time average of observed nucleation time. Also, the cooling rate is known to affect the subcooling point.

Generally, to perform a hydrate kinetic experiment, the cell is initially cooled to temperatures which are about 2 K higher than the hydrate equilibrium temperature. Then, the desired gas/guest is pressurized into the cell up to the desired experimental pressure. The stirrer is turned on, and the system is left to stabilize, after which the system is cooled down to the experimental temperature without stirring during the cooling period. There would be a decrease in the system pressure due to the gas solubility into the liquid phase. When the system pressure becomes constant, at the experimental temperature, the stirrer is turned on. When a rapid pressure drop is noted in the system, the hydrate is assumed to have formed. When the system pressure becomes constant after hydrate formation for more than 3 h, the experiment is considered completed.

1.5.2.1 Estimation of Kinetic Parameters

Induction time is defined as the nucleation time or induction time of gas hydrate formation for a noticeable hydrate nucleus crystal to be formed. It is estimated that the time at which a rapid temperature increases, or pressure drop is observed in the system and in a pressure—temperature verse time plot of any hydrate experiment. However, it is also detected via visual observation using a glass window or camera in some set-ups.

The initial rate of hydrate formation is very important for gas hydrate application as mentioned earlier. It describes how fast or slow the hydrate forms in any given system. Usually, a slow hydrate formation rate is preferred in hydrate testing inhibitors, while hydrate promoters are expected to exhibit fast hydrate formation rates. The initial rate of hydrate formation is usually calculated by most authors following Eq. (1.1):

$$r(t) = \frac{n_i^{i-1} - n_i^{i+1}}{t_{i-1} - t_{i+1}} n_{\mathrm{w}_0}^{-1} \tag{1.1}$$

where n_i^{i-1} and n_i^{i+1} are the amount of moles of gas in the phase at time t_{i-1} and t_{i+1}, respectively, and $n_{\mathrm{w}_0}^{-1}$ is the amount of moles of water in the liquid phase.

The amount of gas consumed or total gas uptake is the amount of gas consumed or converted into hydrate, which is useful to understand the amount of gas that can be trapped in the hydrates. In gas hydrate-based applications such as gas storage and separation, the estimation of the total gas uptake is very important. Interestingly, the total amount of gas consumed during hydrate formation is not completely dependent on its formation rate. That is to say, the high rate of hydrate formation does not guarantee high moles of gas consumed and vice versa. However, kinetic hydrate inhibitors are required to reduce the moles of gas consumed during hydrate formation, while kinetic hydrate promoters are expected to enhance it. The real gas equation (Eq. 1.2) is generally adopted to determine the total amount of gas consumed during hydrate kinetic studies. This is valid for isothermal experiments with the assumption that no water volume changes during hydrate formation.

$$n_{\mathrm{g}} = \left[\left(\frac{PV}{RTz}\right)_0 - \left(\frac{PV}{RTz}\right)_t\right] \tag{1.2}$$

where *P, T, Z*, and *V* are the hydrate reactor pressure, temperature, gas compressibility factor, and volume of the gas phase, respectively. *Z* can be determined by employing any equation states (however, the Peng–Robinson equation of state is mostly used in the literature). *R* represents the universal gas constant, while the subscript 0 denotes the initial time at which the experiment was started; *t* denotes anytime *t* of the experiment. The total gas uptake is usually normalized to eliminate the sample size using Eq. (1.3). In reality, the normalized amount of gas consumed (n_{N}) indicates the total quantity of gas trapped in one mole of a loaded solution.

$$n_{\mathrm{N}} = \frac{n_{\mathrm{g}}}{n_{\mathrm{w}}} \tag{1.3}$$

Storage capacity (SC) is employed in applications such as gas transportation and storage to quantify the amount of gas that can be trapped in any hydrate system. However, it can also be used in also all hydrate kinetic studies for analysis. The storage capacity describes the volume of gas captured under standard conditions (STP) per volume. It can be determined as follows:

$$\mathrm{SC} = \frac{V_{\mathrm{g}}^{\mathrm{STP}}}{V_{\mathrm{H}}} = \frac{n_{\mathrm{g}} R T^{\mathrm{STP}} / P^{\mathrm{STP}}}{V_{\mathrm{H}}} \tag{1.4}$$

where V_{H} is the gas hydrate volume and estimated using Eq. (1.5).

$$V_{\mathrm{H}} = M n_{\mathrm{g}} v_{\mathrm{W}}^{B} \tag{1.5}$$

where $v^{B}{}_{W}$ is the molar volume of empty hydrate lattice.

$$v_{\mathrm{W}}^{B} = \left(11.835 + 2.217 \times 10^{-5} T + 2.242 \times 10^{-6} T^{2}\right)^{3} \times \frac{10^{-30} N_{\mathrm{A}}}{46} - 8.006 \times 10^{-9} P + 5.448 \times 10^{-12} P^{2} \tag{1.6}$$

where P(MPa) and T(K) denote the pressure and temperature of the system. N_{A} is Avogadro's constant. Also, it is assumed that the molar volume of gas hydrate and empty hydrate lattice are the same. Hence, the trapping mechanism of gas into hydrogen water molecules is expressed in the reaction below (see Eq. 1.7):

$$G + M\mathrm{H_2O} \leftrightarrow G.(\mathrm{H_2O})_{M} \tag{1.7}$$

where G is the type of guest and M represents the hydration number. This is linearly related to the fractional cage occupancy. However, this is true for sI hydrates. For sII hydrates, the constant 46 in the equation would be 136.

$$M = \frac{\eta_{\mathrm{k}}}{\sum \upsilon_{\mathrm{m}} \left(\sum \theta_{\mathrm{m,i}}\right)} \tag{1.8}$$

where η_{k} is the number of water molecules in a unit cell, υ_{m} is the number of cavities of type m in the unit cell, and θ_{m} is the fractional occupancy of cavity of type m, which are mostly calculated using the Langmuir adsorption theory, as follows.

$$\theta_{\mathrm{m,i}} = \frac{C_{\mathrm{m,i}} f_{\mathrm{i}}}{1 + \sum C_{\mathrm{m,i}} f_{\mathrm{i}}} \tag{1.9}$$

where $C_{\mathrm{m,i}}$ represents the gas Langmuir constant of the guest (G) in type i cavity and f denotes the fugacity of the guest (G) in the gas phase. The Langmuir constant of gas ($C_{\mathrm{m,i}}$) is given in Eq. (1.10):

$$C_{\mathrm{m,i}} = \frac{A_{\mathrm{m,i}}}{T} \exp\left(\frac{B_{\mathrm{m,i}}}{T}\right) \tag{1.10}$$

$A_{\mathrm{m,i}}$ and $B_{\mathrm{m,i}}$ are constants. T(K) is the temperature. The fugacity of guest in the gas phase can be determined by any equation of state.

Water-to-hydrate conversion ratio describes the portion of water molecules that is converted to gas hydrate per mole of initial solution. It is very useful in hydrate-based desalinating studies. A high water conversion-to-hydrate ratio would guarantee high water desalination efficacy. Equation (1.11) is usually adopted to calculate the water-to-hydrate conversion ratio.

$$\text{Conversion} = \frac{M n_{\mathrm{g}}}{n_{\mathrm{w_o}}} \tag{1.11}$$

1.5.3 Hydrate Dissociation and Preservation Measurements

Dissociation and preservation tests for hydrates are usually performed first by cooling the system. After the hydrate forms in a typical manner as explained in the previous section, the temperature of the reactor is then lowered to the hydrate equilibrium temperature at the pressure which the hydrates are expected to be preserved. Mostly, the hydrate is expected to be preserved at an atmospheric pressure until they are dissociated. Hence, after the reduction in temperature to 263.2 K, the pressure in the reactor is decreased to atmospheric pressure and allowed to stabilize. These experiments are used to determine how stable the hydrate would be especially for CO_2 storage and hydrate pellets applications due to climate concerns.

1.5.4 Hydrate Phase Behaviour Measurement

In order to measure the hydrate phase behaviour, the isochoric temperature cycle (T-cycle) or pressure search mode is used [23]. During this experimental mode, the reactor is first cleaned and vacuumed. Then, the temperature of the system is set to about 2–3 K above the hydrate equilibrium temperature of the studied experimental pressure. The solution under study is then loaded into the cell, after which the system is compressed with the guest molecules. The system is then left to stabilize while the stirrer is turned on. When the pressure becomes constant, the system temperature is then lowered to an adequate temperature, which would allow hydrate formation. A sharp pressure drop in the system shows hydrate formation. After gas hydrates are formed, the system is heated slowly, stepwise, at about 0.5 K/step for 3 h at each step as proposed by Tohidi et al. [71]. Figure 1.5 illustrates the hydrate formation and dissociation process during hydrate phase behaviour measurement. The hydrate phase equilibrium point is determined as the point where the cooling curve intersects with the heating curve as described in Fig. 1.6.

1.5.4.1 Average Depression Temperature ($\overline{T}$)

The average depression temperature ($\overline{T}$) is calculated using Eq. (1.12) [36]. It is used to quantitatively analyse the impact of hydrate phase behaviour shift in the presence of inhibitors/promoters.

$$\overline{T} = \frac{1}{m} \sum_{i=1}^{m} \Delta T \tag{1.12}$$

where m is the number of data points and ΔT is the difference between measured hydrate dissociation temperature in the presence of inhibitor and pure water. The

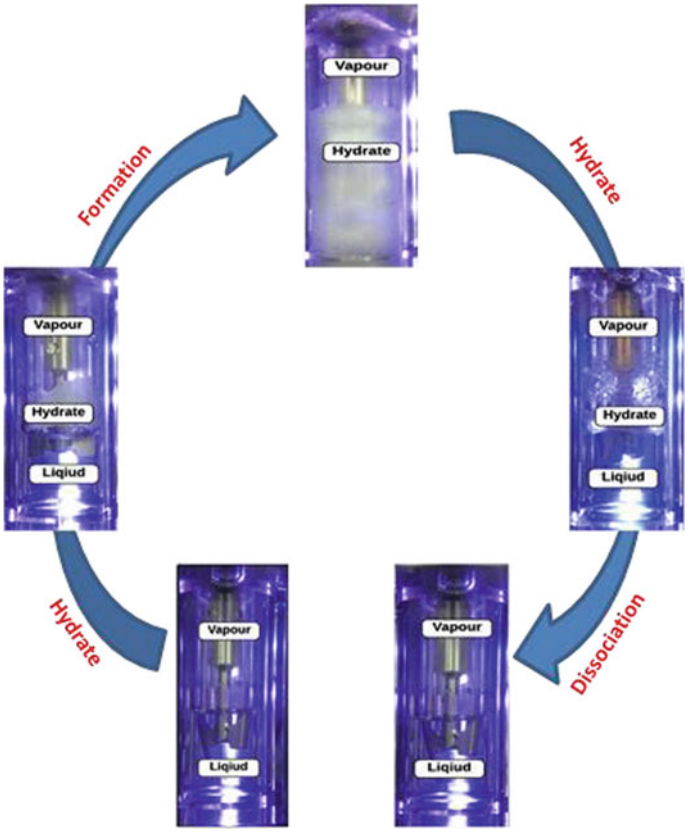

Fig. 1.5 Pictures of hydrate formation and dissociation

pure water equilibrium temperature can be determined using CSMGem, PVTsim, or any hydrate model at constant pressure [19].

1.5.4.2 Calculation of Methane Hydrate Dissociation Enthalpy

Determining of hydrate dissociation enthalpy is critical in understating the hydrate structure and guest cage occupancy, which is related to the relative size of the guest molecule and cavity size. Generally, the gas hydrate formation disassociation enthalpy is defined as the heat required to decompose hydrate and to release one mole of guest gas molecule, with a reaction formula as:

$$M.n\mathrm{H_2O}_{(s)} = M + n\mathrm{H_2O}_{(l)} \tag{1.13}$$

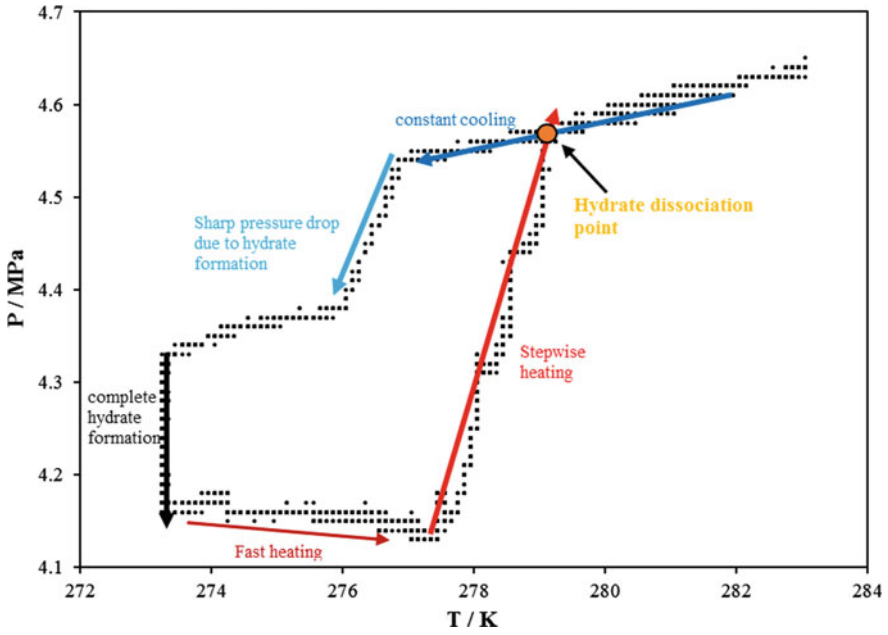

Fig. 1.6 Typical pressure–temperature profile measured during methane + deionized water experiment

where M and n are the guest and hydration numbers, respectively. The enthalpy of hydrate dissociation can be determined calorimetrically as a direct method or indirectly by using the Clausius–Clapeyron equation via the aid of the measured HL_wVE points. The hydrate dissociation enthalpy is estimated by employing the Clausius–Clapeyron equation (Eq. 1.14) as follows [1]:

$$\frac{d(\ln P)}{d\left(T^{-1}\right)} = \frac{-\Delta H_d}{zR} \tag{1.14}$$

where P, T, ΔH_d, z, and R are pressure, temperature, dissociation enthalpy, compressibility factor, and universal gas constant, respectively.

1.6 Gas Hydrate Models

Based on the knowledge of hydrate structure and formation mechanisms, effective hydrate themodynamic and kinetic predictive methods have been formulated by several authors. These predictive models are needed and are constantly modified for more accurate prediction, especially kinetic models.

1.6.1 Nucleation and Growth Models

Hydrate nucleation and growth processes have a lot of measurement challenges, resulting in the difficulty to model their formation processes. However, there has been a rise in the attempts to model hydrate kinetics from the Bostnia days till now. Both nucleation and growth models have been used in literature. Vysniauskas and Bishnoi et al., in their seminal work, reviewed the kinetics of hydrate formation and developed a semi-empirical model to correlate experimental data on methane and ethane hydrate formation. In their work, the hydrate formation modelling did not include the hydrate nucleation. They further followed up with other modifications of their model. Kvamme et al. developed a generic hydrate nucleation model based on the phase field theory for describing the nucleation of CO_2 hydrates in aqueous solutions. Other forms of hydrate nucleation and growth theories including CNT have been reviewed in Chap. 4 of this book. However, due to the probabilistic nature of hydrate nucleation and its dependence on apparatus and many other factors, very poor accurate hydrate kinetic prediction has been reported.

1.6.2 Thermodynamic Models

The use of thermodynamic hydrate models has made hydrate formation pressure and temperature prediction much easier for industrial applications. This model has been extended to several hydrate systems and is very accurate in predictions by comparing them with its kinetic counterpart. On the other hand, simple hydrate phase behaviour models can be developed. The model proposed by van der Waals and Platteeuw (1959) discussed the basics of the modern hydrate models with or without inhibitors. Since new hydrate inhibitors such as ionic liquids, and amino acids have been reported, constant modification of the models has been developed to suit such systems. The advantage of this model is that it is able to predict macroscopic property such as pressure. Chapter 4 gives a detailed method of all the hydrate thermodynamic models used recently in the presence and absence of hydrate inhibitors.

1.7 The Connection of This Chapter to Those That Follow

This chapter provides a background for hydrate formation and applications. Considering the fact that the focus of this book is to provide recent advances on the progress of hydrate chemical additives, the next chapter will provide the state-of-the-art development on recent hydrate inhibitors devel and their inhibition mechanisms. Similarly, Chap. 3 deals with gas hydrate additives (promoter) that enhance hydrate formation

for gas separation, desalination, and CO_2 storage. It also provides the hydrate promotion mechanism for these additives. Lastly, Chap. 4 details the thermodynamic and kinetic models for gas hydrates in the presence and absence of additives, including recently introduced novel additives.

References

1. Sloan ED, Koh CA (2007) Clathrate hydrates of natural gases, 3rd edn. CRC Press, Boca Raton, p 758
2. Hammerschmidt EG (1934) Formation of gas hydrates in natural gas transmission lines. Ind Eng Chem 26:851–855
3. Englezos P (1993) Clathrates hydrates. Ind Eng Chem Res 32:1251–1274
4. Javanmardi J, Moshfeghian M (2003) Energy consumption and economic evaluation of water desalination by hydrate phenomenon. Appl Therm Eng 23:845–857
5. Javanmardi J, Nasrifar K, Najibi SH, Moshfeghian M (2005) Economic evaluation of natural gas hydrate as an alternative for natural gas transportation. Appl Therm Eng 25:1708–1723
6. Xu C-G, Li X-S (2015) Research progress on methane production from natural gas hydrates. RSC Adv 5:54672–54699
7. Lang X, Fan S, Wang Y (2010) Intensification of methane and hydrogen storage in clathrate hydrate and future prospect. J Nat Gas Chem 19(3):203–209
8. Li S, Fan S, Wang J et al (2009) CO_2 capture from binary mixture via forming hydrate with the help of tetra-n-butyl ammonium bromide. J Nat Gas Chem 18:15–20
9. Chun-Gang X, Xiao-Sen L (2014) Research progress of hydrate-based CO_2 separation and capture from gas mixtures. RSC Adv 4:18301–18316
10. Duc NH, Chauvy F, Herri JM (2007) CO_2 capture by hydrate crystallization—a potential solution for gas emission of steelmaking industry. Energy Convers Manag 48:1313–1322
11. Babu P, Linga P, Kumar R et al (2015) A review of the hydrate-based gas separation (HBGS) process for carbon dioxide pre-combustion capture. Energy 85:261–279
12. Park S, Lee S, Lee Y et al (2013) CO_2 capture from simulated fuel gas mixtures using semi-clathrate hydrates formed by quaternary ammonium salts. Environ Sci Technol 47:7571–7577
13. Mohammadi AH, Anderson R, Tohidi B (2005) Carbon monoxide clathrate hydrates: equilibrium data and thermodynamic modeling. AIChE J 51:2825–2833
14. Li S, Fan S, Wang J (2010) Clathrate hydrate capture of CO_2 from simulated flue gas with cyclopentane/water emulsion. Chin J Chem Eng 18:202–206
15. Kim SM, Lee JD, Lee HJ et al (2011) Gas hydrate formation method to capture the carbon dioxide for pre-combustion process in IGCC plant. Int J Hydrogen Energy 36:1115–1121
16. Ameripour S (2005) Prediction of gas-hydrate formation conditions in production and surface facilities. Doctoral dissertation, Texas A&M University
17. Harrison SE (2010) Natural gas hydrates. Stanford University, p 4
18. Obanijesu EO, Gubner R, Barifcani A et al (2014) The influence of corrosion inhibitors on hydrate formation temperature along the subsea natural gas pipelines. J Pet Sci Eng 120:239–252
19. Koh CA, Sloan ED, Sum AK et al (2011) Fundamentals and applications of gas hydrates. Ann Rev Chem Biomol Eng 2:237–257
20. Jeffrey GA (1984) Hydrate inclusion compounds. J Incl Phenom 1:211–222
21. Jeffery GA (1972) Pentagonal dedecahedral water structure in crystalline hydrates. Mat Res Bull 7:1259–1270
22. Ripmeester JA, Tse JS, Ratcliffe CI et al (1987) A new clathrate hydrate structure. Nature 325:135–136
23. Partoon B, Wong NMS, Sabil KM et al (2013) A study on thermodynamics effect of [EMIM]-Cl and [OH-C_2MIM]-Cl on methane hydrate equilibrium line. Fluid Phase Equilib 337:26–31

24. Tariq M, Rooney D, Othman E et al (2014) Gas hydrate inhibition: a review of the role of ionic liquids. Ind Eng Chem Res 53:17855–17868
25. Ke W, Svartaas TM, Chen D (2019) A review of gas hydrate nucleation theories and growth models. J Nat Gas Sci Eng 61:169–196
26. Ranieri U, Koza MM, Kuhs WF et al (2017) Fast methane diffusion at the interface of two clathrate structures. Nat Commun 8:1–7
27. Jacobson LC, Hujo W, Molinero V (2010) Amorphous precursors in the nucleation of clathrate hydrates. J Am Chem Soc 132:11806–11811
28. Durham WB, Stern LA, Kirby SH (2003) Ductile flow of methane hydrate. Can J Phys 81:373–380
29. Davidson DW, Handa YP, Ripmeester JA (1986) Xenon-129 NMR and the thermodynamic parameters of xenon hydrate. J Phys Chem 90:6549–6552
30. Waite WF, Gilbert LY, Winters WJ et al (2005) Thermal conductivity of THF hydrate between −25 and +4 °C, and their application to methane hydrate. In: Proceedings of fifth international conference on gas hydrates, pp 1724–1733
31. Christiansen RL, Sloan ED (1994) Mechanisms and kinetics of hydrate formation. Ann N Y Acad Sci 715:283–305
32. Kashchiev D, Firoozabadi A (2002) Nucleation of gas hydrates. J Cryst Growth 243:476–489
33. Li XS, Liu YJ, Zeng ZY et al (2011) Equilibrium hydrate formation conditions for the mixtures of methane + ionic liquids + water. J Chem Eng Data 56:119–123
34. Boyun G, Shanhong S, Ghalambor A (2014) Offshore pipelines design, installation, and maintenance, 2nd edn. Elsevier, p 383
35. Xiao C, Adidharma H (2009) Dual function inhibitors for methane hydrate. Chem Eng Sci 64:1522–1527
36. Sabil KM, Nashed O, Lal B et al (2015) Experimental investigation on the dissociation conditions of methane hydrate in the presence of imidazolium-based ionic liquids. Thermodyn J Chem 84:7–13
37. Xiao C, Wibisono N, Adidharma H (2010) Dialkylimidazolium halide ionic liquids as dual function inhibitors for methane hydrate. Chem Eng Sci 65:3080–3087
38. Bavoh CB, Partoon B, Lal B et al (2016) Effect of 1-ethyl-3-methylimidazolium chloride and polyvinylpyrrolidone on kinetics of carbon dioxide hydrates. Int J Appl Chem 12:6–11
39. Nashed O, Sabil KM, Lal B et al (2014) Study of 1-(2-hydroxyethyle) 3-methylimidazolium halide as thermodynamic inhibitors. Appl Mech Mater 625:337–340
40. Nashed O, Dadebayev D, Khan MS et al (2018) Experimental and modelling studies on thermodynamic methane hydrate inhibition in the presence of ionic liquids. J Mol Liq 249:886–891
41. Khan MS, Liew CS, Kurnia KA et al (2016) Application of COSMO-RS in investigating ionic liquid as thermodynamic hydrate inhibitor for methane hydrate. Procedia Eng 148:862–869
42. Bavoh CB, Lal B, Khan MS et al (2018) Combined inhibition effect of 1-ethyl-3-methylimidazolium chloride + glycine on methane hydrate. J Phys: Conf Ser 1123:012060
43. Bavoh CB, Lal B, Keong LK et al (2016) Synergic kinetic inhibition effect of EMIM-CL + PVP on CO_2 hydrate formation. Procedia Eng 148:1232–1238
44. Khan MS, Bavoh BC, Lal B et al (2018) Kinetic assessment of tetramethyl ammonium hydroxide (ionic liquid) for carbon dioxide, methane and binary mix gas hydrates. Recent Adv Ion Liq 9:159–179
45. Bavoh CB, Lal B, Nashed O et al (2016) COSMO-RS: an ionic liquid prescreening tool for gas hydrate mitigation. Chin J Chem Eng 11:1619–1624
46. Sa J-H, Kwak G-H, Lee BR et al (2013) Hydrophobic amino acids as a new class of kinetic inhibitors for gas hydrate formation. Sci Rep 3:2428
47. Bavoh CB, Partoon B, Lal B et al (2016) Methane hydrate-liquid-vapour-equilibrium phase condition measurements in the presence of natural amino acids. J Nat Gas Sci Eng 37:425–434
48. Bavoh CB, Lal B, Osei H et al (2019) A review on the role of amino acids in gas hydrate inhibition, CO_2 capture and sequestration, and natural gas storage. J Nat Gas Sci Eng 64:52–71
49. Merey Ş (2017) Drilling of gas hydrate reservoirs. J Nat Gas Sci Eng 35:1167–1179

50. Sami NA, Sangwai J, Subramanian B (2013) Gas hydrate applications and problems in oil and gas industry. Int J Sci Eng Res 4:1–5
51. Fan S, Li S, Wang J et al (2009) Efficient capture of CO_2 from simulated flue gas by formation of TBAB or TBAF semiclathrate hydrates. Energy Fuels 23:4202–4208
52. Partoon B, Sabil KM, Roslan H et al (2016) Impact of acetone on phase boundary of methane and carbon dioxide mixed hydrates. Fluid Phase Equilib 412:51–56
53. Partoon B, Malik SNA, Azemi MH et al (2013) Experimental investigations on the potential of SDS as low-dosage promoter for carbon dioxide hydrate formation. Asia-Pac J Chem Eng 8:258–261
54. Deschamps J, Dalmazzone D (2009) Dissociation enthalpies and phase equilibrium for TBAB semi-clathrate hydrates of N_2, CO_2, $N_2 + CO_2$ and $CH_4 + CO_2$. J Therm Anal Calorim 98:113–118
55. Nashed O, Partoon B, Lal B et al (2018) Review the impact of nanoparticles on the thermodynamics and kinetics of gas hydrate formation. J Nat Gas Sci Eng 55:452–465
56. Veluswamy HP, Kumar A, Seo Y et al (2018) A review of solidified natural gas (SNG) technology for gas storage via clathrate hydrates. Appl Energy 216:262–285
57. Ganji H, Manteghian M, Rahimi Mofrad H (2007) Effect of mixed compounds on methane hydrate formation and dissociation rates and storage capacity. Fuel Process Technol 88:891–895
58. Darbouret M, Cournil M, Herri J-M (2005) Rheological study of TBAB hydrate slurries as secondary two-phase refrigerants. Int J Refrig 28:663–671
59. Sabil KM, Witkamp G-J, Peters CJ (2010) Estimations of enthalpies of dissociation of simple and mixed carbon dioxide hydrates from phase equilibrium data. Fluid Phase Equilib 290:109–114
60. Linga P, Babu P, Nambiar AP (2018) A clathrate hydrate desalination method. WO/2018/156083
61. Nambiar A, Babu P, Linga P (2019) Improved kinetics and water recovery with propane as co-guest gas on the hydrate-based desalination (hydesal) process. Chem Eng 3:31
62. Mannar N, Bavoh CB, Baharudin AH et al (2017) Thermophysical properties of aqueous lysine and its inhibition influence on methane and carbon dioxide hydrate phase boundary condition. Fluid Phase Equilib 454:57–63
63. Bavoh CB, Partoon B, Lal B et al (2017) Inhibition effect of amino acids on carbon dioxide hydrate. Chem Eng Sci 171:331–339
64. Khan MSMS, Bavoh CB, Partoon B et al (2017) Thermodynamic effect of ammonium based ionic liquids on CO_2 hydrates phase boundary. J Mol Liq 238:533–539
65. Trueba AT, Radović IR, Zevenbergen JF et al (2012) Kinetics measurements and in situ Raman spectroscopy of formation of hydrogen-tetrabutylammonium bromide semi-hydrates. Int J Hydrogen Energy 37:5790–5797
66. Khan MSMS, Partoon B, Bavoh CB et al (2017) Influence of tetramethylammonium hydroxide on methane and carbon dioxide gas hydrate phase equilibrium conditions. Fluid Phase Equilib 440:1–8
67. Mohammadi AH, Richon D (2010) Gas hydrate phase equilibrium in the presence of ethylene glycol or methanol aqueous solution. Ind Eng Chem Res 49:8865–8869
68. Odutola TO, Ajienka JA, Onyekonwu MO et al (2016) Hydrate Inhibition in laboratory flow loop using polyvinylpyrrolidone, N-Vinylcaprolactam and 2-(Dimethylamino)ethylmethacrylate. J Nat Gas Sci Eng 36:54–61
69. Talaghat MR (2014) Experimental investigation of induction time for double gas hydrate formation in the simultaneous presence of the PVP and l-Tyrosine as kinetic inhibitors in a mini flow loop apparatus. J Nat Gas Sci Eng 19:215–220
70. Sowa B, Zhang XH, Hartley PG et al (2014) Formation of Ice, tetrahydrofuran hydrate, and methane/propane mixed gas hydrates in strong monovalent salt solutions. Energy Fuels 11:6877–6888
71. Tohidi B, Burgass RW, Danesh A et al (2000) Improving the accuracy of gas hydrate dissociation point measurements. Gas Hydrates Chall Futur 912:924–931

Chapter 2
Gas Hydrate Inhibitors

Muhammad Saad Khan, Bhajan Lal and Mohamad Azmi Bustam

2.1 Introduction

In the oil and gas industry, one of the chief impediment faced in flow assurance is the formation of gas hydrate in pipelines, which can cause the blockage of the hydrocarbon production, transportation, and processing. In petroleum transmission lines, the presence of foreign impurities such as rust, dust, or microparticles can possibly catalyse the hydrate nucleation through heterogeneous nucleation attributed to the hydrate plug.

Initially, Hammerschmidt [1] found the hydrate blockage problem in the gas pipeline, and since then extensive research activities are being performed to find better and more proficient mitigation solutions, especially chemical inhibitors [1]. Gas hydrate formation may perhaps lead to catastrophic economic losses and ecological risks. Hydrates also arise in the drilling fluids that are used in deep offshore drilling operations which could result in severe threats towards operational safety. Hydrate formation issues are frequently encountered in deep waters like Gulf of Mexico, Caspian Sea, North Sea, and permafrost region like Alaska.

The low-temperature and high-pressure conditions may cause natural gas and water transported in the pipelines to form gas hydrates. Oil and gas wells always produce undesired water along with hydrocarbons. As the working areas of the gas and oil production are moving into the deeper ocean areas, i.e. the pressure is much higher, and the temperature is much colder, which is favourable for the hydrate formation [2]. The reason for hydrate formation is that oil can dissolve some water in small amounts. The oil is produced up the wellbore, followed by temperature decrease, and liquid water comes out of the solution, remaining in the suspension as microdroplets. In a static condition, the microdroplets gradually coalesce and precipitate. After enough saturation with gas molecule water and the presence of suitable temperature and pressure conditions, the hydrate formation begins leading to blockages and clogging of the gas flow in the pipelines. The gas hydrates that form in the oil and gas transmission line frequently consist of sI and sII structures [2].

B. Lal and O. Nashed, *Chemical Additives for Gas Hydrates*, Green Energy and Technology, https://doi.org/10.1007/978-3-030-30750-9_2

2.1.1 Conventional Gas Hydrate Mitigation Method

There are four conventional methods employed in oil and gas industry for preventing gas hydrates, which are thermal heating, depressurization, dehydration, and insertion of chemical inhibitors. Thermal heating involves insulation of the entire pipeline which caused an enormous amount of economic losses. Since the pipelines span hundreds of miles, and the capital cost is 1 million US$/mile, it becomes a counteractive method once gas hydrate is formed inside the pipeline. Similarly, depressurization is also considered as a corrective method for hydrate plug removal. Depressurization should be done cautiously since sudden pressure drops cause a rapid increase in hydrate plug velocity that can lead to catastrophic damages to platform or infrastructure. Dehydration refers to the preventive method for avoiding gas hydrate plug formation. Offshore dehydration may not be likely due to physical footprint constraints in the production facility at the offshore facility. The most effective method for prevention of gas hydrate is the insertion of chemicals [3, 4].

Chemical inhibition involves the addition of certain chemicals to prevent or delay the gas hydrate plug formation [5–8]. Therefore, under many circumstances, the use of inhibitors for gas hydrate inhibition is the only practical and feasible choice. From the knowledge of the chemical composition requirements and the thermodynamics of hydrates formation, the industry has tried to prevent the hydrate formation by using conventional anti-freezing methods. These methods are either inefficient or require an enormous amount of chemical solvents resulting in high operation cost and high environmental impact of operating gas and oil facilities. Thus, in most of the cases, the hydrate inhibition by adding chemical inhibitors is the only viable option [9–12]. The subsequent section further elaborates the type and nature of gas hydrate inhibitors. Accordingly, investigations to understand hydrate nucleation and growth process with or without inhibitors are still in progress.

2.1.2 Chemical Inhibition of Gas Hydrates

The mitigation of hydrate formation using chemical inhibitors can be categorized into two fundamental types according to their utilized dosage: high dosage hydrate inhibition (HDHI) [thermodynamic hydrate Inhibitors (THIs)] and low dosage hydrate inhibitors (LDHIs) [7, 13–17]. Figure 2.1 represents the different types of inhibitors.

2.1.2.1 Thermodynamic Hydrate Inhibitors (THIs)

Thermodynamic hydrate inhibitors (THIs) are mainly based on organic solvents such as methanol, polyethylene oxide (PEO), polyethylene glycol (PEG), and conventional salts such as sodium chloride (NaCl), potassium chloride (KCl). THIs shift

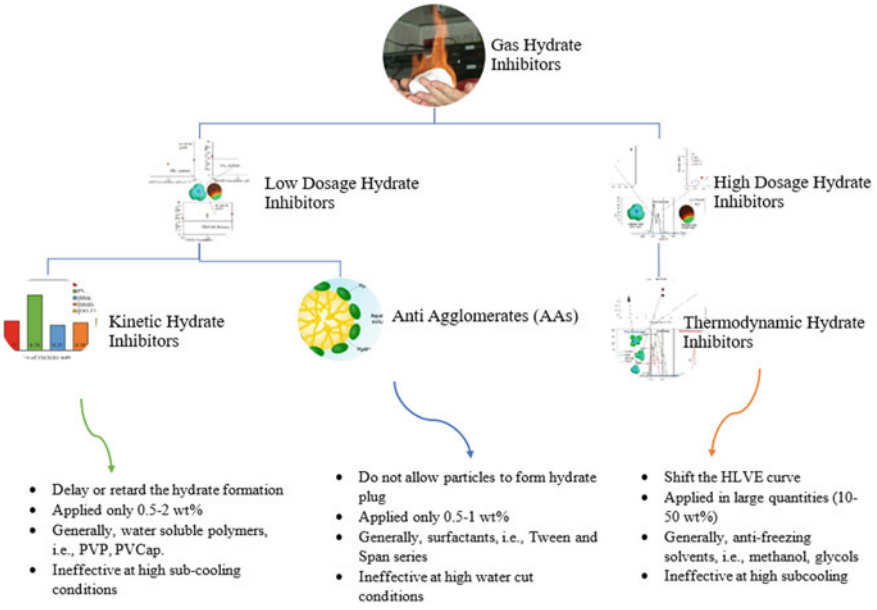

Fig. 2.1 Different types of hydrate inhibitors applied in petroleum pipelines

the hydrate equilibrium curve towards lower temperature and higher-pressure regions and hence keeping the system out of hydrate formation region [15, 18–21].

Organic solvent-based particles usually disrupt the activity of water via hydrogen bonding ability with water molecules. The hydrogen bonding ability of organic solvent is attributed to the presence of hydroxyl [OH^-] groups such as ethylene glycol and alcohols. While salts like NaCl or KCl are also able to induce this behaviour due to the presence of ions, known as the Coulombic effect, the Coulombic effect is induced due to the presence of positive (cations) and negative (anions) charged particles, which overcome the hydrogen bonding, network of water molecules. Increasing the concentration of this results in more hydrogen bonding disruption among the gas and water molecules, which decelerates further hydrate formation resulting in more hydrate-free zone.

The typical example was presented by the Koh and co-worker [23] 50 miles long natural gas pipeline from well head to production platform for the deep water field located in the Gulf of Mexico. Thermodynamic inhibitors such as methanol, in this case, are added to the pipeline at different mass percentages to ensure the operating condition is set outside the hydrate formation region. The degree of shifting of the hydrate equilibrium curve in hydrate-forming regions to the hydrate-free regions describes the inhibition impact of methanol.

In contrast, the produced gas contains significant amounts of water formation, which contains various types of salts at different concentrations. The presence of salts reduces the ability of gas hydrate formation, i.e. works as an inhibitor. However, in

most of the deep water cases, saline water inhibition is insufficient; therefore, aqueous solution of organic inhibitor (anti-freezing solvents) such as methanol, mono ethylene glycol (MEG) is injected into the pipeline. In comparison, among the inhibitors, the methanol is the most effective inhibitor due to the presence of two hydroxyl [OH^-] groups along with the shortest alkyl chain radical methyl in its structure. However, MEG is also frequently used in the industry due to the less volatility and higher density in comparison with methanol.

These applications in the pipeline are expensive (regarding operational cost) and are used in quite high concentrations. At higher subcooling conditions, sometimes up to 40 wt% or more is required for efficient inhibition (specifically four Barrels (bbls) of methanol injection for every six bbls of produced water) [23]. According to Carroll [24], methanol mixed with liquefied petroleum gas (LPG) components (Propane and mixed butane) forms azeotropes and becomes difficult to separate with simple distillation. The addition of methanol may also cause corrosion problems in the pipelines and environmental prohibitive [25]. These led to the discovery of low dosage hydrate inhibitors (LDHIs) in the early 1990s.

2.1.2.2 Low Dosage Hydrate Inhibitors (LDHIs)

The history of LDHIs began from the early 1970s when a Russian engineer named Kuliev, who was facing gas hydrate complications in his gas wells. He tried small quantities of commercial surfactants on the wells, and surprisingly, revealed that the gas hydrate problems were resolved [12]. Although Kuliev was unable to understand the mechanism of mitigation, nevertheless, it led to the discovery of LDHIs.

The advanced hydrate mitigation strategies are moving from hydrate elimination to hydrate managements with LDHIs. LDHIs are used in distinctly fewer quantities, to be precise 0.5–2.0 wt% of water cuts. This means LDHIs required in less order of magnitude (wt%) compared to thermodynamic inhibitors (10–50 wt%) for safe operation under comparable subcooling conditions. Such a hefty decrease in inhibitor requirements offers the opportunity of major OPEX and CAPEX savings. Moreover, since LDHIs are non-volatile, they provide the added benefits of actually condensing the environmental impact. Therefore, they are more economical, environmentally benign and attractive for industrial perspective. They are non-volatile and relatively environmentally friendly and are further divided into kinetic hydrate inhibitors (KHIs) and anti-agglomerates (AAs). KHIs are water-soluble polymers such as polyvinylpyrrolidone PVP and polyvinylcaprolactam PVCap; whereas, AAs are mostly surfactants molecules [26]. KHIs are discussed extensively in the next section.

Kinetic Hydrate Inhibitors (KHIs)

Kinetic hydrate inhibitors (KHIs) have been used commercially since 1995. KHIs inhibit gas hydrate formation by delaying hydrate nucleation time or induction time

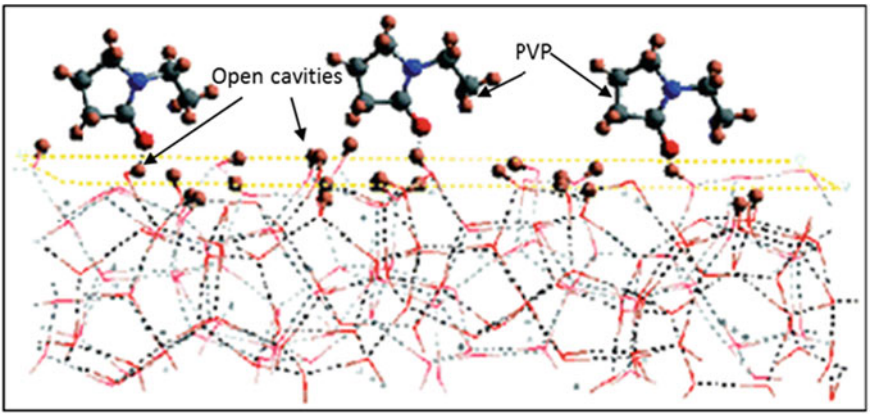

Fig. 2.2 Adsorption of the monomer unit of PVP on the {111} crystal surface of sI hydrate obtained from Monte Carlo simulation

[27, 28]. They are used in low concentrations usually below 2 wt%. KHIs are mainly based on water-soluble polymers such as PVP and PVCap. However, ILs anti-freezing proteins (AFPs) and biomolecules had also used [12, 29].

The two fundamental KHI mechanisms reported by Sloan et al. [2] are that KHIs inhibit hydrate nuclei particles from reaching a critical size for spontaneous growth through the disturbance of the local water structure via hydrophobic interactions. Secondly, KHIs condense or prevent further hydrate growth process by captivating onto freshly grown hydrate crystals. The (alkyl) groups in KHIs imitate small hydrocarbon guest molecules and intermingle with open cavities on the hydrate surface. Figure 2.2 shows the absorption of dimer units of PVP on CH_4 hydrate crystal through hydrogen bonding at hydrate growth sites depending on the type of hydrate gas present [30].

As can be perceived from Fig. 2.2, the PVP perfectly follows the mechanism proposed by Sloan et al. [1]. It adsorbs on the open cavities of water, hence providing steric hindrances to the gas and water interaction via hydrophobic interactions.

Important factors that affect the performance of KHIs are the subcooling temperature (ΔT = temperature below the equilibrium temperature) in the system and pressure. Most often, KHIs perform poorly at higher subcooling and pressures. The effective subcooling temperature of many KHIs is between 7 and 10 K indicating limitations of their use in deep water field applications [2].

Moreover, the new type of KHIs also evolves in the form of hyper-branched polymers, which are relatively non-toxic, cheaper, and biodegradable KHIs compared to conventional KHIs (PVP or PVCap). Hyper-branched polymers possess a combination of anti-agglomerates (AAs) and kinetic inhibitor properties. The reason behind these dual properties is lying in their structure. They are made by condensing of dialkanolamine with a cyclic acid anhydride. This provides a polymer with [OH–] groups at the tips. The three reactive groups of dialkanolamine caused the hyper-branching in the polymer. Moreover, by addition of the third molecule, i.e.

secondary amine to the reaction mixture efficiently modified to tips of the polymer to hydrophilic which is a criterion for the gas hydrate inhibition.

Anti-agglomerates (AAs)

Typical anti-agglomerates are surfactants and quaternary ammonium salts (QAS) which are a longer chain which composes of hydrophilic and hydrophobic ends. The hydrophilic (anionic) tail is attached to the water molecules; whereas, the hydrophobic (cationic part includes long chain) head is dissolved in the oil or gas phase. Initially, at the end of the 1993, the Shell Oil Company patented their results for quaternary ammonium surfactants with two or three n-butyl, n-pentyl, and isopentyl groups, which showed exceptionally well anti-agglomeration characteristics [12]. Among QAS, tetrapentylammonium bromide (TPAB) has been reported as hydrate inhibitor in the category of anti-agglomerates [12]. Twin-tailed quaternary AAs were also developed which included tetraalkylammonium salts. Among these salts, dicocoyldibutylammonium bromide was most notably applied for field testing by Dutch Shell team; however, it did not perform up to the expectations regarding its biodegradability. Huo et al. [31] used some of the commercial surfactants, namely Span 20, Span 40, Span 60, and Span 80 in their research. Their finding revealed that studied surfactants are able to keep the hydrate particles suspended at the conditions of 277 K and 8.20 MPa. Their performances were also compared with dodecyl-2-(2-caprolactamyl) ethanamide (synthesized AA). However, the synthesized chemical showed better dispersion at higher water cut condition, i.e. 0.75 wt%. The endeavour of developing cost-effective LDHIs for the oil industry leads the Kelland and coworker [32] to extend the AAs research by utilizing polypropoxylates. Polyamine polypropoxylates and other branched polypropoxylates dispersed gas hydrates in a hydrocarbon fluid as long as the fluid was well agitated.

2.1.3 Recent Developments in Gas Hydrate Inhibitors

The oil and gas industry is constantly on the lookout for chemicals that possess better qualities, such as being of a relatively environmentally friendly nature, and less volatility to avoid vapour losses, especially in the case of THI inhibitors. Similarly, the commercial gas hydrate inhibitors (THIs or KHIs) independently are not sufficient to satisfy the prerequisites of the oil and gas industry. For that reason, the quest for new gas hydrate inhibitors is vigorously ongoing for discovering chemicals that hold both (THI and KHI) qualities and could work as dual functional inhibitors. Therefore, the focus had shifted towards the different kind of chemicals, especially, amino acids [33–36] and ionic liquids (ILs) [25, 37–40] as potential dual functional hydrate inhibitors. This section mainly discusses the available literature on the advances of the ILs, besides it also provides an overview on amino acids too as the gas hydrate inhibitors.

2.1.3.1 Innovative Gas Hydrate Inhibitors

The search for innovative gas hydrate inhibitors is vigorously enduring owing to the confines mentioned above for commercial inhibitors. Recently, environmentally friendly, naturally occurring biomolecules known as amino acids are also reported to be promising gas hydrate inhibitors.

Amino acids are biologically organic compounds, which are the building blocks of proteins. There are 20 naturally occurring amino acids found in a living organism. All amino acids consist of an amine ($–NH_2$) and carboxylic acid (–COOH) functional groups as an essential constituent. Additionally, the unique side chain, ranging from a polar alkyl chain (hydrophobic) to a positively or negatively charged moiety (hydrophilic) describes their physical and chemical properties [41–44]. Amino acids can also be classified based on the side chain group (R-group), as they have different physicochemical properties and interact with the water very differently [43]. The general structure of amino acid is presented in Fig. 2.3.

The hydrate–liquid–vapour equilibrium curve of CO_2 hydrates three amino acids (glycine, alanine, and valine) was initially reported in 2011 by Sa et al. [45] at 0.1 and 0.5 mol% concentrations. The results suggested that all the studied amino acids show significant inhibition for CO_2 hydrates. The increasing order of inhibition of amino acids was found to be valine < alanine < glycine. The thermodynamic inhibition impact increased with increasing hydrophobicity of amino acids. Sa et al. [46] further examined the natural hydrophobic amino acids as novel KHIs. Amino acids with lower hydrophobicity were found to be better KHIs to delay nucleation and retard growth, which disrupts the hydrogen-bonded network of water, whereas, those with higher hydrophobicity strengthened the local water structure.

Most recently, Bavoh et al. [34, 47] reported that the amino acids could provide a similar magnitude of inhibition for both CH_4 and CO_2 systems. The overall inhibition impact of 10 wt% amino acids was reported in the increasing order arginine (1.03 K) < serine (1.21 K) < proline (1.44 K) < alanine (1.64 K) < glycine (1.83 K) for both CH_4 and CO_2 hydrates. It was concluded that the shorter side chain length of amino acids exhibited efficient inhibition since glycine had the lowest side chain and arginine possessed the largest side chain among the studied amino acids. However, there is limited literature on the effects of amino acids on the thermodynamics of CH_4 and CO_2 hydrate inhibition in the open literature.

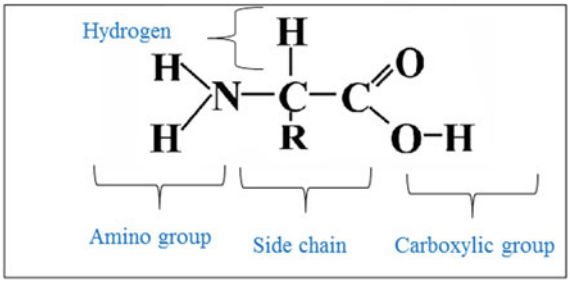

Fig. 2.3 Basic structure of amino acid

2.1.3.2 Ionic Liquids

Ionic liquids (ILs) or room temperature ionic liquids (RTILs) are molten ionic salts composed of a poorly coordinating sizeable organic cation combined with an organic or inorganic anion, which leads to low melting temperature (lower than 373 K). The ionic nature of these liquids offers numerous unique and attractive physical and chemical characteristics encouraging various applications. The main characteristics of most ionic liquids include high thermal stability, negligible vapour pressure, non-flammability, and high solvating capacity for organic, inorganic, and organometallic compounds [48]. Depending on the different cation structures, ILs can be divided into various families which include imidazolium, ammonium, phosphonium, pyridinium, triazolium, and thiazolium. Figure 2.4 shows the various cations structures of different families of ILs.

The more straightforward synthesis (to design ILs with specific functionalities) is one of the greatest attractions together with the other well-known properties compared to the molecular counterparts (organic solvents). The ILs possess distinct advantages over conventional organic solvents such as non-volatility, lower interfacial tensions, and non-flammability together with relatively less toxic nature [49]. Together with their tunable properties, ILs can form extended hydrogen bonds and are highly structured in the liquid state [50]. Attributed to the reasons mentioned above, ILs are attracting more significant interest in varied industrial applications. Some of the core areas are as catalysts and solvents in organic reactions, biomass conversions biological applications, in energy and fuels applications, as functional materials, in electrochemical applications [40, 50–61]. Moreover, ILs also considered as a potential alternative to the conventional hydrate inhibitors attributed to

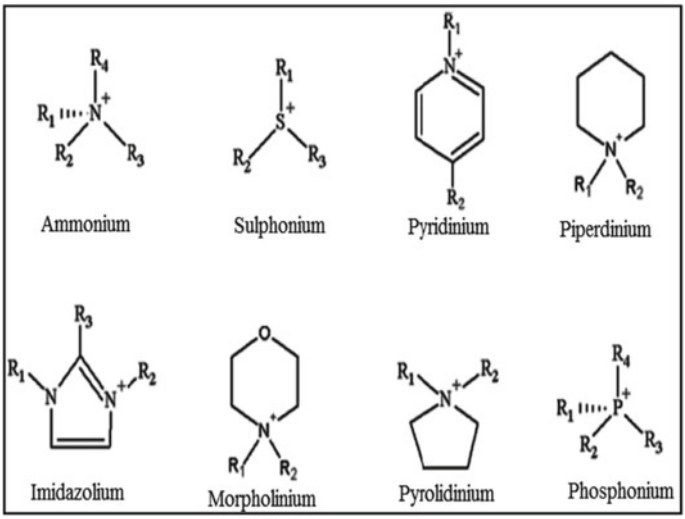

Fig. 2.4 Common cationic structures of different ILs families

their aforementioned excellent physicochemical properties together with the ability to form efficient hydrogen bonding with water [7, 40, 62, 63].

ILs showed an ample potential to work as dual functional gas hydrate inhibitors, as they possess the ability to perform adequate hydrogen bonding with water molecules, which attributed in gas hydrate inhibition. For effective hydrate thermodynamic inhibitions, firstly, ILs must be hydrophilic; otherwise, if the IL is hydrophobic, it tends to reside in a distinct phase, therefore, unable to disrupt hydrogen bonding network of water molecules. Secondly, individual functional groups such as oxygen [O^-] or hydroxyl [OH^-] groups in the structure of the ILs create further intermolecular (hydrogen bonding) disruptions with water molecules, thus effectively prevent the gas hydrate formations [25].

ILs are used as thermodynamic and LDHIs for methane, carbon dioxide, and natural gas hydrates [25, 62, 64, 65]. The application of ILs as gas hydrates inhibitors is relatively a new research area in the gas hydrate field. Xiao and Adhirama [62] initiated the research of ILs as gas hydrate inhibitors in 2009. They examined imidazolium-based ILs and found better results than PEO for both THI and KHI inhibition in the presence of CH_4 hydrates. They found that ionic liquids showed thermodynamic inhibition, and at the same time delay hydrate formation by slowing down the hydrate nucleation rate. This dual functionality was endorsed due to their strong electrostatic charges and ability to form hydrogen bonding with water. Therefore, it provides basis to that ILs perhaps work as both thermodynamic and kinetic inhibitor.

Xiao et al. [66] further reported that imidazolium-based ILs with halides anions showed significant dual functional performance as the kinetic and thermodynamic inhibitors on the methane hydrate formation. Their effects on the shift in equilibrium curve and induction time of CH_4 hydrate formation were measured in a high-pressure microdifferential scanning calorimeter (micro DSC). Their study revealed that ILs have strong electrolyte charges and are capable of hydrogen bonding with the water molecule which causes the shift in HLVE conditions to a lower temperature at a given pressure. On the other hand, due to compelling surface-active phenomenon, they were able to slow down the hydrate nucleation growth rates as well. In another article, they extended the study to six dialkyl imidazolium halide ILs and among all [EMIM][Cl] was reported to be the most effective thermodynamic inhibitor [67].

In general, the ILs show inhibition properties suitable for hydrate dissociation in pipelines. It may address the need for a prosperous solvent for flow assurance issues. Thus, ILs with extraordinary properties offer a unique opportunity to study its potential application as gas hydrate inhibitors [25]. Tariq et al. [25] reviewed ILs extensively for dual functional gas hydrate inhibitors which have led to a certain structure-activity relationship of ILs for gas hydrate inhibition. They concluded that the efficiency of ILs as thermodynamic gas hydrate inhibitors decreases with increasing chain length of the cation [25]. This phenomenon was observed as the increase in alkyl chain length increased the hydrophobicity of ILs. Moreover, the substitution of OH^- groups in the cation enhances the performance of gas hydrate inhibition. Since, the IL with OH-substituted cation can easily be incorporated into the hydrogen bonding network of water, thus making the gas hydrate formation difficult.

The synergist effect usually arises due to the combination of two or more gas hydrate inhibitors and produces an inhibition effect greater than the sum of their individual inhibition effects. The existing KHIs used alone could not encounter the requirement of gas hydrate inhibition under very high subcooling conditions encountered in deep water or ultra deep water during intensive drilling operations. Therefore, many studies had reported on the development of new KHIs and synergists for KHIs [25, 65, 68]. For that reason, a combination of thermodynamic and kinetic inhibitors is required to give better performance in addition to being economic and eco-friendly elucidation. Richard and Adidharma [37] evaluated the synergistic effects of mixtures of ILs containing [EMIM][Cl] and [EMIM][Br] over methane hydrates and found promising results in the presence of MEG at higher pressures. However, at a lower pressure, it is observed that [EMIM][Cl] and MEG do not show any synergistic effects. Table 2.1 presents the overview of the previous studies conducted on the dual functionality of various ILs–gaseous systems.

From Table 2.1, it is evident that the majority of the studied ILs systems dealt with pure methane system. Relatively, lesser studies reported the inhibition impact of ILs in the presence of CO_2 hydrates. There are very few reports that deal with inhibition performance of ILs with the mixed gas hydrates since most of the studied ILs system is based on pure gases (CO_2 or CH_4) hydrates. The literature data for ILs–mixed gas hydrates inhibitors systems are to a certain extent insufficient. The most of the mixed gas–ILs hydrates studies focused on the potential hydrate applications by using ILs as hydrate promoters for gas storage or gas capturing or desalination of saline water purposes [4, 80–84]. Tariq et al. [85] applied choline-chloride ionic liquid as THI inhibitor for Qatari natural gas (QNG) mixture and found that 5 wt% of choline-chloride reduced the equilibrium temperature up to 1.56 K at constant pressure. Likewise, Qureshi et al. [65] studied the Quantary mixture of natural gas (QNG)) in the presence of pyrrolidinium-based ILs for dual functional hydrate inhibition. In the presence of 5 wt% [PMPy][Cl], the phase boundary shifted up to 1 K while it slightly increased the induction time compare to the pure water system. On the other hand, [PMPy][Cl] provided efficient kinetic inhibition as a synergist with PEO by doubled the induction time at 1 wt% concentration. Moreover, Mohamed et al. [86] recently reported the THI behaviour of the 1 and 5 wt% choline-based ILs (namely choline bistriflamide [Cho][Ntf2], choline-chloride [Cho][Cl], and choline acetate [Cho][Ac]) for CH_4 and Qatari natural gas (QNG) systems, respectively. Results revealed that the 5 wt% systems were able to shift average suppression temperature (T) up to 1.5 K for QNG system.

Lee et al. [87] evaluated the pyrrolidinium-based ILs as kinetic hydrate inhibitors in the presence of the tetrafluoroborate [$BF4^-$] anions in synthetic natural gas system. The studied ILs were 1-hydroxyl-1-ethyl-1-methyl pyrrolidinium tetrafluoroborate ([HEMP][BF_4]), 1-butyl-1-methyl pyrrolidinium tetrafluoroborate ([BMP][BF4]), 1-hydroxyl-1-methyl pyrrolidinium tetrafluoroborate ([HMP][BF_4]), and 1-hexyl-1-methyl pyrrolidinium tetrafluoroborate ([OMP][BF^4]). The results revealed that [HEMP][BF4], which contained the hydroxyl functional group in the cation, acted as an auxiliary group which performed much better than the other studied ILs by delaying the induction time from 14 min (pure water) to 89 min at 3 wt% conditions.

Table 2.1 Dual functional ionic liquids systems applied for gas hydrate mitigation

Ionic liquids	System	Conc. (wt%)	Test	(ΔT) K	Relative inhibition power (RIP)	References
[BMIM][BF_4]	CO_2	0.0008–0.6[a]	THI/KHI	0.91	0.65	[70, 71]
[BMIM][BF_4]	CH_4	0.1–10	THI/KHI	0.72	0.90	[62]
[EMIM][BF_4]	CH_4	0.1–10	THI/KHI	0.52	0.94	[62]
[EMIM][BF_4]	CO_2	0.10–1[a]	THI/KHP	1.11	−2.09	[72]
[BMIM][BF_4]	CH_4	0.6–7	THI/KHI	0.74	0.79	[71]
[EMIM][Cl]	CH_4	10.1	THI/KHI	1.01	0.75	[66]
[BMIM][Cl]	CH_4	10.1	THI/KHI	0.58	0.80	[66]
[EMIM][Br]	CH_4	10.1	THI/KHI	0.84	0.82	[66]
[BMIM][Br]	CH_4	10.1	THI/KHI	0.46	0.85	[66]
[PMIM][I]	CH_4	10.1	THI/KHI	0.67	0.72	[66]
[BMIM][I]	CH_4	10.1	THI/KHI	0.34	0.93	[66]
[EMIM][CF_3SO_3]	CH_4	0.1–10	THI/KHI	0.17	0.1	[62]
[BMIM][CF_3SO_3]	CH_4	0.01	THI/KHI	0.61	0.35	[12]
[BMIM] [CH_3SO_4]	CH_4	0.6–7	THI/KHI	1.21	0.5	[71]
[BMIM][CH_3SO_4]	CH_4	0.5	KHI	–	5.18	[73]
[EMIM][$C_2H_5SO_4$]	CH_4	10.10	THI/KHI	0.25	0.56	[61, 74]
[EMIM][$C_2H_5SO_4$]	CH_4	0.5	KHI	–	0.52	[73]
[EMIM)][$N(CN)_2$]	CH_4	0.1–10	THI/KHI	0.58	0.65	[62]
[BMIM][CH_3SO_4]	CH_4	10.1	THI/KHI	0.58	0.38	[28, 75, 76]
[OH-EMIM][Br]	CH_4	10.1	THI/KHI	0.96	0.45	[28, 75, 76]
[EMMor][Br]	CO_2	10	THI	1.72	–	[77]

(continued)

Table 2.1 (continued)

Ionic liquids	System	Conc. (wt%)	Test	(ΔT) K	Relative inhibition power (RIP)	References
[EMMor][BF_4]	CO_2	10	THI	1.54	–	[77]
[OH-EMMor][BF_4]	CH_4	1	THI/KHI	0.7	0.95	[78]
[EMPip][Br]	CO_2	0.1	THI	1.32	–	[77]
[EMPip][BF_4]	CO_2	0.1	THI	1.20	–	[77]
[Cho][iBut]	CH_4	1	THP/KHP	– 0.32	−0.002	[79]
[Cho][Hex]	CH_4	1	THI/KHP	−0.46	0.002	[79]
[TMA][Ac]	CH_4	1	THP/KHP	−0.40	−0.007	[79]
[Cho][But]	CH_4	1	THP/KHI	−0.56	0.05	[79]
[Cho][Oct]	CH_4	1	THP/KHI	−0.67	0.07	[79]
[Cho][iBut]	CH_4	5	THI/KHI	0.49	0.09	[79]
[Cho][Hex]	CH_4	5	THI/KHI	0.07	0.14	[79]
[TMA][Ac]	CH_4	5	THI/KHI	0.87	0.12	[79]
[Cho][But]	CH_4	5	THI/KHI	0.31	0.13	[79]
[Cho][Oct]	CH_4	5	THI/KHI	0.02	0.05	[79]

[a]Concentration in mole%

The performance was further enhanced when [HEMP][BF_4] utilized as synergist with PVCap (0.5 wt% PVCap + 1wt% [HEMP][BF_4]), where no hydrate formation occurred up to 24 h [87].

According to the literature works above, most of the ILs studies focused on CH_4 hydrate inhibition via imidazolium-based ILs [69, 75, 76, 88]. Very few researchers have studied the effects of other gases and families of ILs [65, 89]. Primarily, AILs on gas hydrate mitigation [19, 48–51] were found to be limited and perhaps inadequate for both pure and mixed gas systems [40, 76, 78, 89]. Similarly, we believe that none of the preceding studies dealt dual functional impact of ILs on the binary mixture of CH_4 and CO_2 hydrates as well. In the same way, the information related to dual functionality of ILs in the presence of CH_4 hydrates is not sufficiently available in the literature, and the situation even worsened when dealing with CO_2 or mixed gas hydrates [25].

Ammonium-based ILs have received some attention in the hydrate research community as they exhibit more hydrate inhibition potentials due to the presence of nitrogen donor atom in their structures [91]. Also, they provide much better or greener potentials than imidazolium-based ILs [92, 93]. Ammonium-based ILs (AILs) have various applications across different industries, such as in electrochemistry applications, heavy metal removals, organic syntheses, nanomaterial syntheses, analytical application, mixed gas separation, and gas storage purposes [94].

For gas hydrate inhibitors, Li et al. [67] initially examined the THI influence of the tetramethylammonium chloride ([TMA][Cl]) with dialkyl imidazolium chloride ILs for CH_4 hydrates. Among the studied ILs (IMILs and AILs), the [TMA][Cl]) showed better inhibition impact on CH_4 hydrate as compared to other studied ILs. Keshavarz and co-workers [95] performed the experimental and modelling studies on ILs including [TEA][Cl] from AILs family in 2013. The TEACl was able to shift the HLVE curve towards lower temperature and pressure conditions up to 0.72 K. Recently, Tariq et al. [79] evaluated six (6) AILs as dual functional inhibitors (DFI) for CH_4 gas hydrate. Their findings suggested that all studied AILs exhibited CH_4 hydrate thermodynamic inhibition behaviour at moderate pressure conditions. However, at higher pressures above 7.0 MPa, the inhibition impact seems to be reduced, and some of the ILs behaved as thermodynamic promoters. Among the studied AILs, tetramethylammonium acetate ([TMA][A]) was identified as the best THI, while choline octanoate ([Ch][Oct]) efficiently behaved as a KHI.

The application of AILs as gas hydrate inhibitors are still at the very early stages, and the effects of AILs on hydrate formation are not entirely implicit, with limited studies reported in an open literature on the thermodynamic and kinetic inhibition impact of CO_2 hydrate in the presence of AILs [25]. A critical review of relevant literature related to gas hydrate inhibition is summarized which briefly indicates the issues and challenges in gas hydrate mitigation (Research Gaps) which are tabulated in Table 2.2.

Additionally, the previous kinetic studies performed at less moderate pressures were less than 3.6 and 9 MPa for CO_2 and CH_4, respectively [100]. Usually, authors report the hydrate onset temperature and total gas consumed to determine the formation kinetics [101]. Also, the majority of the kinetics studies for ILs systems are limited and only the induction time is reported [6, 15]. Most of the reported ILs-Kinetic systems dealt with less than 1 wt% systems; above 1 wt% concentrations has not been reported in the literature, and thus their behaviours are either unknown or less understood [25, 102, 103]. Therefore, it is critical to fill the research gaps, as their understanding is essential for the implementation of AILs in practical application.

As a conclusion, the reported literature on gas hydrate inhibition has been reviewed to identify the current focus on gas hydrate inhibition. The basic fundamental concepts on gas hydrate formation and its applications were presented. The hydrates in oil and gas pipelines were discussed in detail including conventional gas hydrate inhibitors together with their associated mechanisms of thermodynamics and kinetics inhibitor. Also, their limitations and the need for new inhibitors have been stated.

Table 2.2 Summary of literature on gas hydrate studies

Author	Remarks
Koh et al. [3] Sloan and Koh [2] Koh [22]	• Conventional THIs are volatile, environmentally unfriendly, and expensive due to higher concentration demand • KHIs are ineffective at higher subcooling and start down conditions • AAIs are ineffective at higher water cut conditions
Sa et al. [45] Talaghat [97] Bhattacharjee et al. [98] Sa et al. [99] Bavoh et al. [34]	• Amino acids were used as potential biocompatible dual functional (KHI and THI) inhibitors • The inhibition impact was found to be affected by the hydrophobicity and side chain length of AAs [67] • However, AAs still have not revealed substantial gas hydrate inhibition impact confines their use for industrial purposes
Xiao and Adidharma [62]	• Ionic liquids are introduced as dual functional inhibitors (both THI and KHI) in 2009 by using six IMILs for methane hydrates • Results revealed that studied ILs were able to act as THI inhibitors together and they are able to hold the hydrate nucleation delay as well
Sabil et al. [75]	• Evaluated the THI performance of nine IMILs and correlated it with electrical conductivity (k) and found significant correlation among ΔT and k • The authors further reported that considered ILs were not participated in hydrate crystalline structure by calculating the enthalpy of hydrate dissociations from Clausius–Clapeyron equation

(continued)

Table 2.2 (continued)

Author	Remarks
Tariq et al. [25]	• The authors systematically reviewed the inhibition performance of ILs for both systems (THIs/KHIs) • They highlighted that most of the research conducted on ILs are restricted to imidazolium-based ionic liquids only, insufficient findings reported for other ILs families • They further highlighted that decidedly fewer studies focused beyond CH_4 hydrates especially none of the previous study dealt with mixed gas hydrates or natural gas hydrates in the presence of ILs
Nashed et al. [28]	• This study reported the KHI performance of nine IMILs at 7.1 MPa pressure for CH_4 hydrates and found only four ILs were able to delay hydrate formations • The reason for effective KHI found in longer alkyl chain ILs which provide better steric hindrance facilitating the prevention of hydrate crystal growth • They further applied Avrami model and reported that the hydrate crystallization partially occurred due the diffusion mechanism
Tariq et al. [79]	• In this work, Tariq et al. [49] evaluated five AILs first time as dual functional hydrate inhibitors for CH_4 hydrate • Their study revealed that THI inhibition of AILs was highly dependent on pressure conditions (At lower-pressure range of 3.50–6.50 MPa, all the studied AILs worked as THI inhibitors; while at a higher-pressure range of 6.6–12.0 MPa, the inhibition impacts found to be lowered for CH_4 hydrates) • Additionally, the studied AILs which have the larger alkyl chains (namely TMAA and Ch-Oct) were able to delay the hydrate nucleation (induction time) as well
Qureshi et al. [65]	• Qureshi et al. [33] studied dual functionality of the pyrrolidinium-based ILs (1-Methyl-1-Propylpyrrolidinium Triflate [PMPy][Triflate] and propylpyrrolidinium chloride [PMPy][Cl]) as Quantary mixture on Qatar natural gas system • Their outcomes revealed that both ILs displayed dual functional impact. At 5 wt% concentration, PMPy-Cl is able to suppress the phase boundary (ΔT) up to 1.0 K while marginally increases the induction time compare to pure water [33]
Tariq et al. [85]	• In this recently reported work, choline-chloride (Ch-Cl) (from AIL family) applied with and without N_2 at low concentrations (1–5 wt%) as THI inhibitor for Qatari natural gas mixture • Found results suggested that 5 wt% of Ch-Cl is able to reduce ΔT up to 1.36 K whereas 1 wt% displayed minor inhibition (ΔT) up to 0.5 K, respectively • When 5 wt% Ch-Cl applied in the presence of N_2 as a synergist, the ΔT is found to be 5.5 K shift perhaps due to the higher pressure required for N_2 hydrates [1]

According to the above literature survey, it can be perceived that various chemicals such as salts or organic solvents are efficient for thermodynamic inhibition only; however, water-soluble polymers or biopolymers possess kinetic inhibition behaviour. Moreover, the chemicals such as ionic liquids and amino acids hold the dual functional tendency. Therefore, future research works should focus on these types of innovative chemicals especially on ionic liquids since they are tuneable chemicals with excellent properties ideal for gas hydrate inhibitors.

References

1. Hammerschmidt EG. (1934) Formation of gas hydrates in natural gas transmission lines. Ind Eng Chem 26:851–855
2. Dendy Sloan E, Koh CA (2008) Gas hydrates of natural gases. In: 3rd edn. CRC Press LLC, London; New York, 2000 Corporate Blvd., N.W., Boca Raton, FL 33431, USA Orders from the USA and Canada (only) to CRC Press LLC
3. Koh CA, Sloan ED, Sum AK, Wu DT (2011) Fundamentals and applications of gas hydrates. Ann Rev Chem Biomolec Eng 2:237–257
4. Khan MS, Bavoh CB, Partoon B, Lal B, Bustam MA, Shariff AM (2017) Thermodynamic effect of ammonium based ionic liquids on CO_2 hydrates phase boundary. J Mol Liq 238:533–539
5. Khan MS, Lal B (2019) Pre-screening of ionic liquids as gas hydrate inhibitor via application of COSMO-RS for methane hydrate. Ion Liq Prog Synth Charact Appl
6. Khan MS, Lal B, Keong LK, Ahmed I (2019) Tetramethyl ammonium chloride as dual functional inhibitor for methane and carbon dioxide hydrates. Fuel 236:251–263
7. Khan MS, Lal B, Shariff AM, Mukhtar H (2019) Ammonium hydroxide ILs as dual-functional gas hydrate inhibitors for binary mixed gas (carbon dioxide and methane) hydrates. J Mol Liq 274:33–44
8. Khan MS, Bavoh CB, Lal B, Keong LK, Mellon NB, Bustam MA et al (2018) Application of electrolyte based model on ionic liquids-methane hydrates phase boundary. IOP Conf Ser Mater Sci Eng 458:012073
9. Erfani A, Varaminian F, Muhammadi M (2013) Gas hydrate formation inhibition using low dosage hydrate inhibitors. In: 2nd national Iranian conference on gas hydrate (NICGH)
10. Koh CA, Westacott RE, Zhang W, Hirachand K, Creek JL, Soper AK (2002) Mechanisms of gas hydrate formation and inhibition. Fluid Phase Equilib 194:143–151
11. Samimi A (2012) Preventing hydrate formation in gas transporting pipe lines with synthetic inhibitors. Int J Sci Investig Fr 1:48–150
12. Kelland MA (2006) History of the development of low dosage hydrate inhibitors. Energy Fuels 20:825–847
13. Kassim Z, Khan MS, Lal B, Partoon B, Shariff AM (2018) Evaluation of tetraethylammonium chloride on methane gas hydrate phase conditions. IOP Conf Ser Mater Sci Eng 458:012071
14. Khan MS, Bavoh CB, Partoon B, Nashed O, Lal B, Mellon NB (2018) Impacts of ammonium based ionic liquids alkyl chain on thermodynamic hydrate inhibition for carbon dioxide rich binary gas. J Mol Liq 261:283–290
15. Foo KS, Khan MS, Lal B, Sufian S (2018) Semi-clathratic impact of tetrabutylammonium hydroxide on the carbon dioxide hydrates. IOP Conf Ser Mater Sci Eng 458:012060
16. Bavoh CB, Khan MS, Lal B, Bt Abdul Ghaniri NI, Sabil KM (2018) New methane hydrate phase boundary data in the presence of aqueous amino acids. Fluid Phase Equilib 478:129–133
17. Bavoh CB, Lal B, Khan MS, Osei H, Ayuob M (2018) Combined inhibition effect of 1-Ethyl-3-methy-limidazolium chloride + glycine on methane hydrate. J Phys Conf Ser 1123:012060

18. Khan MS, Lal B, Keong LK, Sabil KM (2018) Experimental evaluation and thermodynamic modelling of AILs alkyl chain elongation on methane riched gas hydrate system. Fluid Phase Equilib 473:300–309
19. Nashed O, Dadebayev D, Khan MS, Bavoh CB, Lal B, Shariff AM (2018) Experimental and modelling studies on thermodynamic methane hydrate inhibition in the presence of ionic liquids. J Mol Liq 249:886–891
20. Khan MS, Lal B, Bavoh CB, Keong LK, Bustam A (2017) Influence of ammonium based compounds for gas hydrate mitigation: a short review. Indian J Sci Technol 10:1–6
21. Bavoh CB, Lal B, Nashed O, Khan MS, Lau KK, Bustam MA (2016) COSMO-RS: an ionic liquid prescreening tool for gas hydrate mitigation. Chin J Chem Eng 24:1619–1624
22. Koh CA (2002) Towards a fundamental understanding of natural gas hydrates. Chem Soc Rev 31:157–167
23. Patel ZD, Russum J (2009) Flow assurance: Chemical inhibition of gas hydrates in deepwater production systems. Offshore Magzine 4
24. Carroll J (2014) Natural gas hydrates a guide for engineers. In: 3rd edn. Elsevier
25. Tariq M, Rooney D, Othman E, Aparicio S, Atilhan M, Khraisheh M (2014) Gas hydrate inhibition: a review of the role of ionic liquids. Ind Eng Chem Res 53:17855–17868
26. Boyun G, Shanhong S, Ghalambor A, Tian RL (2014) Offshore pipelines design, installation, and maintenance. In: 2nd edn. Elsevier
27. Sloan D, Koh C, Sum AK, Ballard AL, Creek J, Eaton M et al (2010) Natural gas hydrates in flow assurance. Gulf Professional Publishing
28. Nashed O, Sabil KM, Ismail L, Japper-Jaafar A, Lal B (2017) Mean induction time and isothermal kinetic analysis of methane hydrate formation in water and imidazolium based ionic liquid solutions. J Chem Thermodyn 1–8
29. Ke W, Kelland MA (2016) Kinetic hydrate inhibitor studies for gas hydrate systems: a review of experimental equipment and test methods. Energy Fuels 30:10015–10028
30. Carver TJ, Drew MGB, Rodger PM (1995) Inhibition of crystal-growth in methane hydrate. J Chem Soc Trans 91:3449–3460
31. Huo Z, Freer E, Lamar M, Sannigrahi B, Knauss DM, Sloan ED (2001) Hydrate plug prevention by anti-agglomeration. Chem Eng Sci 56:4979–4991
32. Kelland MA, Svartås TM, Andersen LD (2009) Gas hydrate anti-agglomerant properties of polypropoxylates and some other demulsifiers. J Pet Sci Eng 64(1–4):1–10
33. Rufford TE, Smart S, Watson GCY, Graham BF, Boxall J, Diniz da Costa JC (2012) The removal of CO_2 and N_2 from natural gas: a review of conventional and emerging process technologies. J Pet Sci Eng 94–95:123–154
34. Bavoh CB, Partoon B, Lal B, Kok Keong L (2017) Methane hydrate-liquid-vapour-equilibrium phase condition measurements in the presence of natural amino acids. J Nat Gas Sci Eng 37:425–434
35. Sa J-H, Kwak G-H, Han K, Ahn D, Cho SJ, Lee JD, Lee K-H (2016) Inhibition of methane and natural gas hydrate formation by altering the structure of water with amino acids. Sci Rep 6:1–9
36. Roosta H, Dashti A, Mazloumi SH, Varaminian F (2016) Inhibition properties of new amino acids for prevention of hydrate formation in carbon dioxide-water system: Experimental and modelling investigations. J Mol Liq 215:656–663
37. Lim D, Park S, Ro H, Hyery JL, Minchul K, Huen K (2014) Thermodynamic and kinetic effect of a dual-function inhibitor on gas hydrate formation. Int Offshore Polar Eng 3:23–28
38. Shin BS, Kim ES, Kwak SK, Lim JS, Kim KS, Kang JW (2014) Thermodynamic inhibition effects of ionic liquids on the formation of condensed carbon dioxide hydrate. Fluid Phase Equilib 382:270–278
39. Lee W, Shin J-Y, Cha J-H, Kim K-S, Kang S-P (2016) Inhibition effect of ionic liquids and their mixtures with poly (N-vinylcaprolactam) on methane hydrate formation. J Ind Eng Chem 38:211–216
40. Kim K-S, Kang JW, Kang S-P (2011) Tuning ionic liquids for hydrate inhibition. Chem Commun 47:6341–6343

41. Vaitheeswaran S, Thirumalai D (2008) Interactions between amino acid side chains in cylindrical hydrophobic nanopores with applications to peptide stability. Proc Natl Acad Sci U S A 105:17636–17641
42. Vyas N, Ojha AK (2010) Interaction of alanine with small water clusters; Ala–(H2O)n (n=1, 2 and 3): A density functional study. J Mol Struct Theochem 940:95–102
43. Madeira PP, Bessa A, Álvares-Ribeiro L, Raquel Aires-Barros M, Rodrigues AE, Uversky VN et al (2014) Amino acid/water interactions study: a new amino acid scale. J Biomol Struct Dyn 32:959–968
44. Van Oss CJ (2003) Long-range and short-range mechanisms of hydrophobic attraction and hydrophilic repulsion in specific and aspecific interactions. J Mol Recognit 16:177–190
45. Sa JH, Lee BR, Park DH, Lee KH, Han K, Chun HD et al (2011) Amino acids as natural inhibitors for hydrate formation in CO_2 sequestration. Environ Sci Technol 45:5885–5891
46. Sa J-H, Kwak G-H, Lee BR, Park D-H, Han K, Lee K-H (2013) Hydrophobic amino acids as a new class of kinetic inhibitors for gas hydrate formation. Sci Rep 3:2428
47. Bavoh CB, Partoon B, Lal B, Gonfa G, Foo Khor S, Sharif AM (2017) Inhibition effect of amino acids on carbon dioxide hydrate. Chem Eng Sci 171:331–339
48. Kurnia KA, Quental MV, Santos LMNBF, Freire MG, Coutinho JAP (2015) Mutual solubilities between water and non-aromatic sulfonium-, ammonium- and phosphonium-hydrophobic ionic liquids. Phys Chem Chem Phys 17:4569–4577
49. Ratti R (2014) Ionic liquids: synthesis and applications in catalysis. Adv Chem 2014:1–16
50. Marsh KN, Boxall JA, Lichtenthaler R (2004) Room temperature ionic liquids and their mixtures—a review. Fluid Phase Equilib 219:93–98
51. Fallanza M, González-Miquel M, Ruiz E, Ortiz A, Gorri D, Palomar J et al (2013) Screening of RTILs for propane/propylene separation using COSMO-RS methodology. Chem Eng J 220:284–293
52. Vasantha T, Attri P, Venkatesu P, Rama Devi RS (2013) Ammonium based ionic liquids act as compatible solvents for glycine peptides. J Chem Thermodyn 56:21–31
53. Jork C, Kristen C, Pieraccini D, Stark A, Chiappe C, Beste YA et al (2005) Tailor-made ionic liquids. J Chem Thermodyn 37:537–558
54. Xu D, Yang Q, Su B, Bao Z, Ren Q, Xing H (2014) Enhancing the basicity of ionic liquids by tuning the cation-anion interaction strength and via the anion-tethered strategy. J Phys Chem B 118:1071–1079
55. Kärkkäinen J (2007) Preparation and characterization of some ionic liquids and their use in the dimerization reaction of 2-methylpropene
56. Zhou T, Chen LL, Ye Y, Chen LL, Qi Z, Freund H et al (2012) An overview of mutual solubility of ionic liquids and water predicted by COSMO-RS. Ind Eng Chem Res 51:6256–6264
57. Bashir H, Alhanash A (2012) Development of asymmetric ammonium-based room temperature ionic liquids. University of Manchester
58. Chellappan LK (2012) Synthesis of ionic liquids based on new cationic cores
59. Lei Z, Dai C, Chen B (2014) Gas solubility in ionic liquids. Chem Rev 114:1289–1326
60. Safdar R, Omar AA, Ismail L, Lal B (2014) Solubility of CO2 in an aqueous ammonium based ionic liquid. Appl Mech Mater 625:549–552
61. Zhou Z-B, Matsumoto H, Tatsumi K (2004) Novel hydrophobic ionic liquids based on quaternary ammonium and perfluoroalkyltrifluoroborate
62. Xiao C, Adidharma H (2009) Dual function inhibitors for methane hydrate. Chem Eng Sci 64:1522–1527
63. Khan MS, Cornelius BB, Lal B, Bustam MA (2018) Kinetic assessment of tetramethyl ammonium hydroxide (ionic liquid) for carbon dioxide, methane and binary mix gas hydrates. In: Rahman MM (ed) Recent advances in ionic liquids. IntechOpen, London, UK, pp 159–179
64. Kim SM, Lee JD, Lee HJ, Lee EK, Kim Y (2011) Gas hydrate formation method to capture the carbon dioxide for pre-combustion process in IGCC plant. Int J Hydrogen Energy 36:1115–1121
65. Qureshi MF, Atilhan M, Altamash T, Tariq M, Khraisheh M, Aparicio S et al (2016) Gas hydrate prevention and flow assurance by using mixtures of ionic liquids and synergent compounds: combined kinetics and thermodynamic approach. Energy Fuels 30:3541–3548

66. Xiao C, Wibisono N, Adidharma H (2010) Dialkylimidazolium halide ionic liquids as dual function inhibitors for methane hydrate. Chem Eng Sci 65:3080–3087
67. Li X-S, Liu Y-J, Zeng Z-Y, Chen Z-Y, Li G, Wu H-J (2011) Equilibrium hydrate formation conditions for the mixtures of Methane + Ionic Liquids + Water. J Chem Eng Data 56:119–123. doi:10.1021/je100987q
68. Zhao X, Qiu Z, Zhou G, Huang W (2015) Synergism of thermodynamic hydrate inhibitors on the performance of poly (vinyl pyrrolidone) in deepwater drilling fluid. J Nat Gas Sci Eng 23:47–54
69. Richard AR, Adidharma H (2013) The performance of ionic liquids and their mixtures in inhibiting methane hydrate formation. Chem Eng Sci 87:270–276
70. Chen Q, Yu Y, Zeng P, Yang W, Liang Q, Peng X et al (2008) Effect of 1-butyl-3-methylimidazolium tetrafluoroborate on the formation rate of CO_2 hydrate. J Nat Gas Chem 17:264–267
71. Nazari K, Ahmadi AN (2011) Thermodynamic study of methane hydrate formation in the presence of [BMIM][BF_4] and [BMIM][MS] ionic liquids. In: Proceedings of the 7th international conference on gas hydrates (ICGH)
72. Makino T, Matsumoto Y, Sugahara T, Ohgaki K, Masuda H (2011) Effect of ionic liquid on hydrate formation rate in carbon dioxide hydrates. In: Proceedings of the 7th international conference on gas hydrates (ICGH)
73. Zare M, Haghtalab A, Ahmadi AN, Nazari K, Mehdizadeh A (2015) Effect of imidazolium based ionic liquids and ethylene glycol monoethyl ether solutions on the kinetic of methane hydrate formation. J Mol Liq 204:236–242
74. Zare M, Haghtalab A, Ahmadi AN, Nazari K (2013) Experiment and thermodynamic modeling of methane hydrate equilibria in the presence of aqueous imidazolium-based ionic liquid solutions using electrolyte cubic square well equation of state. Fluid Phase Equilib 341:61–69
75. Sabil KM, Nashed O, Lal B, Ismail L, Japper-Jaafar A (2015) Experimental investigation on the dissociation conditions of methane hydrate in the presence of imidazolium-based ionic liquids. J Chem Thermodyn 84:7–13
76. Nashed O, Sabil KM, Lal B, Ismail L, Jaafar AJ (2014) Study of 1-(2-Hydroxymethyl) 3-methylimidazolium halide as thermodynamic inhibitors. Appl Mech Mater 625:337–340
77. Cha JH, Ha C, Kang SP, Kang JW, Kim KS (2016) Thermodynamic inhibition of CO_2 hydrate in the presence of morpholinium and piperidinium ionic liquids. Fluid Phase Equilib 413:75–79
78. Lee W, Shin J, Cha J, Kim K, Kang S (2016) Inhibition effect of ionic liquids and their mixtures with poly(N-vinylcaprolactam) on methane hydrate formation. J Ind Eng Chem 30:3541–3548
79. Tariq M, Connor E, Thompson J, Khraisheh M, Atilhan M, Rooney D (2016) Doubly dual nature of ammonium-based ionic liquids for methane hydrates probed by rocking-rig assembly. RSC Adv 6:23827–23836
80. Shi L, Yi L, Shen X, Wu W, Liang D (2017) The effect of tetrabutylphosphonium bromide on the formation process of CO_2 hydrates. J Mol Liq 229:98–105
81. Kumar A, Bhattacharjee G, Kulkarni BD, Kumar R (2016) Role of surfactants in promoting gas hydrate formation. Ind Eng Chem Res 54:12217–12232
82. Shen X-D, Long Z, Shi L, Liang D-Q (2015) Phase equilibria of CO_2 hydrate in the aqueous solutions of *N*-Butyl - *N*-methylpyrrolidinium Bromide. J Chem Eng Data 60:3392–3396
83. Ilani-Kashkouli P, Mohammadi AH, Naidoo P, Ramjugernath D (2016) Hydrate phase equilibria for CO_2, CH_4, or N2+ tetrabutylphosphonium bromide (TBPB) aqueous solution. Fluid Phase Equilib 411:88–92
84. Ricaurte M, Torré J, Broseta D, Diaz J, Dicharry C, Complexes F et al (2011) CO2 removal From a CO2 – CH4 gas mixture by hydrate formation: Evaluation of additives and operating conditions 33
85. Tariq M, Atilhan M, Khraisheh M, Othman E, Castier M, Garcia G et al (2016) Experimental and DFT approach on the determination of natural gas hydrate equilibrium with the use of excess N_2 and Choline–Chloride ionic liquid as an inhibitor. Energy Fuels 30:2821–2832

86. Mohamed NA, Tariq M, Atilhan M, Khraisheh M, Rooney D, Garcia G et al (2017) Investigation of the performance of biocompatible gas hydrate inhibitors via combined experimental and DFT methods. J Chem Thermodyn 111:7–19
87. Lee W, Shin J-Y, Kim K-S, Kang S-P (2016) Synergetic effect of ionic liquids on the kinetic inhibition performance of poly (N-vinylcaprolactam) for natural gas hydrate formation. Energy Fuels 30:9162–9169
88. Cha M, Shin K, Kim J, Chang D, Seo Y, Lee H, et al (2013) Thermodynamic and kinetic hydrate inhibition performance of aqueous ethylene glycol solutions for natural gas. Chem Eng Sci 99:184–190.
89. Shen X, Shi L, Long Z, Zhou X, Liang D (2016) Experimental study on the kinetic effect of N-butyl-N-methylpyrrolidinium bromide on CO_2 hydrate. J Mol Liq 223:672–677
90. Khan MS, Lal B, Partoon B, Keong LK, Bustam AB, Mellon NB (2016) Experimental evaluation of a novel thermodynamic inhibitor for CH_4 and CO_2 hydrates. Procedia Eng 148:932–940
91. Xiong L, Li X, Wang Y, Xu C (2012) Experimental study on methane hydrate dissociation by depressurization in porous sediments. Energies 5:518–530
92. Armand M, Endres F, MacFarlane DR, Ohno H, Scrosati B (2009) Ionic-liquid materials for the electrochemical challenges of the future. Nat Mater 8:621–629
93. Siedlecka EM, Czerwicka M, Neumann J, Stepnowski P, Fernandez JF, Thoming J (2011) Ionic liquids: methods of degradation and recovery. In: Ionic liquids: theory, properties, new approaches, pp 701–724
94. Govinda V, Venkatesu P, Bahadur I (2016) Molecular interactions between ammonium-based ionic liquids and molecular solvents: current progress and challenges. Phys Chem Chem Phys 18:8278–8326
95. Keshavarz L, Javanmardi J, Eslamimanesh A, Mohammadi AH (2013) Experimental measurement and thermodynamic modeling of methane hydrate dissociation conditions in the presence of aqueous solution of ionic liquid. Fluid Phase Equilib 354:312–318
96. Wilce M, Aguilar M, Hearn M (1995) Physicochemical basis of amino acid hydrophobicity scales: evaluation of four new scales of amino acid hydrophobicity coefficients derived from RP-HPLC of peptides. Anal Chem 67:1210–1219
97. Talaghat MR (2014) Experimental investigation of induction time for double gas hydrate formation in the simultaneous presence of the PVP and l-Tyrosine as kinetic inhibitors in a mini flow loop apparatus. J Nat Gas Sci Eng 19:215–220
98. Bhattacharjee G, Choudhary N, Kumar A, Chakrabarty S, Kumar R (2016) Effect of the amino acid l-histidine on methane hydrate growth kinetics. J Nat Gas Sci Eng 35:1453–1462
99. Rad SA, Khodaverdiloo KR, Karamoddin M, Varaminian F, Peyvandi K (2015) Kinetic study of amino acids inhibition potential of Glycine and L-leucine on the ethane hydrate formation. J Nat Gas Sci Eng 26:819–826
100. Qasim A, Khan MS, Lal B, Shariff AM (2019) Phase equilibrium measurement and modeling approach to quaternary ammonium salts with and without monoethylene glycol for carbon dioxide hydrates. J Mol Liq 282:106–114
101. Bavoh CB, Lal B, Ben-Awuah J, Khan MS, Ofori-Sarpong G (2019) Kinetics of mixed amino acid and ionic liquid on CO2 hydrate formation. IOP Conf Ser Mater Sci Eng 495:012073
102. Muhammad Saad Khan MS, Yaqub S, Manner N, Karthwathi N, Qasim A, Mellon NB, Lal B et al (2018) Experimental equipment validation for methane (CH_4) and carbon dioxide (CO_2) hydrates. IOP Conf Ser Mater Sci Eng 344:1–10
103. Khan MS, Partoon B, Bavoh CB, Lal B, Mellon NB (2017) Influence of tetramethylammonium hydroxide on methane and carbon dioxide gas hydrate phase equilibrium conditions. Fluid Phase Equilib 440:1–8

Chapter 3
Gas Hydrate Promoters

Omar Nashed, Bhajan Lal, Azmi Mohd Shariff and Khalik M. Sabil

3.1 Introduction

The gas hydrates formation is often improved by chemical methods and mechanical methods. The mechanical methods intend to enhance the contact area, as well as the mass transfer between water and gas. It includes use of fixed bed crystallizer with porous media, bubble method, temperature fluctuation, stirrer, ultrasonic waves, and liquid spraying by a nozzle [1, 2]. The chemical approach is used to facilitate the hydrate formation condition at milder condition, increase the formation rate and gas uptake, and improve the selectivity of hydrates [3–6]. The chemicals used to promote gas hydrates are classified into two groups. Firstly, THPs which contribute in the gas structure either as guest molecule such as THF and cyclopentane or change the conventional water cage coordination by forming which so-called semi-clathrate hydrates (SCH) for instance tetra-n-butyl ammonium salts [6, 7]. Secondly, KHPs such surfactant that enhance the induction time, hydrates formation rate, and gas uptake [6, 7]. In the following sections, these chemical methods are reviewed.

3.2 Thermodynamic Promoters (THPs)

THPs are primarily used to reduce hydrate formation pressure or increase hydrate formation temperature. Milder hydrates formation conditions in the presence of THPs are attributed to their notable stabilization effect. There are two types of thermodynamic hydrates promoters. The first one consists of small molecules that occupy the water cavities as guest molecules [5, 8]. The most investigated THPs include cyclic ether compounds, for example, THF, 1,4-dioxane, propylene oxide, and cyclopentane (CP), additionally propane (C_3H_8), neohexene, acetone, and methylcyclohexane (MCH) [8]. Nonetheless, a wide-ranging application of these chemicals is being deterred by high volatility. The released gases are contaminated due to volatility of promoters, therefore, requiring additional separation process [9], which is

B. Lal and O. Nashed, *Chemical Additives for Gas Hydrates*, Green Energy and Technology, https://doi.org/10.1007/978-3-030-30750-9_3

unfavourable for industrial practice. However, the other types, which are an organic phosphonium salts and non-volatile organic quaternary ammonium salts, were introduced as an ionic hydrate former. They can form SCHs at ambient pressure and temperature [9]. They also reduced the required pressure and entrap different gases more effectively than CP and THF [10, 11]. SCHs are a unique group of clathrates, alongside the guest species capability of being merged with the host cavities by replacing water molecules [9]. The formation of SCH crystalline compounds is characterized through the water anion framework, and this includes several large and small cavities. The key difference is that in semi-clathrates there is an interaction between guest molecules and the host [12]. In this chapter, we will review the most common and effective reported promoters. THF, propane, and CP are selected, for an extensive review, as an example for water-miscible, gas, and partially water-miscible promoters, respectively.

THF is a cyclic ether, which is water-miscible, that can form hydrate by its own and only occupying large cages of sII. THF is a widely examined promoter for numerous gas hydrate applications, and these include gas storage and carbon dioxide capture [13–15]. However, THF at several concentrations reduces hydrate phase equilibrium significantly [16–18]. Most likely, an increase of THF concentration causes a decrease in equilibrium hydrate formation pressure at any certain temperature. 5.6 mol% is the stoichiometric concentration of THF hydrate, as THF results in larger reduction in phase hydrate equilibrium conditions. It is perceived that the shifting in equilibrium is depending on promoter concentration. However, exceeding stoichiometric concentration would not result in equilibrium curve shifting.

It has also been confirmed that small amount of THF can shift CH_4 hydrate formation conditions to lower pressures. Furthermore, CH_4 hydrates exist in small cavity, while THF occupies large cavity. Researchers studied the Raman spectroscopy and PXRD pattern of the H_2 and CO_2 hydrate generated with 5.6 mol% of THF in water. The results showed that both H_2 and CO_2 occupy the small cages, while THF occupies the large cages of sII [17, 18]. It is worth to note that THF hydrates can be formed with the absence of guest gas, at atmospheric pressure and appropriate temperature. In Addition, THF can also be combined with KHPs as well. However, the kinetic effects of THF and gas uptake have been discussed in the literature [16, 18].

The impact of THF at several concentrations (0.5, 1.0, and 3.0 mol%) on the kinetics of hydrate formation from fuel gas, revealed an increased rate of hydrate formation with increase in THF concentration from 0.5 to 1.0 mol%, yet the rate reduced when THF concentrations increased further to 3.0 mol% [16]. The induction time reduced with an increase of THF concentration and driving force. This suggested that the existence of concentration dependencies for the kinetics of hydrate formation. A recent study pointed out higher gas uptake for hydrate formation from fuel gas for 5.6 mol% THF solution than 1.0 mol% THF solution at 8.0 MPa and ΔT of 4 K [18]. This suggests that the optimum concentration of a promoter also depends on the experimental conditions. However, the CO_2 selectivity is higher at 1 mol% as hydrate phase CO_2 composition was 94 and 90% in hydrates formed with 1.0 and 5.6 mol% THF concentrations [18]. However, an increase in the driving forces causes an increase in CO_2 content in hydrate phase irrespective of THF concentration [16].

The impact of 1.0 mol% THF spread in silica gel pore in the kinetics of hydrate formation from fuel gas fusion was examined, a gas uptake and water conversion of 0.0175 mol and 9.05% in 4 h at 5.0 MPa and 274.2 K were also described [19]. The results revealed that adding THF, decreased the gas uptake by six times compared to pure water experiments in silica gel. It is observed that the added THF decreased the hydrate growth rate compared to the pure system, without the presence of THF as a promoter in silica gel [16, 19]. The effects of THF on the thermodynamics and kinetics of hydrate formation from fuel gas in glass beads, silica gel, and silica sands has been discussed [20–22]. An earlier study reported that 1.0 mol% THF as the ideal concentration for CO_2 capture from fuel gas with a gas uptake of 0.0085 mol of gas/mol of water for 1.0 mol% THF solution at 279.6 K was the driving force up to 1.87 MPa [16]. Another study showed higher gas uptake for 5.6 mol% THF of the solution, as opposed to the 1.0 mol% sample at 8 MPa with a driving force of 4 K [18].

Propane is a hydrocarbon gas at standard pressures and temperature. The size of propane is a fit for the structure II hydrates. Adding (2.5–3.2 mol%) of propane to the gas decreases the equilibrium pressure significantly [23, 24]. Propane was found to form structure II as indicated by calculating the heat of dissociation using the Clausius–Clapeyron equation [23, 24]. Structure II formation and cage occupancy have been confirmed using Raman spectroscopy, infrared, NMR, and PXRD.

For example, the hydrate formed from $C_3H_8/H_2/CO_2$ (2.6/59.2/38.2 mol%), gas mixture was found to form sII hydrate supporting the estimation based on the Clausius–Clapeyron equation [25]. While, structure I was formed from the ternary gas mixture $C_3H_8/H_2/CO_2$ (1.2/18.8/80 mol%), this suggests that propane can act as a diluent [24]. Another experimental work revealed that adding 2.5 mol% propane to the fuel gas at 278.4 K will reduce the equilibrium pressure from 10.74 to 3.5 MPa. This work found that propane occupies 43% of large cages, CO_2 occupies 57 and 34% of large and small cages, and hydrogen exist in small cages of sII. In addition, gas chromatography tests showed that the hydrate phase consists of 14.6 mol% C_3H_8, 11.2 mol% H_2, and 74.2 mol% CO_2.

In another study, propane (2.5 mol%) was used as a promoter for a two-stage clathrate hydrate/membrane process. The first and second stage of this process operated at 273.7 K and 3.8 and 3.5 MPa, respectively [26]. The separation factor of 27.84 and 91.19 and split fraction of 0.47 and 0.32 were found for the first and second stage, respectively. It was reported that addition of propane reduced the rate of hydrate formation, but did not compromise the separation efficiency. Microscopic studies have been conducted on hydrate formation from $CO_2/H_2/C_3H_8$ (38.1/59.4/2.5 mol%) gas mixtures to understand the mechanism of rate of hydrate formation enhancement in silica sand bed in the presence of propane gas [27]. Morphological observations revealed that the presence of propane as a part of gas mixture can draw water dispersed in the interstitial pore space between silica sand particles towards the hydrate growth front in the gas phase. This behaviour was not observed in the case of CO_2/H_2 (40/60%) mixture hydrate formation in silica sand. The ability to draw water from silica sand is attributed to the presence of propane in the hydrate forming gas mixture due to which the hydrate growth rates which are significantly higher. It is worth to

note that propane enhances the kinetics of hydrate formation in silica sand for different systems like methane, methane/ethane compared to the gas/gas mixtures without propane [28, 29].

Cyclopentane (CP) is a cycloalkane which is partially miscible with water. At ambient temperature and pressure, the binary system {water + cyclopentane} shows liquid–liquid phase separation into a cyclopentane-rich and a water-rich liquid phase, respectively, over a wide range of composition. The first study showed the occurrence of pure sII cyclopentane hydrates, formed without coexisting of small gas molecules by Fan et al. [30]. Recently, thermodynamic and kinetic studies have been reported employing cyclopentane as a promoter for CO_2 capture [30].

Phase equilibrium of CO_2/H_2 mixtures in the occurrence of CP showed that the accumulation of CP decreases the equilibrium hydrate formation pressure [10]. Additionally, it used for two-stage separation where at the end of first and second stages, 84 and 98% CO_2 is captured in the hydrate phase. Experiments with several volumes of CP (0–20 vol%) in stirred tank reactor (STR) at 4.5 MPa and 273.15 K were performed, and a minor improvement of gas uptake was revealed [9]. The gas uptake increased with an increase in CP/water ratio until 3 vol%. No further increment in gas uptake was revealed when the CP/water ratio increased further. The occurrence of CP in an unstirred tank reactor (UTR) under quiescent conditions was more efficient for gas uptake, compared to STR at same experimental conditions [11]. In an STR, CP remained as an emulsion suspended in water, whereas in the UTR configuration, CP formed a layer above water. In a STR, it was shown that the increase in the amount of CP did not enhance the gas uptake [9], whereas in an UTR [11], the amount of CP or CP layer thickness affected the gas uptake for hydrate formation. Under the same experimental conditions, UTR resulted in 2.28 times gas uptake compared to STR. Moreover, in an UTR, the effect of volume of CP, i.e. thickness of the CP layer above the water layer was examined at 6.0 MPa and 275.7 K, and 15 ml CP, which was found to be the optimum, based on the induction time, gas uptake, and rate of hydrate formation compared to 7 and 22 ml. A gas uptake of 0.0264 mol of gas/mol of water for 15 ml CP, while for 7.5 ml it was 0.0202 mol of gas/mol of water [11]. It was reported that hydrate nucleation occurred at the CP-water interface and hydrate grew along the crystallizer wall and radially. Upon the complete hydrate formation at CP-water interfacial, hydrates started to grow downwards and afterwards, the water level quickly dropped due to continuous hydrate growth in all three directions. Comparison studies between THF, CP, and TBAB reported that CP consumed more flue gas compared to THF and TBAB, while more CH_4 was consumed in the presence of THF than CP [31].

The ternary system (water + cyclopentane + CO_2) was investigated by Zhang and Lee, in the sII mixed hydrate stability region [10, 32]. Four-phase (hydrate–liquid water–organic liquid–vapour) equilibrium pressures were determined in the temperature range from 286.7 to 292.6 K. The hydrate dissociation pressures varied from 0.89 to 3.15 MPa at the low and high temperatures, respectively.

Mohammadi and Richon [33] introduced similar data from the ternary system of water, cyclopentane, and CO_2 in the temperature interval from 284.3 to 291.8 K [33]. Their data corresponded well with the pressures measured by Zhang and Lee [32, 34].

However, they extended the low end of the temperature interval compared to Zhang and Lee, by approximately 2 K. At 284.3 K, Mohammadi and Richon determined the mixed hydrate equilibrium pressure at 0.35 MPa [35]. The immiscibility of CP with water is a key drawback for its use as a promoter since the hydrate forming gas must diffuse via the CP layer and reach the water interface to form hydrates. This may be a challenge during process scale-up, since the height of the CP layer is crucial in such a situation.

3.2.1 Semi-clathrate Hydrate (SCH)

SCH is a term given by Davidson for a type of clathrate hydrates, in which the guest molecule shares with the water molecules the host framework and also reside the hydrate cages [36]. More specifically, the charged centres of the cation and anion substituted water at certain position in hydrate lattice and the alkyl chains of the salt occupied larger cages of the structures Fig. 3.1. These larger cages were either tetrakaidecahedral (with twelve pentagonal faces and two hexagonal faces, in short hand $5^{12}6^2$), pentakaidecahedral ($5^{12}6^3$), or hexakaidecahedral ($5^{12}6^4$), and between these large cages smaller dodecahedral (5^{12}) cages filled the space [36]. The structural studies also revealed that each peralkylonium salt could form several different SCH structures with differing hydration numbers. At least three different hydration numbers (27, 32.8, and 38); the structure that forms is dependent on the ratio of salt to water in the solution and the accompanying temperature [36].

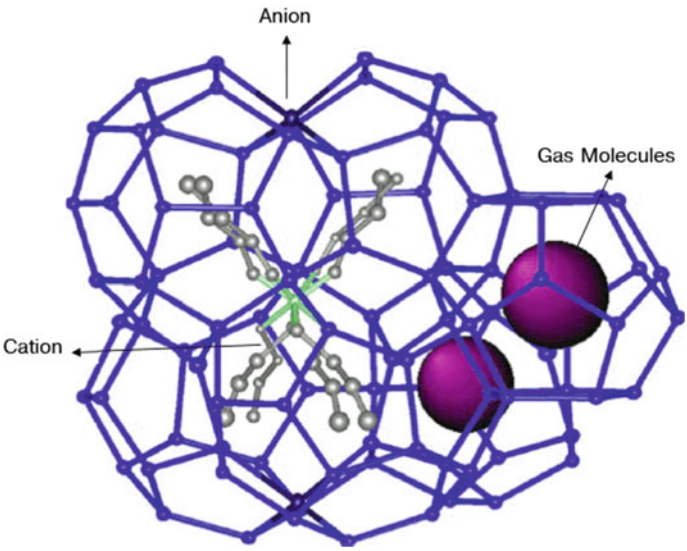

Fig. 3.1 Semi-clathrate hydrate structure

Quaternary ammonium/phosphonium salts form SCH. Semi-clathrate hydrates have gained significant attention as THP for several applications such as CH_4 and H_2 storage, CO_2 capture from flue gas, and refrigeration [37]. This is because they can form hydrates at milder experimental conditions compared to the conventional gas hydrates. Small gas molecules such as CH_4, H_2, and CO_2 reside the small cages of SCH. The most common SCH former is tetra-n-butyl ammonium bromide (TBAB), tetra-n-butyl ammonium chloride (TBAC), tetra-n-butyl ammonium fluoride (TBAF), and tetra-n-butyl ammonium nitrate ($TBANO_3$), tetra-i-sopentylammonium fluoride, tetra-n-butylphosphonium bromide (TBPB), tributylphosphine oxide (TBPO) [38, 39]. All SCH hydrates are capable to shift the hydrate equilibrium curve to lower pressures and higher temperature conditions. In addition, it was found that SCH have better selectivity compared to other promoters such as THF. However, they also have impact on the kinetic of gas hydrates formation. Their performance is uneven and should be compared under the same conditions. Following is a comparison between the most studied semi-clathrate hydrates in literature.

The literature data shows that TBAB hydrate phase equilibrium conditions for CO_2/H_2 in presence of various concentrations of TBAB at various pressure and temperature range were reduced for fuel gas mixture significantly [40–42]. The increase in TBAB concentrations decreased the hydrate formation conditions further until the stoichiometric concentrations were achieved. Further increase in TBAB concentrations above stoichiometric concentrations resulted in the increase in the phase equilibrium [41, 43]. Addition of TBAF as a promoter to a system with a fuel gas mixture shifted the phase equilibrium to much lower pressure and higher temperatures [43]. The maximum shift was achieved for the stoichiometric concentration of 3.3 mol% TBAF. Addition of TBAF beyond this concentration increased the hydrate phase equilibrium conditions. $TBANO_3$ also reduced the phase equilibrium significantly in the range of 0.5–3.7 mol% [44]. The heat of dissociation increased with increase in $TBANO_3$ concentrations. However, tetra-n-butyl ammonium halides are more effective THPs compared to $TBANO_3$. The kinetic effect of $TBANO_3$ on CO_2 hydrates formation was evaluated at 6.0 MPa and 274.2 K. CO_2 preferentially occupies the SCH regardless of the $TBANO_3$ concentration. The results showed that 1.0 mol% $TBANO_3$ is the optimum concentration. Several kinetic studies have been investigated TBAB at various experimental conditions, reactor configurations and concentrations [41–44]. TBAB has the ability to improve the kinetic of fuel gas by reducing the induction time and increased the CO_2 uptake in hydrates phase [45, 46]. An increase in TBAB loading more than 0.29 mol% resulted in decreased in the gas uptake and a decrease in the amount of CO_2 captured. Another study reported that with the increase in TBAB concentration, the induction time decreased. When the TBAB concentration was increased from 0.5 to 1.0 mol%, the hydrate formation rate increased, but when the TBAB concentration was increased from 1.0 to 3.0 mol%, the rate decreased [41]. A hydrate phase CO_2 composition of 85, 89, and 88% for 0.5, 1.0, and 3.0 mol% TBAB, respectively, was reported. The separation and split fraction for 0.29 and 0.61 mol% were 15.7 and 0.41 and 28.0 and 0.48, respectively. Experimental work on TBAB at concentrations of 0.6 and 3.7 mol% at 8.0 MPa and

subcooling of 4 K revealed that the total obtained gas uptake was much lower than that with pure water at the same experimental conditions [43]. The effect of TBAB concentrations on gas uptake and separation efficiency was systematically evaluated at 6.0 MPa and 279.2 K in a recent study [47]. The TBAB concentrations employed were 0.3, 1.0, 1.5, 2.0, and 3.0 mol%. A longer induction time and higher total gas uptake and separation factor was reported for 0.3 mol% TBAB solution. On the other hand, for 1.0 mol% TBAB, shorter induction time and higher hydrate growth rate was reported. Although TBAB concentrations of 1.5, 2.0, and 3.0 mol% had shorter induction time, low gas uptake, slow rate of hydrate growth, and low separation factor were reported. An important aspect of TBAB hydrate formation at 0.3 mol% concentration was that before nucleation, the gas consumption was very high (70.4 $\pm$ 11.77% of the total gas uptake) compared to the hydrate growth region.

The kinetics of hydrate formation in the presence of TBAF was also evaluated at 8.0 MPa and subcooling of 4 K with TBAF concentration of 0.8 and 3.3 mol%. The addition of TBAF did not improve the kinetics instead lowered the gas uptake for hydrate formation considerably. Meanwhile, the gas uptake increased with the increase in $TBANO_3$ concentrations from 0.5 to 1.0 mol% but decreased with further increase in $TBANO_3$ concentration. Microscopic observations were also presented to understand the SCH formation kinetics. Microscopic observation revealed extensive SCH formation for $TBANO_3$ concentrations above 1.0 mol% at 6.0 MPa and 274.2 K. In the case of 1.0 mol% $TBNAO_3$ concentrations, gradual SCH formation was observed. Among the quaternary ammonium salt investigated in a stirred tank reactor, 0.29 mol% TBAB resulted in the highest normalized gas uptake of 0.0187 mol of gas/mol of water at 5.0 MPa and 278.15 K. The optimum concentration of TBAB for enhanced kinetics (higher gas uptake) varies in the literature, which can be attributed to the different experimental conditions and different reactor configurations [41, 45, 47, 48]. The normalized gas uptake was found to be very lower for TBAF concentrations of 0.6 and 3.3 mol% than that of TBAB at same driving force. Among the various $TBANO_3$ concentrations investigated at 6.0 MPa and 274.2 K in an STR, 1.0 mol% $TBANO_3$ was found to be optimum and yielded a normalized gas uptake of 0.0138 mol of gas/mol of water.

3.3 Kinetic Hydrate Promoters (KHPs)

As has been described in Chap. 1, the main issue that hindered the industrial applications of gas hydrates technology is the slow hydrate formation rate. Therefore, in the quest to achieve fast hydrates formation, researchers have focused on developing KHPs. The main advantages of kinetic hydrates promoters are that they do not occupy the water cages as well as help to increase the gas uptake. In addition, KHPs are used at low concentrations <10,000 ppm.

Reducing the surface tension between gas and liquid phase is the main function of KHPs. This is could be done using surfactants or high surface materials. One literature paper has reported that surfactants shift the hydrate formation conditions,

but most of the literature works proved that KHPs do not change the phase equilibria of gas hydrate system. In the following sections, the most common types of KHPs are presented.

3.3.1 Surfactants

Surfactants refer to surface-active agents' materials having both hydrophobic and hydrophilic component. Thus, they can dissolve polar and non-polar substances. The hydrophobic and hydrophilic groups; characteristic of each surfactant is the property determining factors. Surfactants can alter the surface or interfacial tension and modify the contact angle between the phases and thus changing surface charge and surface viscosity. At suitable concentrations, the surfactant molecules aggregate in water to form various kinds of structures (called micelles) with different shapes and orientations (spherical, rod-like micelles, multilayer structures, etc.). Surfactants mainly categorized into four groups depending on the moieties they contain, namely anionic, cationic, non-ionic, and Zwitterionic surfactants. Zwitterionic surfactants consist of both cationic and anionic centres attached to the same molecule. Use of surfactants in gas hydrate-related studies has been ongoing since the early 1990s. Karaaslan et al. studied three different types of surfactants (anionic, cationic, and non-ionic); they found that anionic surfactant enhances the hydrate formation kinetics significantly as compared to a pure water system. The effects of the non-ionic surfactant (ETHOXALATE) was less pronounced while the cationic surfactant showed promotional behaviour at concentrations less than 0.1 wt%, which was exactly opposite to that at high concentrations [49]. Kang et al. have concluded from their experimental work that use of an optimum concentration of SDS acts as a promoter but an excess amount of the same can inhibit hydrate growth [50]. Another study compared the storage capacity of CH_4 hydrates in the presence of surfactant at concentrations of 300, 500, and 1000 ppm. Maximum promotion effect of SDS on CH_4 hydrate was observed at the concentration of 500 ppm, linear alkyl benzene sulphonate (LABS) at the concentration of 1000 ppm, and cationic surfactant cetyl trimethyl ammonium bromide (CTAB) is a promoter at only high concentrations of 1000 ppm. The non-ionic surfactant 9 molar ethoxylated nonylphenol (ENP) showed close results to that of CTAB [51]. Kumar et al. studied the three types of surfactants (cationic, anionic, and non-ionic) for CO_2 hydrate formation kinetics. Anionic surfactant (SDS) was found to be most effective in enhancing the rate of hydrate formation as well as reducing the induction time. Non-ionic surfactant (Tween-80) was found to be better than the cationic surfactant DTACl [52]. Dependencies on the surfactant concentration for hydrate formation rate and the final water to hydrate conversion ratio had been established for many guest species. However, it is not clear whether such dependencies exist, or it is more to do with different reactor configuration used in these studies.

Karaaslan et al. concluded that IGEPAL-520 is the most effective hydrate formation promoter among three non-ionic surfactants, polyoxyethylene (5) nonylphenyl

ether (IGEPAL-520), Brij-58 and Tween-40. An amount of 1 wt% IGEPAL-520 accelerates the CH_4 hydrate formation rate by a factor of 2.4, compared to CH_4 hydrate formation rate in pure water.

Veluswamy et al. have also used such types of cationic and non-ionic surfactants (DTACl and Tween-20, respectively) for mixed hydrogen/THF and methane/THF hydrate formation. They observed a remarkable progress in the hydrogen THF hydrate formation rates, while the reduction of hydrate formation rates for Methane/THF mixed hydrates were observed. Thus, the effects of surfactants depend upon the guest gas and the system itself [53]. Zhong and Rogers have found that by adding about 284 ppm of SDS to an ethane-water system, the rate of hydrate formation increased by a factor greater than about 700 as compared to a system having only pure water [54]. Furthermore, it was suggested that the formation of micelles could enhance ethane solubility as well as act as nucleating sites to lower induction time [54]. Considering such contradicting reports regarding faster hydrate nucleation in presence of micelles, it is concluded that the surfactant micelle hypothesis has not been tested extensively and at this point of time there is no concrete evidence in the literature to support this claim. It has been observed that presence of THPs like THF and CP reduces the influence of SDS and its effects as a hydrate promoter compared to a pure water system. Zhong et al. studied the influence of cyclopentane (CP) and SDS on CH_4 separation from low concentration coal mine gas [54]. They found that the gas uptake and rate of hydrate formation were dependent on SDS concentration, but the presence of SDS did not show any clear influence on CH_4 recovery. The CH_4 recovery obtained in the presence of SDS was 33.3%, while that obtained without SDS was 33.1% [55, 56]. They have reported that SDS was not very effective in promoting CH_4 enclathration in presence of CP. Gemini surfactants are a new and unique class of surfactants; they are dimeric surfactants having two hydrophilic head groups and two hydrophobic tails; the hydrophilic head groups of the surfactants are linked by a spacer group of varying length [57]. Gemini surfactants not only have lower CMC values but also show lower surface tension at their respective CMC values. They found that the multichain disulphonate surfactant synthesized exhibited higher CH_4 storage capacity than SDS (sodium dodecyl sulphate) even at lower surfactant concentrations. This observation was attributed to the lower CMC and surface tension value for the Gemini surfactant as compared to an SDS-water solution having similar concentrations [58].

3.3.2 Nanomaterials

In 2006, Li et al. reported copper nanoparticles as kinetic hydrate promoters [59]. Nanoparticles refer to tiny particles having at least one dimension in a size ranging from 1 to 100 nm. Compared to micron-sized particles, nanoparticles have much larger relative surface areas and a high potential for heat transfer enhancement. Since 2010, a huge number of publications have been produced on the usage of nanomaterials to enhance hydrate formation. The thermal conductivity of a liquid can

be increased by adding a more thermally conductive liquid or solids. Solid materials are inherently more thermally conductive than liquids, but due to the high surface energy of nanoparticles, it is easy for nanoparticles to coagulate and consequently, difficult to disperse in the base fluid. This phenomenon could lead to the unstable/less stable colloidal system. If particles are aggregated, it changes the hydrodynamic size and the morphology, and sometimes reduces the volume fraction as a result of settling out, ultimately lowering the thermal conductivity of the colloidal. The most important factor affecting the stability of suspensions are the nanoparticle's concentration, dispersant, viscosity of the base liquid, and pH value. The diameter, density of the nanoparticles, and ultrasonic vibration also influence the stability of the nanofluids. If the attractive force is larger than the repulsive force, the two particles will collide, and the suspension will become unstable. If the particles have a sufficient high repulsion, the suspensions will exist in a stable state. For stable nanofluids or colloids, the repulsive forces between particles must be dominant. Typically, surfactants are added to stabilize nanofluid. In general, when the base fluid of the nanofluids is a polar solvent, water-soluble surfactants are recommended (e.g. for hydrate studies).

Several types of nanomaterials have been investigated such as metal, metal oxide, silica, graphite, and single and multi-wall carbon nanotubes. These nanomaterials are naturally stable or stabilized using surfactants. Hence, researchers should differentiate between the influence of stabilizer and nanomaterial.

Pristine and surface-modified carbon nanotube was investigated. Single-wall carbon nanotube (SWCNT) can reduce the induction time 75.5% compared with SDS [60]. Multi-wall carbon nanotubes have been investigated widely due to its lower cost compared to SWCNT. Pristine, oxidized (OMWCNT), hydroxylated (OHMWCNT), carboxylated (COOHMWCNT), and SDS-doped multi-wall carbon nanotubes were also explored. Functionalized carbon nanotubes were more effective than pristine MWCNT. For example, OMWCNT has the most impact on the induction time Song et al. [61]. The positive effect of acid treatment on the MWCNTs is attributed to the appreciable defects made on the MWCNTs' surface, which destroys the graphitic integrity and formation of small graphitic fragments. Therefore, the produced defective sites with more oxygen-containing groups contributed to the higher dispersion and stability of nanotubes in the aqueous phase [61]. OMWCNT showed maximum gas consumption at a concentration of 0.003 wt%, which is less than the previously reported 0.004 wt% value for MWCNT [62]. In addition, the 0.003 wt% of OMWCNT increased the gas consumption by 450% compared to the pure water experiments, which is also higher than the enhancement rate observed by MWCNT. It is worth to mention that the combination of surfactant and nanomaterial result in higher improvement rate in comparison with single promoter. However, COOHMWCNT increased CO_2 hydrates formation rate considerably compared to pure water and SDS. A synergic effect has been found when MWCNT was mixed with THPs such as TBAB and THF. Comparative studies were done for graphene (GP), graphene oxide (GO), and sulfonated graphene oxide (SGO) nanosheets. It was found that SGO was the most efficient promoter in terms of the time needed to completely form hydrates, rate of hydrate formation, and storage capacity followed

by GP then GO. The poor promotional effects shown by GO was speculated due to the existence of oxygen-containing groups could destroy the conjugated structure of the nanosheets, and hence decreased the heat transfer efficiency [63]. The performance of nano graphite was also enhanced further when it was combined with 0.04 wt% SDBS solution, as a 86.4% gas consumption enhancement rate obtained [64]. Moreover, 0.08 wt% of graphite show the maximum enhancement among studied concentrations (0–0.1 wt%) for CO_2 hydrates in the presence of 9.01 wt% TBAB [65]. Experiments which have been conducted on silver nanoparticles revealed that the shape of nanoparticles could play a vital role for hydrates promotion. Copper was also reported as an effective hydrate promoter, as it prepared the cationic surfactant solution or anionic surfactant solutions. CuO, ZnO, Al_2O_3, SiO_2, CeO_2, Zeolite, MgO, TiO_2, and Fe_3O_4 are other investigated nanoparticles that have shown promotional effects. Since the nanomaterials enhance the gas consumption, the storage capacity as well as water to hydrates conversion also increased. However, like other KHP, the reported nanomaterials do not show selectivity for a specific gas type.

1. Gas hydrate formation is an exothermic event that leads to an increase in the temperature, thus decreasing the driving force for hydrate formation. Therefore, the heat of formation can be removed from the system much more effectively and much faster by using a higher thermal conductivity fluid. This will provide a more suitable temperature profile that is required for better nucleation. It should be noted that the MWCNT nanofluids, which have a very high thermal conductivity, have shown the highest enhancement rate.
2. Mass transfer is enhanced by reducing the surface tension because of the high surface area of nanoparticles.
3. Due to the presence of solid nanoparticles in the solution, hydrate crystal nuclei are formed easily by providing more nucleation sites, which enhance the nucleation process, as well as heterogeneous nucleation. Moreover, some researchers demonstrated the solubility of gas in water based on the adhesion of the gas to carbon nanotubes.
4. The Brownian motion of nanoparticles in the fluid can act as a stirrer and enhance the driving force. The movement of nanoparticles reduces films resistance in the gas/water interface.
5. The modification of the surface or the properties of the nanoparticles such as adding functional group or lowering the surface charge will positively affect the stability of the nanofluid. Hence, heat transfer will be enhanced.
6. The enhancement rate of the nanomaterials is less for soluble gases (CO_2) than other hydrophobic gases such as methane.

3.3.3 Amino Acid

Amino acid, any of a group of organic molecules that contain a basic amino group ($–NH_2$), an acidic carboxyl group (–COOH), and an organic R group (or side chain)

that are unique to each amino acid. The term amino acid is short for α-amino [alpha-amino] carboxylic acid. Each molecule consists of a central carbon (C) atom, known as α-carbon, to which both an amino and a carboxyl group are enclosed. The remaining two bonds of the α-carbon atom are commonly satisfied by a hydrogen (H) atom and the R group.

Recent studies claimed that amino acids are potential gas hydrate promoters, which are environmentally friendly, relatively cheap, and do not support foam formation, and hence they can be applied in hydrate-based commercial operations [66]. Liu et al. [67] are the first group to study natural amino acids as CH_4 hydrate promoters, at low concentrations up to 1 wt% [67]. In their study, leucine showed the highest CH_4 hydrate promotion result as compared to tryptophan, phenylalanine, methionine, glutamic acid, histidine, and arginine at 0.5 wt%. Leucine can convert 95% of water into CH_4 hydrate with a gravimetric capacity of 144 mgg^{-1} at an optimum concentration of 0.5 wt%. The occurrence of leucine did not cause foaming upon degassing. They further demonstrated that the tryptophan can promote CH_4 hydrate formation more than arginine and histidine but could not beat leucine. They also argued that the amino acid side chain properties have a significant role in hydrate promotion as amino acids with aromatic side chains improved hydrate formation better than those with aliphatic side chain. The combination of hydrophobic and aromatic side chain can promote hydrate formation more effectively. This may be true for CH_4 hydrates, as the amino acids promotion influence is composition dependent. All studied amino acids with aromatic sided chain and hydrophobic nature (tryptophan, leucine, phenylalanine) have shown significant CH_4 hydrate promotion.

However, leucine shows inhibition effect in ethane and THF hydrates [68, 69]. The behaviour of amino acid can change for CO_2 or hydrocarbons. In addition, histidine showed kinetic promotional effects on CH_4 hydrate [70]. On the contrary, histidine is reported to kinetically inhibit CO_2 hydrates, indicating that the kinetic promotion/inhibition effect of amino acids is depending on the type of guest compound present [71]. Interestingly, tryptophan and methionine can promote both CO_2 and CH_4 hydrates [72]. Other factors that contribute to the promotion/inhibition effects of amino acids are their side-chain length and hydropathy index. For every gas system, all amino acids have an optimum concentration above which their promotion/inhibition impact is decreased. For example, the optimum promotion impact of leucine in CH_4 hydrate ranges between 0.3 and 0.5 wt% [66]. In CH_4 hydrate system, the optimum concentration for tryptophan is 0.3 wt%, while for arginine and histidine is 1 wt%. In CO_2 hydrate L-methionine has an optimum concentration of 0.2 wt%. This shows that both arginine and valine can promote CH_4 hydrate formation more than SDS. Valine exhibits the most efficient average CH_4 hydrate promotional effect of about 10 and 1.3 times moles consumption of CH_4 than pure water and SDS. But the induction time for CH_4 hydrate nucleation was less compared to SDS [73]. The occurrence of methionine and phenylalanine improved the formation kinetics of hydrate formation with about 90% gas to hydrate conversion and over 85% water to hydrate conversion within an hour. Nonetheless, methionine promotes hydrate formation better than phenylalanine in both the gas systems, however, phenylalanine is more recommended for CH_4 hydrates only. These findings

further confirm that amino acids form structure I hydrates. This finding reveals an interesting bio potential for the separation of CH_4 gas from $CO_2 + CH_4$ gas mixtures and natural gas storage [74].

Amino acids hydrate promotion mechanism is controlled by various factors, which are not completely understood yet [67]. The suggested amino acids hydrate promotion effect is speculated by authors to arise from their surface activity and adsorption behaviour through capillary action [67, 72]. The surface activity of amino acids resulting in hydrate formation enhancement is same as conventional surfactants. Most amino acids molecular structure consists of both hydrophilic and hydrophobic nature arising from the occurrence of amine and carboxylic acid groups and side chain. Furthermore, the amino acids side chain may also vary based on its structure, charge, and polarity. This makes them amphiphilic molecules; thus, they can act as surfactants. This surfactant behaviour allows such amino acids to prevent the formation and agglomeration of hydrate nucleus crystals film at the gas/liquid interface, hence, enabling more gas to dissolve in the liquid phase for high hydrate gas uptake. Linga's laboratory demonstrated that hydrates formed in amino acids solution are very flexible and porous in nature, which is responsible for their hydrate promotion effect [66]. The presence of porous and flexible hydrates increases the surface adsorption ability at the gas/liquid interface. This enables the sucking of more liquids to the gas/liquid interface through improved capillary effect, resulting in high gas uptake into hydrate formation. It is crucial to highlight that amino acids promotion/inhibition mechanism in CO_2 systems is partly affected by the reaction between CO_2 molecules and amino acids.

3.4 Overview on Mechanical Methods

In order to reduce energy consumption and enhance hydrate formation efficiencies, several mechanical techniques were explored. It should be observed that the discussions within previous sections were mainly research activities carried out by laboratory experiments using a stirred tank reactor. However, in stirred tank reactors, the accumulation of hydrate crystals turns out to be an obstacle for reducing the water/gas interface area and, thus, the rate of hydrate formation and water conversion. The fixed bed crystalliser along with porous silica gel was extensively studied to solve this problem. The porous nature of the silica used in fixed bed can significantly improve the contact area between water and gas, enabling more gas to be enclathrated in a short time, therefore, enhancing the whole gas uptake and induction time. A study by Seo and Kang revealed that over 93% of small cages and 100% of large cages were occupied by CO_2 when porous silica gels were used [50]. Enhanced CO_2 selectivity and hydrate formation rates are also being achieved by using the silica bed [75]. Moreover, the disseminated water in silica pores reacts instantly with gas mixtures, which in turn disregards the need for energy-intensive mechanical agitation and excess water. This remains a strong economic advantage that keeps the need for research going [19].

The silica bed is further categorized into silica sand bed and silica gel bed types. Silica is cheap and more economically advantageous for large scale CO_2 separation. Babu et al. stated that water conversion reached to 36% in the silica sand bed and only 13% in the silica gel bed [76]. They also claimed that the silica sand bed gave better performance for hydrate-based CO_2 capture due to higher gas uptake. Another study confirmed that silica sand bed gave a higher rate of hydrate formation and total gas uptake, compared to stirred crystallizer [28]. Changing the physical properties (pore and particle sizes of the porous silica gel), can enhance the kinetics of hydrate formation. Kang et al. [77] claimed that pores which are too small lead to inhibition of their effect on hydrate formation due to the reduced water activity in the pores [77]. Increasing pore size can solve this problem. Greater pores and particle sizes tend to enhance CO_2 recovery, gas consumption, separation factor, and water conversion to hydrate, hence reducing the operating pressure [18]. This is due to the lower flow resistance across a larger pore than a smaller pore. This means that the larger exposed surface area of the silica gel significantly reduces induction time due to the better contact between water and gas within the gel [52]. The bubble method has also been attempted for gas hydrate-based CO_2 separation. Findings indicate that the hydrate shell formation around the bubble may delay the formation of hydrate within the bubble, due to isolation of the liquid from the gas [78]. However, this can be enhanced by using a smaller bubble size. It was reported that an ideal size of gas bubbles for CO_2 separation is 50 mm [79]. Unlike stirring and the packed bed crystalliser, the bubble method requires a large bubbling column, which is not easily built and run on an experimental scale. This makes the method limited for further examinations. Recent studies have revealed that temperature fluctuation (via vibration) is used to enhance CO_2 hydrate formation [7, 80]. This method is based on the fact that, when the temperature decreases, the solubility of CO_2 decreases in the hydrate forming region while increasing in the non-hydrate forming region [81]. The authors reported that, in the experiments using temperature fluctuation, pressure drop was increased by 30%. A 30–35% increase in total gas consumption also was observed. The positive effect of the temperature fluctuation was mostly observed during the early period of hydrate growth. The method was proven to be efficient when the reaction scale was increased by 100-fold [82].

Studies which have been conducted in a small scale setup showed that bubbling method replaces the stirring method [82]. It should be highlighted that for such a bubbling method, controlling the gas bubble size and avoiding hydrate plugs along the column is a big challenge.

This practice includes the gas bubbles fragmentation at the front of the shock wave and their involvement in the movement related to the liquid. It improves the heat transfer from the interphase and leads to a rapid hydrate shell formation over the bubble [83]. Stirring is one of the most common methods used to enhance mass and heat transfer in the CH_4 hydration process: induction times was reduced, formation rates accelerated, and storage capacity was increased when stirring was applied. Stirring reactors are widely used in laboratory settings to carry out fundamental studies on formation and dissociation of gas hydrates. As this has already been established, there are numerous problems with stirring in an industrial size process.

Energy costs from stirring increase as slurry thickens. Thickening slurry of a stirred system may limit the hydrate mass in the water to as low as 5% at which time filtering or clarification would be necessary. The separation of hydrates from the slurry requires additional work as does packing the hydrates in a storage vessel. Furthermore, hydrate particles entrain substantial amounts of interstitial water.

The bubble tower reactor is a standard industrial reactor type suitable for gas–liquid reactant system, and it was tested for hydrate formation. However, findings from using this type of reactor are not advancing in terms of hydrate formation rate, and hydrate shells formed are not easily broken. Spraying reactor is an alternative type of reactor for gas–liquid reactant systems. Application of water spraying into a gas phase to form CH_4 hydrates has been examined by Mori and co-workers, who designed and modified spraying reactors. We believe this technique is worthy of further development for applications to scaled-up systems. Zhong and Rogers found that the crystallization can also be induced abruptly from the supercooled solution with a 5 s pulse of 100 W ultrasonic energy [54]. The impact of ultrasonic on natural gas hydrate has been explored and showed that the nucleation of hydrate appears simultaneously when ultrasonic was used and less depends on the supercooling. It is also reported that the induction time decreased with the increase of ultrasonic power or reaction pressure [84].

References

1. Makogon IF, Makogon IF, Makogon YF (1997) Hydrates of hydrocarbons. Pennwell Books
2. Sabil KM, Partoon B (2018) Recent advances on carbon dioxide capture through a hydrate-based gas separation process. Curr Opin Green Sustain Chem 11:22–26
3. Nashed O, Partoon B, Lal B, Sabil KM, Shariff AM (2018) Review the impact of nanoparticles on the thermodynamics and kinetics of gas hydrate formation. J Nat Gas Sci Eng 55:452–465
4. Ganji H, Manteghian M, Omidkhah MR, Mofrad HR (2007) Effect of different surfactants on methane hydrate formation rate, stability and storage capacity. Fuel 86:434–441
5. Partoon B, Nashed O, Kassim Z, Sabil KM, Sangwai J, Lal B (2016) Gas hydrate equilibrium measurement of methane + carbon dioxide + tetrahydrofuran + water system at high CO_2 concentrations. Procedia Eng 148:1220–1224
6. Babu P, Linga P, Kumar R, Englezos P (2015) A review of the hydrate based gas separation (HBGS) process for carbon dioxide pre-combustion capture. Energy 85:261–279
7. Dashti H, Yew LZ, Lou X (2015) Recent advances in gas hydrate-based CO_2 capture. J Nat Gas Sci Eng 23:195–207
8. Veluswamy HP, Kumar A, Seo Y, Lee JD, Linga P (2018) A review of solidified natural gas (SNG) technology for gas storage via clathrate hydrates. Appl Energy 216:262–285
9. Li X-S, Xu C-G, Chen Z-Y, Wu H-J (2011) Hydrate-based pre-combustion carbon dioxide capture process in the system with tetra-n-butyl ammonium bromide solution in the presence of cyclopentane. Energy 36:1394–1403
10. Zhang J, Yedlapalli P, Lee JW (2009) Thermodynamic analysis of hydrate-based pre-combustion capture of CO_2. Chem Eng Sci 64:4732–4736
11. Ho LC, Babu P, Kumar R, Linga P (2013) HBGS (hydrate based gas separation) process for carbon dioxide cap-ture employing an unstirred reactor with cyclopentane. Energy 63:252–259
12. Kim S, Kang SP, Seo Y (2015) Semiclathrate-based CO_2 capture from flue gas in the presence of tetra-n-butyl ammonium chloride (TBAC). Chem Eng J 276:205–212

13. Veluswamy HP, Linga P (2013) Macroscopic kinetics of hydrate formation of mixed hydrates of hydrogen/tetrahydrofuran for hydrogen storage. Int J Hydrogen Energy 38:4587–4596
14. Timothy A, Strobel et al (2006) Molecular hydrogen storage in binary THF–H_2 clathrate hydrates
15. Yoshioka H, Ota M, Sato Y, Watanabe M, Inomata H, Smith RL, Peters CJ (2011) Decomposition kinetics and recycle of binary hydrogen-tetrahydrofuran clathrate hydrate. AIChE J 57:265–272
16. Lee HJ, Lee JD, Linga P, Englezos P, Kim YS, Lee MS, Kim Y Do (2010) Gas hydrate formation process for pre-combustion capture of carbon dioxide. Energy 35:2729–2733
17. Hashimoto S, Murayama S, Sugahara T, Ohgaki K (2006) Phase equilibria for H_2 + CO_2 + tetrahydrofuran + water mixtures containing gas hydrates. J Chem Eng Data 51(5):1884–1886
18. Park S, Lee S, Lee Y, Lee Y, Seo Y (2013) Hydrate-based pre-combustion capture of carbon dioxide in the presence of a thermodynamic promoter and porous silica gels. Int J Greenhouse Gas Control 14:193–199
19. Adeyemo A, Kumar R, Linga P, Ripmeester J, Englezos P (2010) Capture of carbon dioxide from flue or fuel gas mixtures by clathrate crystallization in a silica gel column. Int J Greenhouse Gas Control 4:478–485
20. Yang M, Song Y, Liu W, Zhao J, Ruan X, Jiang L, Li Q (2013) Effects of additive mixtures (THF/SDS) on carbon dioxide hydrate formation and dissociation in porous media. Chem Eng Sci 90:69–76
21. Babu P, Ho CY, Kumar R, Linga P (2014) Enhanced kinetics for the clathrate process in a fixed bed reactor in the presence of liquid promoters for pre-combustion carbon dioxide capture. Energy 70:664–673
22. Song Y, Wang X, Yang M, Jiang L, Liu Y, Dou B, Wang S (2013) Study of selected factors affecting hydrate-based carbon dioxide separation from simulated fuel gas in porous media. Energy Fuels 27:3341–3348
23. Kumar R, Wu H, Englezos P (2006) Incipient hydrate phase equilibrium for gas mixtures containing hydrogen, carbon dioxide and propane. Fluid Phase Equilib 244:167–171
24. Babu P, Yang T, Veluswamy HP, Kumar R, Linga P (2013) Hydrate phase equilibrium of ternary gas mixtures containing carbon dioxide, hydrogen and propane. J Chem Thermodyn 61:58–63
25. Kumar R, Englezos P, Moudrakovski I, Ripmeester JA (2009) Structure and composition of CO_2/H_2 and $CO_2/H_2/C_3H_8$ hydrate in relation to simultaneous CO_2 capture and H_2 production. AIChE J 55:1584–1594
26. Kumar R, Linga P, Ripmeester JA, Englezos P (2009) Two-stage clathrate hydrate/membrane process for precombustion capture of carbon dioxide and hydrogen. J Environ Eng 135:411–417
27. Babu P, Kumar R, Linga P (2014) Unusual behavior of propane as a co-guest during hydrate formation in silica sand: potential application to seawater desalination and carbon dioxide capture. Chem Eng Sci 117:342–351
28. Linga P, Daraboina N, Ripmeester JA, Englezos P (2012) Enhanced rate of gas hydrate formation in a fixed bed column filled with sand compared to a stirred vessel. Chem Eng Sci 68:617–623
29. Daraboina N, Ripmeester J, Englezos P (2013) The impact of SO_2 on post combustion carbon dioxide capture in bed of silica sand through hydrate formation. Int J Greenhouse Gas Control 15:97–103
30. Fan SS, Liang DQ, Guo KH (2001) Hydrate equilibrium conditions for cyclopentane and a quaternary cyclopentane-rich mixture. J Chem Eng Data 46:930–932
31. Xu C-G, Yu Y-S, Ding Y-L, Cai J, Li X-S (2017) The effect of hydrate promoters on gas uptake. Phys Chem Chem Phys 19:21769–21776
32. Zhang JS, Lee JW (2009) Equilibrium of hydrogen + cyclopentane and carbon dioxide + cyclopentane binary hydrates †. J Chem Eng Data 54:659–661
33. Mohammadi AH, Richon D (2009) Phase equilibria of clathrate hydrates of cyclopentane + hydrogen sulfide and cyclopentane + methane. Ind Eng Chem Res 48:9045–9048
34. Zhang J, Lee JW (2009) Enhanced kinetics of CO_2 hydrate formation under static conditions. Ind Eng Chem Res 48:5934–5942

35. Herslund PJ, Thomsen K, Abildskov J, von Solms N, Galfré A, Brântuas P, Herri J-M (2013) Thermodynamic promotion of carbon dioxide–clathrate hydrate formation by tetrahydrofuran, cyclopentane and their mixtures. Int J Greenhouse Gas Control 17:397–410
36. Hughes TJ, Marsh KN (2011) Methane semi-clathrate hydrate phase equilibria with tetraisopentylammonium fluoride. J Chem Eng Data 56:4597–4603
37. Veluswamy HP, Kumar R, Linga P (2014) Hydrogen storage in clathrate hydrates: current state of the art and future directions. Appl Energy 122:112–132
38. Sales Silva LP, Dalmazzone D, Stambouli M, Arpentinier P, Trueba A, Fürst W (2016) Phase behavior of simple tributylphosphine oxide (TBPO) and mixed gas (CO_2, CH_4 and CO_2 + CH_4) + TBPO semiclathrate hydrates. J Chem Thermodyn 102:293–302
39. Li X Sen, Zhan H, Xu CG, Zeng ZY, Lv QN, Yan KF (2012) Effects of tetrabutyl-(ammonium/phosphonium) salts on clathrate hydrate capture of CO_2 from simulated flue gas. Energy Fuels 26:2518–2527
40. Xu C, Li X, Cai J, Chen Z (2012) Hydrate-based carbon dioxide capture from simulated integrated gasification combined cycle gas. J Nat Gas Chem 21:501–507
41. Kim SM, Lee JD, Lee HJ, Lee EK, Kim Y (2011) Gas hydrate formation method to capture the carbon dioxide for pre-combustion process in IGCC plant. Int J Hydrogen Energy 36:1115–1121
42. Xu C-G, Zhang S-H, Cai J, Chen Z-Y, Li X-S (2013) CO_2 (carbon dioxide) separation from CO_2–H_2 (hydrogen) gas mixtures by gas hydrates in TBAB (tetra-n-butyl ammonium bromide) solution and Raman spectroscopic analysis. Energy 59:719–725
43. Park S, Lee S, Lee Y, Seo Y (2013) CO_2 capture from simulated fuel gas mixtures using semi-clathrate hydrates formed by quaternary ammonium salts. Environ Sci Technol 47:7571–7577
44. Babu P, Yao M, Datta S, Kumar R, Linga P (2014) Thermodynamic and kinetic verification of tetra-n-butyl ammonium nitrate ($TBANO_3$) as a promoter for the clathrate process applicable to precombustion carbon dioxide capture. Environ Sci Technol 48:3550–3558
45. Li X-S, Xia Z-M, Chen Z-Y, Wu H-J (2011) Precombustion capture of carbon dioxide and hydrogen with a one–stage hydrate/membrane process in the presence of tetra-n-butylammonium bromide (TBAB). Energy Fuels 25:1302–1309
46. Li X-S, Xia Z-M, Chen Z-Y, Yan K-F, Li G, Wu H-J (2010) Gas hydrate formation process for capture of carbon dioxide from fuel gas mixture. Ind Eng Chem Res 49:11614–11619
47. Babu P, Chin WI, Kumar R, Linga P (2014) Systematic evaluation of tetra-n-butyl ammonium bromide (TBAB) for carbon dioxide capture employing the clathrate process. Ind Eng Chem Res 53:4878–4887
48. Gholinezhad J, Chapoy A (2011) Separation and capture of carbon dioxide from CO_2/H_2 syngas mixture using semi–clathrate hydrates. Chem Eng Res Des 89:1747–1751
49. Karaaslan U, Parlaktuna M (2000) Surfactants as hydrate promoters? Energy Fuels 14:1103–1107
50. Kang S-P, Lee J-W (2010) Kinetic behaviors of CO_2 hydrates in porous media and effect of kinetic promoter on the formation kinetics. Chem Eng Sci 65:1840–1845
51. Ganji H, Manteghian M, Rahimi Mofrad H (2007) Effect of mixed compounds on methane hydrate formation and dissociation rates and storage capacity. Fuel Process Technol 88:891–895
52. Kumar A, Sakpal T, Linga P, Kumar R (2013) Influence of contact medium and surfactants on carbon dioxide clathrate hydrate kinetics. Fuel 105:664–671
53. Veluswamy HP, Ang WJ, Zhao D, Linga P (2015) Influence of cationic and non-ionic surfactants on the kinetics of mixed hydrogen/tetrahydrofuran hydrates. Chem Eng Sci 132:186–199
54. Zhong Y, Rogers RE (2000) Surfactant effects on gas hydrate formation. Chem Eng Sci 55:4175–4187
55. Zhong D-L, Ding K, Yan J, Yang C, Sun D-J (2013) Influence of cyclopentane and SDS on methane separation from coal mine gas by hydrate crystallization. Energy Fuels 27:7252–7258
56. Zhang JS, Lo C, Somasundaran P, Lee JW (2010) Competitive adsorption between SDS and carbonate on tetrahydrofuran hydrates. J Colloid Interface Sci 341:286–288
57. Menger FM, Littau CA (1991) Gemini-surfactants: synthesis and properties. J Am Chem Soc 113:1451–1452

58. Kwon Y-A, Park J-M, Jeong K-E, Kim C-U, Kim T-W, Chae H-J, Lee J (2011) Synthesis of anionic multichain type surfactant and its effect on methane gas hydrate formation. J Ind Eng Chem 17:120–124
59. Li J, Liang D, Guo K, Wang R, Fan S (2006) Formation and dissociation of HFC134a gas hydrate in nano-copper suspension. Energy Convers Manag 47:201–210
60. Ghozatloo A, Shariaty-Niassar M, Hassanisadi M (2014) Effect of single walled carbon nanotubes on natural gas hydrate formation. Iran J Chem Eng 11:67–73
61. Song Y, Wang F, Liu G, Luo S, Guo R (2017) Promotion effect of carbon nanotubes-doped SDS on methane hydrate formation. Energy Fuels 31:1850–1857
62. Kim N-J, Park S-S, Kim HT, Chun W (2011) A comparative study on the enhanced formation of methane hydrate using CM-95 and CM-100 MWCNTs. Int Commun Heat Mass Transf 38:31–36
63. Wang F, Meng H-L, Guo G, Luo S-J, Guo R-B (2017) Methane hydrate formation promoted by-SO_3–coated graphene oxide nanosheets. ACS Sustain Chem Eng 5:6597–6604
64. Yu YS, Xu CG, Li XS (2018) Evaluation of CO_2 hydrate formation from mixture of graphite nanoparticle and sodium dodecyl benzene sulfonate. J Ind Eng Chem 59:64–69
65. Zhou S, Jiang K, Zhao Y, Chi Y, Wang S, Zhang G (2018) Experimental investigation of CO_2 hydrate formation in the water containing graphite nanoparticles and tetra-n-butyl ammonium bromide. J Chem Eng Data 63(2):389–394
66. Veluswamy HP, Hong QW, Linga P (2016) Morphology study of methane hydrate formation and dissociation in the presence of amino acid. Cryst Growth Des 16:5932–5945
67. Liu Y, Chen B, Chen Y, Zhang S, Guo W, Cai Y, Wang W (2015) Methane storage in a hydrated form as promoted by leucines for possible application to natural gas transportation and storage. Energy Technol 3:815–819
68. Abbasian Rad S, Rostami Khodaverdiloo K, Karamoddin M, Varaminian F, Peyvandi K (2015) Kinetic study of amino acids inhibition potential of glycine and L-leucine on the ethane hydrate formation. J Nat Gas Sci Eng 26:819–826
69. Naeiji P, Mottahedin M, Varaminian F (2014) Separation of methane–ethane gas mixtures via gas hydrate formation. Sep Purif Technol 123:139–144
70. Bhattacharjee G, Choudhary N, Kumar A, Chakrabarty S, Kumar R (2016) Effect of the amino acid l-histidine on methane hydrate growth kinetics. J Nat Gas Sci Eng 35:1453–1462
71. Roosta H, Dashti A, Mazloumi SH, Varaminian F (2016) Inhibition properties of new amino acids for prevention of hydrate formation in carbon dioxide–water system: experimental and modelling investigations. J Mol Liq 215:656–663
72. Cai Y, Chen Y, Li Q, Li L, Huang H, Wang S, Wang W (2017) CO_2 hydrate formation promoted by a natural amino acid L–methionine for possible application to CO_2 capture and storage. Energy Technology 5:1195–1199
73. Bavoh CB, Nashed O, Khan MS, Partoon B, Lal B, Sharif AM (2018) The impact of amino acids on methane hydrate phase boundary and formation kinetics. J Chem Thermodyn 117:48–53
74. Sa J-H, Kwak G-H, Lee BR, Ahn D, Lee K-H (2014) Abnormal incorporation of amino acids into the gas hydrate crystal lattice. Phys Chem Chem Phys 16:26730–26734
75. Kang S-P, Lee J, Seo Y (2013) Pre-combustion capture of CO_2 by gas hydrate formation in silica gel pore structure. Chem Eng J 218:126–132
76. Babu P, Kumar R, Linga P (2013) Medium pressure hydrate based gas separation (HBGS) process for pre-combustion capture of carbon dioxide employing a novel fixed bed reactor. Int J Greenhouse Gas Control 17:206–214
77. Kang S-P, Lee J-W, Ryu H-J (2008) Phase behaviour of methane and carbon dioxide hydrates in meso–and macro–sized porous media. Fluid Phase Equilib 274:68–72
78. Luo Y-T, Zhu J-H, Fan S-S, Chen G-J (2007) Study on the kinetics of hydrate formation in a bubble column. Chem Eng Sci 62:1000–1009
79. Xu C-G, Li X-S, Lv Q-N, Chen Z-Y, Cai J (2012) Hydrate-based CO_2 (carbon dioxide) capture from IGCC (integrated gasification combined cycle) synthesis gas using bubble method with a set of visual equipment. Energy 44:358–366

80. Liu N, Chen W, Liu D, Xie Y (2011) Characterization of CO_2 hydrate formation by temperature vibration. Energy Convers Manag 52:2351–2354
81. Kojima R, Yamane K, Aya I (2003) Dual nature of CO_2 solubility in hydrate forming region. In: 6th international conference greenhouse gas control technologies, pp 825–830
82. Xu C-G, Cai J, Li X-S, Lv Q-N, Chen Z-Y, Deng H-W (2012) Integrated process study on hydrate-based carbon dioxide separation from integrated gasification combined cycle (IGCC) synthesis gas in scaled-up equipment. Energy Fuels 26:6442–6448
83. Elistratov DS, Meleshkin AV, Pil'Nik AA, Bartashevich MV, Chernov AA, Mezentsev IV, Vlasenko MG (2017) New hydrate formation methods in a liquid-gas medium. Sci Rep 7:1–9
84. Park S-S, Kim N-J (2013) Study on methane hydrate formation using ultrasonic waves. J Ind Eng Chem 19:1668–1672

Chapter 4
Gas Hydrate Models

Behzad Partoon, S. Jai Krishna Sahith, Bhajan Lal and Abdulhalim Shah Bin Maulud

4.1 Introduction

Since the first announcement by Hammerschmidt regarding the blockage of transportation pipelines by gas hydrates, the attempt to overcome the situation was looked into [1]. The first exercises were to utilize the anti-freezing agents, such as methanol or ethylene glycol as additives to prevent the hydrate formation [2]. The presence of these chemicals in the solution was to shift the equilibrium phase boundary conditions of the gas hydrates to much lower temperatures and higher pressure. The addition of methanol to the solution shifted the gas hydrate phase boundary to the left, where gas hydrate formed at much lower temperatures and higher pressure conditions. This behaviour was due to the hydrogen bonding between the water and methanol molecules, which decreased the water activity and the tendency to form hydrate cages [3]. This group of chemicals was referred to as thermodynamic inhibitors. Thermodynamic inhibitors have been widely used in the oil and gas industry for the prevention of gas hydrate formation and blockage in the pipelines and cold processes [4]. On the other hand, some chemicals enhance the hydrate formation by shifting the phase boundary to the right. These additives are thermodynamic promoters. Thermodynamic promoters are normally captured in the hydrate crystalline structure along with the gas molecules. These molecules help to stabilize the hydrate structure at a higher temperature and/or lower pressure. In 1991, Dyadin et al. summarized the hydrate equilibrium temperature of few cyclic esters, such as trimethylene oxide, ethylene oxide, 1,3- and 1,4-dioxane, 1,3-dioxolane, and tetrahydrofuran, at low and high pressures. They claimed that these chemicals, which can form sII under atmospheric pressures, are also able to form hydrates at higher pressures with the help of small gases [5]. These stabilizing chemicals might be effectively used for storing natural gas in solid hydrate state because of their effect on the shift of hydrate forming equilibrium temperature and pressure to milder ones and the large increase in storage capacity. The attempt of predicting the impact of these additives on the gas hydrate phase boundary started with Hammerschmidt in the 1930s. It was very important for the oil and gas industries to predict the proper amount of inhibitors that was required

B. Lal and O. Nashed, *Chemical Additives for Gas Hydrates*, Green Energy and Technology, https://doi.org/10.1007/978-3-030-30750-9_4

to eliminate the risks of pipelines' blockage with gas hydrate. The Hammerschmidt formula was based on the suppression of the hydrate formation temperature in the presence of inhibitors, as shown in Eq. (4.1).

$$\Delta T = \frac{k_{\mathrm{H}} W}{M(100 - W)} \tag{4.1}$$

Although the thermodynamic-based approaches were developed in the 1950s, the suppression temperature method is still practiced due to its simplicity and acceptable accuracy. The suppression temperature is the reduction of the equilibrium temperature as a result of additives, and thus, its accuracy is tied in with the accuracy of hydrate equilibrium temperature estimation in the presence of pure samples. On the other hand, the thermodynamic models are mainly based on the equality of chemical potentials of each component in all phases. Hence, any additive to the mixture could also be included in the calculation, if required parameters for prediction of chemical potentials are available. In the following pages, the recent advances on both methods are collected and discussed.

4.2 Classic Thermodynamic Model

The first research for determining the properties of gas hydrate using a statistical thermodynamic approach was done carried out by Barrer and Stuart at 1957 [6]. With the knowledge of the crystal structure of hydrates and using a similar approach, a statistical thermodynamic model of hydrate phase equilibria was conceived by van der Waals and Platteuw at in 1959 [7]. In their work, expressions for the chemical potential of water in sI and sII hydrate structures were developed using an approach analogous to the Langmuir gas adsorption.

The classic van der Waals and Platteeuw (vdWP) model was based on the difference between the chemical potential of water in the hydrate phase μ_{w}^{H} and a hypothetical empty lattice hydrate phase (μ_{w}^{β}) as shown in Eq. (4.2).

$$\frac{\Delta\mu_{\mathrm{w}}^{H}}{RT} = \frac{\mu_{\mathrm{w}}^{\beta} - \mu_{\mathrm{w}}^{H}}{RT} = \sum_{m=1}^{2} \upsilon_{\mathrm{m}} \ln\left(1 + \sum_{i=1}^{nc} C_{\mathrm{mi}} f_{\mathrm{i}}\right) \tag{4.2}$$

where υ_{m} is the number of cages of type m in the crystalline structure, C_{mi} is the Langmuir constant of hydrate former i in the type m cage of the crystalline structure, and f_{i} is the fugacity of hydrate formers.

The vdWP model led Saito et al. [8] and Parrish and Prausnitz [9] to predict the gas hydrate equilibria by equating the chemical potential of water in hydrate, with that in the aqueous (or ice) phase and introducing an algorithm in a form suitable for use on a computer. The expression of the chemical potential of water in an aqueous or ice phase has been simplified by some researchers such as Holder et al. [10] and

John et al. [11] as shown in Eq. (4.3).

$$\frac{\Delta\mu_{\mathrm{w}}^{\alpha}}{RT}=\frac{\mu_{\mathrm{w}}^{\beta}-\mu_{\mathrm{w}}^{\alpha}}{RT}=\frac{\Delta\mu_{\mathrm{w}}^{0}}{RT}-\int_{T_0}^{T}\frac{\Delta h_{\mathrm{w}}}{RT^2}\mathrm{d}T+\int_{P_0}^{P}\frac{\Delta v_{\mathrm{w}}}{RT}\mathrm{d}P-RT\ln\left(a_{\mathrm{w}}^{\alpha}\right) \tag{4.3}$$

where α denotes liquid water or ice phase, and 0 superscript/subscripts stands for reference condition. Δh_{w} and Δv_{w} are enthalpy change and volume difference between the empty hydrate lattice and water in α phase, respectively. The parameters for Eqs. (4.2) and (4.3) are provided in Tables 4.1 and 4.2.

The impact of any additives in the mixture can be seen on three parameters of Eqs. (4.2) and (4.3), i.e. fugacity, activity of water, and Langmuir constant. The first parameter is fugacity of components in Eq. (4.2). Addition of any extra component in the mixture will change the phase equilibria, and consequently the fugacity of each component in the mixture. In the calculation of fugacity in the vdWP model, it commonly assumed that at equilibrium, the amount of hydrate particles is very small, and the system mainly consisted of two phases of vapour and liquid/solid water. Therefore, any VLE or VSE calculation with proper mixing rule could lead to an acceptable prediction of fugacity. Thus, the most critical task in the calculation of fugacity is a selection of suitable equation of state and mixing rule. While EOSs such as Peng–Robinson [12] or Soave–Redlich–Kwang [13] with van der Waals mixing

Table 4.1 Geometry of different hydrate structures and parameters used in Eqs. (4.2), (4.5), and (4.6)

Hydrate structure	Structure I		Structure II		Structure H		
	Small	Large	Small	Large	Small	Medium	Large
Cavity name	5^{12}	$5^{12}6^2$	5^{12}	$5^{12}6^4$	5^{12}	$4^35^66^3$	$5^{12}6^8$
Average radius (R) (Å)	3.91	4.33	3.9	4.68	3.94	4.04	5.79
Coordination number (z)	20	24	20	28	20	20	36
Cavities/unit cell	2	6	16	8	3	2	1
Cavities/H_2O (υ_{m})	1/23	3/23	2/17	1/17	1/12	1/18	1/36
H_2O/unit cell	46		136		36		
Crystal type	Cubic		Cubic		Hexagonal		
Lattice constant (m)	1.20×10^{-11}		1.72×10^{-11}		$a=1.22\times10^{-11}$ $c=1.01\times10^{-11}$		

Table 4.2 Thermodynamic properties of the empty hydrate lattice relative to liquid water, Eq. (4.3)

Parameter	Structure sI	Structure sII
$\Delta\mu_{\mathrm{w}}^{\circ}$ (J/mol)	1263.6	882.8
$\Delta h_{\mathrm{w}}^{ol}$ (J/mol)	−4858.9	−5202.2
$\Delta v_{\mathrm{w}}^{l}$ (cm^3/mol)	4.6	5.0
ΔC_{Pw} (J/mol K)	$-38.12+0.141(T-273.15)$	

rule can be used for hydrocarbon systems, for more complex systems, including electrolytes or very polar components, a more advanced equation of state, such as Valderrama–Patel–Teja [14], Nasrifar–Bolland [15], CPA [16], or statistical associating fluid theory (SAFT) equations of state [17], leads to better prediction. Moreover, the G-excess mixing rules such as MHV1 [18] or MHV2 [19] would increase the accuracy of fugacity calculations.

The second parameter is the activity of water, which is presented in Eq. (4.3). The water activity will change significantly in the presence of additives, especially thermodynamic hydrate inhibitors. Therefore, to predict the impact of these additives on the hydrate equilibria, it is important to calculate the water activity quite accurate. This is not an easy task, as hydrate equilibrium involves multicomponents system at high-pressure and low-temperature conditions and most of activity models are designed for low pressures and binary systems. However, combining VLE calculation with G-excess mixing rules and exploitation of a predictive activity model such as UNIFAC or UNIQUAC could lead to reasonable accuracy in calculation of water activity in the liquid phase.

The third parameter, which is the Langmuir constant, is more important for systems containing thermodynamic promoters. While the majority of thermodynamic inhibitors are not involving in the crystalline structure of gas hydrate, some of the promoters either work as hydrate formers (e.g. tetrahydrofuran, acetone, 1-4 dioxane [20]) or as part of crystalline building blocks (e.g. tetra-n-butyl ammonium bromide [21]). While prediction of hydrate formation condition in the presence of second group is needed more complicated modelling, the first group, i.e. that work as hydrate formers, can be predicted by considering as a hydrate former. This includes calculating fugacity, activity, and Langmuir constant for these chemicals.

To calculate the Langmuir constant, two methods are generally used in literature. The first and easier method was developed by Parrish and Prausnitz [9] which is a correlation suitable for the temperature range of 260–300 K, as shown in Eq. (4.4)

$$C_{\mathrm{m,i}}(T) = \left(A_{\mathrm{m,i}}/T\right)\exp\left(B_{\mathrm{m,i}}/T\right) \tag{4.4}$$

The values for $A_{\mathrm{m,i}}$ and $B_{\mathrm{m,i}}$ parameters are given for each hydrate former i that filled cavity type m in either structure sI or sII by Parrish and Prausnitz [9] and presented in Table 4.3.

The more accepted method is based on the intermolecular interaction between hydrate former and water molecules in a hydrate cavity, Van der Waals and Platteeuw by using Lennard–Jones–Devonshire cell theory to calculate the Langmuir constant, as shown in Eq. (4.5).

$$C_{\mathrm{m,i}}(T) = 4\frac{\pi}{kT}\int_{0}^{R_{\mathrm{m}}-2a_i}\exp\left[-\frac{\omega_{\mathrm{m,i}}(r)}{kT}\right]r^2\mathrm{d}r \tag{4.5}$$

Table 4.3 Parameters for calculating Langmuir constants by Eq. (4.4) between 260 and 300 K

Guest	Structure I				Structure II			
	Small (K)		Large (K)		Small (K)		Large (K)	
	$A_{m,i} \times 10^3$	$B_{m,i} \times 10^{-3}$	$A_{m,i} \times 10^3$	$B_{m,i} \times 10^{-3}$	$A_{m,i} \times 10^3$	$B_{m,i} \times 10^{-3}$	$A_{m,i} \times 10^3$	$B_{m,i} \times 10^{-3}$
Nitrogen	3.8087	2.2055	18.42	2.3013	3.0284	2.175	75.149	1.8606
Carbon dioxide	1.1978	2.8605	8.507	3.2779	0.9091	2.6954	48.262	2.5718
Methane	3.7237	2.7088	18.372	2.7379	2.956	2.6951	76.068	2.2027
Ethane	0	0	6.906	3.6316	0	0	40.818	3.0384
Propane	0	0	0	0	0	0	12.353	4.4061
Isobutane	0	0	0	0	0	0	1.573	4.453
Ethylene	0.083	2.3969	5.448	3.66638	0.0641	2.0425	34.94	3.1071
Propylene	0	0	0	0	0	0	20.174	4.0057
Hydrogen sulphide	3.0343	3.736	16.74	3.6109	2.3758	3.7506	73.631	2.8541

where k is the Boltzmann constant, $\omega(r)$ is the spherically symmetric cell potential that is a function of cell radius, r, and T is the absolute temperature. R_m is the type m cavity radius and ai is the hydrate former i core radius. Parrish and Prausnitz recommend the Kihara theory for calculation of cell potential, as shown in Eq. (4.6).

$$\omega_{m,i}(r) = 2z_m\epsilon_i\left[\frac{\sigma_i^{12}}{R_m^{11}r}\left(\delta^{10} + \frac{a_i}{R_m}\delta^{11}\right) - \frac{\sigma_i^6}{R_m^5 r}\left(\delta^4 + \frac{a_i}{R_m}\delta^5\right)\right] \tag{4.6}$$

where ε_i is the minimum potential, $\sigma_i + 2\ a_i$ is the collision diameter, z_m is the coordination number of each cavity, and δ^N is calculating with Eq. (4.7) for N equals to 4, 5, 10, and 11.

$$\delta^N = \frac{\left[\left(1 - \frac{r}{R_m} - \frac{a_i}{R_m}\right)^{-N} - \left(1 + \frac{r}{R_m} - \frac{a_i}{R_m}\right)^{-N}\right]}{N} \tag{4.7}$$

ε_i, σ_i, and a_i are the Kihara potential parameters that are optimized with hydrate equilibrium data and given for each hydrate former. The values for common hydrate formers are given in Table 4.4. The z_m and R_m values also given in Table 4.1.

Table 4.4 Kihara parameters of common hydrate formers and thermodynamic promoters [22]

Component	a (Å)	σ (Å)	$\bar{\varepsilon}/\mathrm{k}$ (K)
Nitrogen	0.3526	3.0124	125.15
Carbon dioxide[a]	0.6358	2.9681	169.09
Methane	0.3834	3.1650	154.54
Ethane	0.5651	3.2641	176.40
Propane	0.6502	3.3093	203.31
Isobutane	0.8706	3.0822	225.16
Ethylene	0.4700	3.2910	172.87
Propylene	0.6500	3.2304	202.42
Hydrogen sulphide	0.3600	3.1530	204.85
THF[a]	0.8830	3.0020	301.95
Acetone[a]	0.96785	2.9297	283.62

[a]Optimized values [23]

4.3 Suppression Temperature Models

As mentioned before, the hydrate equilibrium temperature gradually reduces in the presence of inhibitors due to the intermolecular interaction between these chemicals and water molecules. From a thermodynamic point of view, these interactions reduce the water molecule's activity. Pieroen [24] formulated a relationship between enthalpy of hydrate formation, water activity, and suppression temperature, as shown in Eq. (4.8).

$$\ln(a_{\mathrm{w}}) = \frac{-\Delta H^{\mathrm{d}}}{n_{\mathrm{H}} R}\left(\frac{1}{T} - \frac{1}{T_{\mathrm{w}}}\right) \tag{4.8}$$

In this equation, a_{w} is the water activity in the presence of additives, n_{H} is the hydration number and ΔH^{d} is the enthalpy of hydrate dissociation, and T and T_{w} are the hydrate equilibrium temperature in the presence of additives and pure water, respectively. Since the values of a_{w}, n_{H}, and ΔH^{d} cannot be easily calculated, Pieroen showed that by a good approximation, this equation could be simplified to calculate the suppression temperature, as shown in Eq. (4.9).

$$\Delta T = -\frac{n_{\mathrm{H}} R T_0^2}{\Delta H^{\mathrm{d}}} \frac{18W}{M(100 - W)} \tag{4.9}$$

Equation (4.9) is very similar to Eq. (4.1) that was developed by Hammerschmidt based on the experimental data. Later, Maddox et al. [25] used the Pireroen formula to calculate the hydrate equilibrium temperature in the presence of alcohols. They suggested using Margules's equation for calculating the activity coefficient of water, as shown in Eq. (4.10). Additionally, they developed a model to calculate $\Delta H^{\mathrm{d}}/n_{\mathrm{H}}R$, as presented in Eq. (4.11).

$$\ln(\gamma_w) = (1 - x_w)^2[B + 2x_w(A - B)] \tag{4.10}$$

$$\frac{\Delta H^d}{n_H R} = \frac{-2063}{\alpha + \frac{\beta P}{1000} + \delta \ln P} \tag{4.11}$$

In these equations, A and B are the Margules constant for each electrolyte or alcohol, x_w is the mole fraction of water in the solution, and α, β, and δ are the coefficients that encounter the pressure dependency of enthalpy of hydrate dissociation. Later, Javanmardi et al. [26] modified the enthalpy equation and included the ionic strength of solution in order to use this method for electrolytes system.

$$\frac{\Delta H^d}{n_H R} = \frac{e_1 I^{e_2}}{1 + e_3 P + e_4 \ln P} \tag{4.12}$$

In this equation, I is ionic strength and e_1 to e_4 are global constants. Javanmardi and his co-workers [26, 27] calculated the coefficients' value by fitting the equilibrium data of different gas hydrate system in the presence of various electrolytes. Later, Nasrifar et al. [28] optimized the parameters of Eq. (4.12) by increasing the database. Partoon et al. [29] also extended the model to ionic liquid systems. However, they provided another set of parameters for ionic liquids. The coefficients of Eq. (4.12) are presented in Table 4.5.

Javanmardi et al. suggested to use more complicated model of Pitzer and Mayorga [30], as shown in Eqs. (4.13)–(4.17).

$$\ln a_w = \frac{-vmM_w}{\varphi} \tag{4.13}$$

$$-1 = \left|z^+ z^-\right| f^\varphi + m\left(\frac{2v^+v^-}{v}\right)\beta^\varphi_{MX} + m^2\left(\frac{2\left(v^+v^-\right)^{\frac{3}{2}}}{v}\right)C^\varphi \tag{4.14}$$

$$f^\varphi = -A_\varphi \frac{I^{\frac{1}{2}}}{1 + bI^{\frac{1}{2}}} \tag{4.15}$$

$$\beta^\varphi_{MX} = \beta^{(0)} + \beta^{(1)} \exp\left(-aI^{\frac{1}{2}}\right) \tag{4.16}$$

Table 4.5 Parameters of Eq. (4.12)

Parameter	Electrolytes [26]	Electrolytes [28]	Ionic liquids [29]
e_1	597.33	1000.0	222.24
e_2	-4.090×10^{-2}	1.237×10^{-2}	-7.796×10^{-2}
e_3	2.270×10^{-5}	-1.205×10^{-2}	3.854×10^{-5}
e_4	-7.510×10^{-2}	4.073×10^{-2}	2.530×10^{-2}

$$I = 0.5 \sum m_i z_i^2 \tag{4.17}$$

In these equations, φ is the osmotic coefficient, M_w is water molecular weight, v^+ and v^- are number of ions in the salt formula, and z^+ and z^- are number of cation and anion charges, respectively. Also, $v = v^+ + v^-$, m is the conventional molality of each ion (anion and cation) and z_i is the number of each cation and anion charges. As suggested by Pitzer and Mayorga, $a = 2$ and $b = 1.2$ for all electrolytes. $\beta^{(0)}$, $\beta(1)$ and C^{φ} are model parameters that are available for each electrolyte. The parameter A_{φ} is the Debye–Hückel coefficient. Javanmardi et al. [26] used a value of 0.392 for water at 25 °C in their study; however, A_{φ} is a weak function of temperature. Therefore, Partoon et al. [29] suggested to use the temperature-dependent Debye–Hückel coefficient, as presented in Eq. (4.18) [31], for calculating the activity coefficient.

$$A_{\varphi} = 0.3769 + 0.0005(T - 273.15) + 0.000004(T - 273.15)^2 \tag{4.18}$$

The described method, however, is limited to a single additive. For a mixture of electrolytes, Nasrifar et al. [28] suggested to use Patwarthan and Kumar's [32] mixing rule for activity coefficient, as shown in Eq. (4.19).

$$\ln a_w = \sum_k \left(m_k / m_k^0\right) \ln a_{w,k}^0 \tag{4.19}$$

In addition, Nasrifar et al. [28] suggested another mixing rule for a mixture containing both electrolytes and alcohols, as it is the most probable case for real application of inhibitors in the oil and gas transportation pipelines. First, for calculating the water activity, Nasrifar et al. [28] suggested that the non-idealistic reasoning to suppress water in the presence of electrolytes and alcohols are independent. Therefore, the total non-idealistic factor is cumulative, as shown in Eq. (4.20).

$$\ln a_{w,mix} = \ln a_{w,el} + \ln a_{w,al} \tag{4.20}$$

where $a_{w,mix}$ the is calculated be Eq. (4.14) and $a_{w,al}$ is calculated by Eq. (4.10). In addition, the enthalpy of hydrate dissociation for the mixture of electrolytes and alcohols are calculated by Eq. (4.21).

$$\left(\frac{\Delta H^d}{n_H R}\right)_{mix} = \frac{2\left(\frac{\Delta H^d}{n_H R}\right)_{el}\left(\frac{\Delta H^d}{n_H R}\right)_{al}}{\left(\frac{\Delta H^d}{n_H R}\right)_{el} + \left(\frac{\Delta H^d}{n_H R}\right)_{al}} \tag{4.21}$$

where $\left(\frac{\Delta H^d}{n_H R}\right)_{al}$ and $\left(\frac{\Delta H^d}{n_H R}\right)_{el}$ are calculated by Eqs. (4.11) and (4.12), respectively.

Another approach for the calculation of hydrate suppression temperature was developed by Dickens and Quinby-Hunt [33]. The model considered the Pieroen

equation (Eq. 4.8) as the base for calculation for the suppression temperature. However, as the calculation of the activity coefficient was complicated, they suggested to use the freezing point suppression temperature instead of activity coefficient, as shown in Eq. (4.22).

$$\ln a_{\mathrm{w}} = \frac{\Delta H_{\mathrm{Fus}}}{R}\left(\frac{1}{T_{\mathrm{f}}^{0}} - \frac{1}{T_{\mathrm{f}}}\right) \tag{4.22}$$

where ΔH_{Fus} is the enthalpy of fusion of pure water, T_{f}^{0} is the ice point and is the suppressed melting point of solution. Combining Eqs. (4.8) and (4.22), the activity of water in the presence of additives is eliminating from the formula, as presented in Eq. (4.23), resulting in simpler method for prediction of hydrate suppression temperatures.

$$\left(\frac{1}{T_{\mathrm{w}}} - \frac{1}{T}\right) = \frac{n_{\mathrm{h}}\Delta H_{\mathrm{Fus}}}{\Delta H^{\mathrm{d}}}\left(\frac{1}{T_{\mathrm{f}}^{0}} - \frac{1}{T_{\mathrm{f}}}\right) \tag{4.23}$$

However, as the activity calculations are well developed for electrolytes and alcohols, other researchers have not practiced the model. Nonetheless, recently, Bavoh et al. [34] and later Khan et al. [35] showed the potential of this model for calculation of the hydrate suppression temperature in the presence of natural amino acids and ionic liquid, where the activity coefficient cannot be estimated due to the presence of electrolytes and alcohols.

The Pieroen formula was also used to predict the hydrate equilibrium temperature in the presence of acetone by Mainusch et al. [36]. The major modification in this model was in the calculation of $\Delta H^{\mathrm{d}} \big/ n_{\mathrm{H}} R$, as shown in Eq. (4.24).

$$\frac{\Delta H^{\mathrm{d}}}{n_{\mathrm{H}} R} = \frac{-31.3 - \left(3.0 \times 10^{3}\right)x_{\mathrm{a}} - \left(3.7 \times 10^{5}\right)x_{\mathrm{a}}^{4.5} + \left(3.36 \times 10^{8}\right)x_{\mathrm{a}}^{13.5}}{1 - \left(9.3 \times 10^{-2}\right)\ln\left(P \big/ P^{\circ}\right)} \tag{4.24}$$

where x_{a} is the mole fraction of acetone in the mixture and P is the system pressure. The P^{0} is the reference pressure and is equal to 1 kPa. The activity coefficient of water in the presence of acetone was calculated using the van Laar equation [36]. However, this formula can only be used for CH_4 hydrates, where the acetone acts as promoter, while, for other gases like CO_2, it can act as inhibitor. Partoon [23] modified the Pieroen formula to adapt it for other hydrate thermodynamic promoters, i.e. water soluble hydrate hydrocarbons, by introducing the polarity index ratio in the calculation as shown in Eq. (4.25) and (4.26).

$$\ln(a_{\mathrm{w}}) = \frac{-\Delta H^{\mathrm{d}}}{n_{\mathrm{H}} R}\mathrm{PIC}\left(\frac{1}{T} - \frac{1}{T_{\mathrm{w}}}\right) \tag{4.25}$$

$$\mathrm{PIC} = 10\left(\sum_{i=1}^{nc} j_i.\mathrm{PIR}.\ln\left[\frac{1-x_i}{\sum_{\substack{j=1\\ j\neq w}}^{nc} x_j}\right]\right) \tag{4.26}$$

$$\mathrm{PIR} = \ln\left(\frac{2\mathrm{PI}_i + 1}{\mathrm{PI}_w}\right) \tag{4.27}$$

where PI_i is the polarity index of solvent and PI_w is the polarity index of water which is equal to 10.2 [37]. x_i is the mole fraction of gases in the pure water at hydrate equilibrium temperature and pressure. j_i is an index number that shows the impact of solvent on the pure gas hydrate. The value of j_i is equal to $+1$ if the impact of solvent on pure gas i hydrate is promotion and is equal to -1 if the solvent acts as inhibitor for gas i hydrate. Finally, the enthalpy of the hydrate disassociation is calculated using Eq. (4.28).

$$\frac{\Delta H^{\mathrm{d}}}{n_{\mathrm{H}} R} = \frac{-56.7 + a x_{\mathrm{a}} + b x_{\mathrm{a}}^{\mathrm{PI}} + c x_{\mathrm{a}}^{2\mathrm{PI}}}{1 + d\ln(P/P^{\circ})} \tag{4.28}$$

4.4 Kinetic Models for Growth of Gas Hydrates

The growth of gas hydrates usually takes place after nucleation and is a complex phenomenon as it includes multiphase studies at various levels of research. On a macroscopic scale, the kinetics of gas hydrate growth usually depends on the mole consumption rate of gases. At the microscopic level, the growth of gas hydrates can be quantified as:

1. Mass transfer of H_2O and gases for the growth of hydrate surface.
2. Transportation of exothermic heat produced during crystal growth of gas hydrates.
3. The intrinsic kinetics of gas hydrates growth.

Based on all these factors, the structure of gas hydrates has been classified.

A substantial amount of literature has been published (Table 4.6) in which all major gas hydrate growth models on kinetics are displayed since 1980. Most of these models that are mentioned here are not developed from the principles, and most of them cover the multiphase patterns. Moreover, there is no uniform model, which covers all the significant aspects of kinetics of growth of gas hydrates. So, still, there is a significant research contribution that needs to be made in this area.

Table 4.6 Summary of kinetic growth models

Controlling mechanism	Model features/driving force/rate equation	References	Chemical combination
Reaction kinetics	Arrhenius-type rate equation $r = Aa_s \exp\left(-\frac{\Delta E_a}{RT}\right)\exp\left(-\frac{a}{\Delta T^b}\right)P^\gamma$ The reaction rate law for first order (mole fraction) $r = K_R * x_G(t)$ Pseudo-reactions that are elementary and included with rate constants Arrhenius-type rate equation with sub cooling as the driving force $r = uk_1 \exp\left(-\frac{k_2}{RT}\right)A_s\left(T_{eq} - T_{sys}\right)$	[38, 39] [40] [41–43]	CH_4 + Glycol C_2H_6 + Glycol CO_2 + Ethylene Glycol CH_4 + Methanol
Mass transfer	Model due to concentration difference between phases of gas and liquid Fugacity difference if gas phase with population balance model $r = \sum_1^2 K_j^* A_p\left(f - f_{eq}\right)_j$ Concentration difference of CH_4 between the oil phase and equilibrium $r = k_{g-0}A_{g-0}\left(C^{eq}_{CH4,0} - C_{CH4,0}\right)$ Model due to concentration difference (advanced nucleation) $r = k_g\left(C_b - C_{eq}\right)$	[44, 45] [46] [47] [48, 49]	CH_4,C_2H_6 CH_4 + Glycol C_2H_6 + Glycol CO_2 + Glycol CH_4 + Methanol CH_4 + Glycol
Heat transfer	1D H.T model due to conduction 1D H.T model due to conduction and convection $v_f\delta = \Delta T^{3/2}$ 1D H.T model due to convection $v_f\delta = \psi \Delta T^{5/2}$ 2D H.T model due to conduction	[50–53]	CO_2 CO_2 CH_4, C_2H_4, CH_4 + C_2H_4 CO_2

(continued)

Table 4.6 (continued)

Controlling mechanism	Model features/driving force/rate equation	References	Chemical combination
Models based on kinetic reactions and mass transfer	Concentration difference with mass transfer and reaction kinetics $r = K\left(C_{\text{sol}} - C_{\text{eq}}\right)$ $\frac{1}{K} = \frac{1}{k_{\text{L}} A_{\text{g}}} + \frac{1}{k_{\text{S}} A_{\text{C}}}$ Mass transfer at liquid–vapour interface and reaction kinetics $r = \frac{1}{A_{\text{p}}}\left(\frac{1}{k_{\text{H-L}}} + \frac{1}{k_{\text{r}}}\right) + \frac{1}{k_{\text{G-L}}}$ Shrinking core model with diffusion or reaction coupled $(1-\alpha)^{1/3} = \left(-\frac{(2k)^{1/2}}{r_0}\right)(t-t^*)^{1/2} + (1-\alpha^*)^{1/3}$ Molecular diffusion with first-order formation kinetics of water Molecular diffusion with first-order formation and dissociation kinetics of H_2O Molecular diffusion with first-order formation kinetics of CO_2 Reaction-limited and diffusion-limited schemes with induction time	[54] [55] [56–58] [59–62] [63] [64]	CH_4 + Methanol C_3H_8 + MEG $CH_4 + H_2O$ $CH_4 + D_2O$ CO_2 $CO_2(LCO_2)$, CO_2 CO_2 $CH_4 + CaCl_2$
Models based on kinetic reactions and heat transfer	Kinetic rate joined with H.T. model $\frac{\mathrm{d}X}{\mathrm{d}t} = \frac{\Delta T}{\rho_{\text{h}} \lambda\left(\frac{1}{k\Delta T^n} + \frac{1}{h_{\text{avg}}(t)}\right)}$ Surface kinetic rate joined with H.T. model $\frac{\mathrm{d}X}{\mathrm{d}t} = \frac{T_{\text{eq}} - T_{\text{bulk}}}{\frac{\Delta H}{k_{\text{h}} A_{\text{h}}} + \frac{1}{k_{\text{r}} A_{\text{r}}}}$ Kinetic rate joined with a heat convection model $\frac{\mathrm{d}X}{\mathrm{d}t} = \frac{T_{\text{eq}} - T_{\text{bulk}}}{\rho_{\text{h}} \lambda\left(\frac{1}{k} + \frac{1}{h}\right)}$ Equilibrium model in sandy porous medium	[65] [66] [67] [68–71]	Tetrahydrofuran CH_4, CO_2 CH_4 + Diesel Oil CH_4
Fluid flow heat flow and reaction kinetics	Kinetic rate equation of hydrate formation and hydrate dissociation Kinetic rate equation based on the model of Kim et al. Simple slug flow model joined with kinetic rate and heat flow	[72] [73]	CH_4, CO_2 CH_4 CH_4

4.4.1 Models Based on Chemical Reaction

Experiments were conducted for investigation of the kinetics of growth rate of gas hydrates of methane and ethane, and a two-step procedure is described which starts with the formation of the crystal due to the interface between gas and water molecules. The following is the three-step rate equations that are considered as the Arrhenius equations:

$$M + H_2O + (H_2O)_{y-1} \rightleftarrows M \ldots (H_2O)_y \tag{4.29}$$

$$M + H_2O + M(H_2O)_z \rightleftarrows M.(H_2O)_c \tag{4.30}$$

$$M + H_2O + M(H_2O)_m \rightleftarrows M \ldots (H_2O)_n \tag{4.31}$$

By a combination of these equations, the rate of hydrate formation is termed as follows:

$$r = k_r a_s [H_2O]^m [H_2O]_c^n [M]^q \tag{4.32}$$

where

k_r	constant of reaction rate for lumped Arrhenius type
a_s	total surface area of the gas–water interface
m, n, and q	parameters indicating the order of reaction for each component
c	critical cluster size.

This kinetic model is adopted by many researchers in later years to study the rate of growth of gas hydrates. These studies included bubble theory in deep sea conditions that affect gas hydrate formation. This bubble theory was further used to analyse blow-out conditions of oil wells in the presence of water. Later, this model is further improved by the addition of heat and mass balance equations alongside considering the drag effect of a slug on the multiphase flow. Later around 1993, research interest was concentrated on liquid water approach with CH_4 gas to analyse the kinetics of gas hydrate growth. A critical model was proposed with five elemental processes considering three-step analysis of hydrate formation:

1. The dissolution of CH_4 gas into H_2O phase
2. The build-up of CH_4 hydrate precursor
3. The growth of CH_4 hydrate by an autocatalytic process.

This model was also accounted for in the development of a kinetic model for analysis of gas hydrate formation in oil-dominated systems. These intrinsic models are used and impended into commercial software like CSMhyk for analysis of different hydrate formation kinetics.

The concentration shifted slowly from CH_4 to CO_2 with the time. The study of carbon dioxide hydrates came into importance and studies mentioned that the hydrate

growth is dependent on interfacial temperatures and pressures of phases. Experimental results were claimed that the multiphase flow regimes affect the rate of formation of gas hydrates. Also, studies presented displayed that the kinetic models based on heat transfer and mass transfer are not much different when it comes to results of the kinetics of growth rate of gas hydrates. However, some of the models are unclear, and many errors were still included in the model due to the difficulty in predicting the accuracy of gas–liquid interphase. Moreover, the models developed based on experimental results have a limitation as many of them are apparatus dependent. They might not be applicable to real-time systems as their capacity is higher compared to laboratory scale equipment. Later, an advanced model proposed by Lekvam et al. states that the rate of reaction can be estimated and validated by means of vital statistics. This helps as a significant model that reduces the research gap between the microscopic and macroscopic level of study on the kinetics of gas hydrates. It also can be displayed as the proof for the representation of "chemical reaction" for the formation of gas hydrates.

4.4.2 Models Based on Mass Transfer

The reported kinetic model was proposed in 1987 with referring to the methane and ethane gas hydrates. The major part of their study was reported because of the fugacity differences dissolved gas and multiphase hydrate equilibrium at a constant temperature *T*. the model was developed based on the theory of the growth of crystallization of gas hydrates. Surprisingly, this model gave a very less dependence on *T*, unlike chemical reaction models. According to the proposed model, the following two consecutive steps of hydrate particle growth were proposed:

- Diffusion of the dissolved gas from the bulk of solution to the crystal–liquid interface
- Adsorption process that incorporates the gas molecules into the water molecules and the subsequent stabilization of the framework of the structured water.

An assumption is made in this model about the shape of the hydrate particles which are spherical and uniformly distributed. The fugacity changed from initial stages to final stages in diffusion and adsorption layers, and the difference between initial and final conditions can be termed as an overall driving force. The rate of growth of hydrate particles can be found by:

$$\frac{\mathrm{d}n}{\mathrm{d}t} = K^* A_\mathrm{p}\left(f_\mathrm{b} - f_\mathrm{eq}\right) \tag{4.33}$$

$$\frac{1}{K^*} = \frac{1}{K_\mathrm{r}} + \frac{1}{K_\mathrm{d}} \tag{4.34}$$

where

A_p surface area of hydrate particle
K^* overall kinetic rate constant
K_r Rate of reaction due to adsorption
K_d mass transfer rate.

The overall rate of reaction for all included particles can be found by integrating each particle of all sizes. It can be found by

$$R_y(t) = \int_0^\infty \left(\frac{dn}{dt}\right) \varnothing(r,t)dr = 4\pi K^* \mu_2 \left(f - f_{eq}\right) \tag{4.35}$$

$$\mu_2 = \int_0^\infty r^2 \varnothing(r,t)dr \tag{4.36}$$

where $\varnothing$ is the particle size of hydrate and μ_2 is the second moment of the particle size.

When the gas phase encounters liquid phase, two-film theory was adopted. In this theory, quasi-steady-state condition is considered. Thus, the diffusion rate of gas from the interface of gas–liquid was balanced. The mass balance of gas molecules is given by:

$$D\frac{d^2C}{dy^2} = 4\pi K * \mu_2(t)\left(f - f_{eq}\right) \tag{4.37}$$

B.C. 1: $C_{(0)} = C_{eq}$
B.C. 2: $C_{(\delta)} = C_b$
where "δ" = liquid film thickness.

After adopting Henry's law of fugacity to develop a profile of fugacity of the gas, the flux of gas that is being transported can be derived by

$$f_{(y)} = f_{eq} + \left(\frac{1}{\sin h\gamma}\right)\left\{\left(f_g - f_{eq}\right)\sin h\left(\gamma\left(1 - \frac{y}{\delta}\right)\right) + \left(f_b - f_{eq}\right)\sin h\left(\gamma\frac{\gamma}{\delta}\right)\right\} \tag{4.38}$$

$$\frac{dn}{dt} = J_{y=0}A_{g-1} = \left(\frac{D^*\gamma A_{g-1}}{\delta}\right)\frac{\left(\left(f_g - f_{eq}\right)\cos h\gamma - \left(f_b - f_{eq}\right)\right)}{\sin h\gamma} \tag{4.39}$$

$$\gamma = \delta\sqrt{\frac{4\pi K^*\mu_2}{D^*}} \tag{4.40}$$

$$D^* = \frac{DC_{wo}}{H} \tag{4.41}$$

where

γ Hatta number
H Henry's law constant
D diffusion coefficient
C_{wo} initial water concentration
f_g fugacity of pure gas
f_b gas fugacity of liquid bulk.

Alongside these advanced studies, many more studies on the kinetics of gas hydrates have been done. Some of them are kinetic models that are developed using concentration difference between gases, models that are based on the combination of mass and heat transfer due to chemical reactions of gas and fuels during hydrate formation. Some studies also covered the kinetics of gas hydrates in porous media.

So, as discussed in this chapter from the past 30 years, considerable progress has been made regarding the study of the kinetics of gas hydrate growth. In brief, this chapter covered most of the significant kinetic models that involve various combinations regarding the growth of gas hydrates. This will serve as a reference for the development of advanced models in future. Interestingly, among all the models discussed, none of them covered both physical behaviours of the formation of gas hydrates. So, still, there is a need for the united kinetic growth model proposal. This unified model should cover all the physical parameters that influence the kinetics of gas hydrates. Even though many models that are developed are used industrially, still there is a lack of accuracy when scaling them upon more extensive apparatus. So, by the study done here, a next-generation model can be made to bridge the gap between the applications of the developed models on an industrial perspective.

References

1. Hammerschmidt EG (1934) Formation of gas hydrates in natural gas transmission lines. Ind Eng Chem 26:851–855
2. Campbell JM (1992) Gas conditioning and processing-volume 2: the equipment modules. Campbell Petroleum Series.
3. Sloan ED, Koh CA (2008) Clathrate hydrates of natural gases third edition. CRC Press, Boca Raton, p 119
4. Carroll JJ (2009) Natural gas hydrates: a guide for engineers, 2nd edn. Gulf Professional Publishing, Burlington
5. Dyadin YA, Zhurko FV, Bondaryuk IV, Zhurko GO (1991) Clathrate formation in water-cyclic ether systems at high pressures. J Incl Phenom Mol Recogn Chem 10(1):39–56
6. Barrer RM, Stuart WI (1957) Non-stoichiometric clathrate compounds of water. Proc R Soc Lond Ser A. Math Phys Sci 243(1233):172–189
7. Waals JVD, Platteeuw JC (1958) Clathrate solutions. Adv Chem Phys 1–57
8. Saito S, Marshall DR, Kobayashi R (1964) Hydrates at high pressures: Part II. Application of statistical mechanics to the study of the hydrates of methane, argon, and nitrogen. AIChE J 10(5):734–740
9. Parrish WR, Prausnitz JM (1972) Dissociation pressures of gas hydrates formed by gas mixtures. Ind Eng Chem Process Des Dev 11:26–35

10. Holder GD, Corbin G, Papadopoulos KD (1980) Thermodynamic and molecular properties of gas hydrates from mixtures containing methane, argon, and krypton. Ind Eng Chem Fundam 19:282–286
11. John VT, Papadopoulos KD, Holder GD (1985) A generalized model for predicting equilibrium conditions for gas hydrates. AIChE J 31:252–259
12. Peng DY, Robinson DB (1976) A new two-constant equation of state. Ind Eng Chem Fundam 15:59–64
13. Soave G (1972) Equilibrium constants from a modified Redlich-Kwong equation of state. Chem Eng Sci 27:1197–1203
14. Valderrama JO (1990) A generalized Patel-Teja equation of state for polar and nonpolar fluids and their mixtures. J Chem Eng Jpn 23:87–91
15. Nasrifar K, Bolland O (2006) Simplified hard-sphere and hard-sphere chain equations of state for engineering applications. Chem Eng Commun 193(10):1277–1293
16. Kontogeorgis GM, Voutsas EC, Yakoumis IV, Tassios DP (1996) An equation of state for associating fluids. Ind Eng Chem Res 35:4310–4318
17. Chapman WG, Gubbins KE, Jackson G, Radosz M (1989) SAFT: equation-of-state solution model for associating fluids. Fluid Phase Equilibria 52:31–38
18. Michelsen ML (1990) A modified Huron-Vidal mixing rule for cubic equations of state. Fluid Phase Equilibria 60:213–219
19. Dahl S, Michelsen ML (1990) High-pressure vapor-liquid equilibrium with a UNIFAC-based equation of state. AIChE J 36:1829–1836
20. Saito Y (1996) Methane storage in hydrate phase with water soluble guests. In: Proceedings of 2nd international conference on natural gas hydrates, Toulouse, France, 2, pp 459–465
21. Oyama H, Shimada W, Ebinuma T, Kamata Y, Takeya S, Uchida T, … Narita H (2005) Phase diagram, latent heat, and specific heat of TBAB semiclathrate hydrate crystals. Fluid Phase Equilibria 234:131–135
22. Sloan Jr ED, Koh CA (2007) Clathrate hydrates of natural gases. CRC Press, Boca Raton
23. Partoon B (2017) Separation of carbon dioxide and methane via hydrate formation with utilization of modified spray reactor and thermodynamic promoters. Ph.D. Chemical Engineering Department, Universiti Teknologi PETRONAS, Perak, Malaysia
24. Pieroen AP (1955) Gas hydrates-approximate relations between heat of formation, composition and equilibrium temperature lowering by "inhibitors". Recl Des Trav Chim Des Pays-Bas 74:995–1002
25. Maddox RN, Moshfeghian M, Lopez E, Tu CH, Shariat A, Flynn AJ (1991) Predicting hydrate temperature at high inhibitor concentration. In: Proceedings of Laurance Reid gas conditioning conference, Norman, Oklahoma, pp 273–294
26. Javanmardi J, Moshfeghian M, Maddox RN (1998) Simple method for predicting gas-hydrate-forming conditions in aqueous mixed-electrolyte solutions. Energy Fuels 12:219–222
27. Javanmardi J, Moshfeghian M, Maddox RN (1997) Simple method for predicting gas-hydrate-forming conditions in aqueous mixed-electrolyte solutions, 521–524
28. Nasrifar K, Moshfeghian M, Maddox RN (1998) Prediction of equilibrium conditions for gas hydrate formation in the mixtures of both electrolytes and alcohol. Fluid Phase Equilibria 146:1–13
29. Partoon B, Wong NM, Sabil KM, Nasrifar K, Ahmad MR (2013) A study on thermodynamics effect of [EMIM]-Cl and [OH-C2MIM]-Cl on methane hydrate equilibrium line. Fluid Phase Equilibria 337:26–31
30. Pitzer KS, Mayorga G (1993) Thermodynamics of electrolytes.: II. Activity and osmotic coefficients for strong electrolytes with one or both ions univalent. In: Molecular structure and statistical thermodynamics: selected papers of Kenneth S Pitzer, pp 396–404
31. Zemaitis Jr JF, Clark DM, Rafal M, Scrivner NC (2010) Handbook of aqueous electrolyte thermodynamics: theory & application. Wiley, New York
32. Patwardhan VS, Kumar A (1986) A unified approach for prediction of thermodynamic properties of aqueous mixed-electrolyte solutions. Part I: vapor pressure and heat of vaporization. AIChE J 32:1419–1428

33. Dickens GR, Quinby-Hunt MS (1997) Methane hydrate stability in pore water: a simple theoretical approach for geophysical applications. J Geophys Res Solid Earth 102:773–783
34. Bavoh CB, Partoon B, Lal B, Gonfa G, Khor SF, Sharif AM (2017) Inhibition effect of amino acids on carbon dioxide hydrate. Chem Eng Sci 171:331–339
35. Khan MS, Bavoh CB, Partoon B, Nashed O, Lal B, Mellon NB (2018) Impacts of ammonium based ionic liquids alkyl chain on thermodynamic hydrate inhibition for carbon dioxide rich binary gas. J Mol Liq 261:283–290
36. Mainusch S, Peters CJ, de Swaan Arons J, Javanmardi J, Moshfeghian M (1997) Experimental determination and modeling of methane hydrates in mixtures of acetone and water. J Chem Eng Data 42:948–950
37. Snyder LR (1974) Classification of the solvent properties of common liquids. J Chromatogr A 92:223–230
38. Sun C, Chen G, Guo T, Lin W, Chen J (2002) Kinetics of methane hydrate decomposition. J Chem Ind Eng-China 53:899–903
39. Vysniauskas A, Bishnoi PR (1985) Kinetics of ethane hydrate formation. Chem Eng Sci 40:299–303
40. Lekvam K, Ruoff P (1993) A reaction kinetic mechanism for methane hydrate formation in liquid water. J Am chem Soc 115:8565–8569
41. Boxall J, Davies S, Koh C, Sloan ED (2009) Predicting when and where hydrate plugs form in oil-dominated flowlines. SPE Projects Facil Constr 4:80–86
42. Zerpa LE, Sloan ED, Sum AK, Koh CA (2012) Overview of CSMHyK: a transient hydrate formation model. J Pet Sci Eng 98:122–129
43. Yang D, Le LA, Martinez RJ, Currier RP, Spencer DF (2011) Kinetics of CO_2 hydrate formation in a continuous flow reactor. Chem Eng J 172:144–157
44. Englezos P, Kalogerakis N, Dholabhai PD, Bishnoi PR (1987) Kinetics of gas hydrate formation from mixtures of methane and ethane. Chem Eng Sci 42:2659–2666
45. Englezos P, Kalogerakis N, Dholabhai PD, Bishnoi PR (1987) Kinetics of formation of methane and ethane gas hydrates. Chem Eng Sci 42:2647–2658
46. Skovborg P, Rasmussen P (1994) A mass transport limited model for the growth of methane and ethane gas hydrates. Chem Eng Sci 49:1131–1143
47. Herri JM, Pic JS, Gruy F, Cournil M (1999) Methane hydrate crystallization mechanism from in-situ particle sizing. AIChE J 45:590–602
48. Clarke MA, Bishnoi PR (2005) Determination of the intrinsic kinetics of CO_2 gas hydrate formation using in situ particle size analysis. Chem Eng Sci 60:695–709
49. Turner DJ, Miller KT, Sloan ED (2009) Methane hydrate formation and an inward growing shell model in water-in-oil dispersions. Chem Eng Sci 64:3996–4004
50. Uchida T, Ebinuma T, Kawabata JI, Narita H (1999) Microscopic observations of formation processes of clathrate-hydrate films at an interface between water and carbon dioxide. J Crystal Growth 204:348–356
51. Mori YH (2001) Estimating the thickness of hydrate films from their lateral growth rates: application of a simplified heat transfer model. J Crystal Growth 223(1–2):206–212
52. Peng BZ, Dandekar A, Sun CY, Luo H, Ma QL, Pang WX, Chen GJ (2007) Hydrate film growth on the surface of a gas bubble suspended in water. J Phys Chem B 111:12485–12493
53. Mochizuki T, Mori YH (2006) Clathrate-hydrate film growth along water/hydrate-former phase boundaries—numerical heat-transfer study. J Crystal Growth 290:642–652
54. Hashemi S, Macchi A, Servio P (2007) Gas hydrate growth model in a semibatch stirred tank reactor. Ind Eng Chem Res 46:5907–5912
55. Bergeron S, Servio P (2008) Reaction rate constant of propane hydrate formation. Fluid Phase Equilibria 265:30–36
56. Salamatin AN, Hondoh T, Uchida T, Lipenkov VY (1998) Post-nucleation conversion of an air bubble to clathrate air–hydrate crystal in ice. J Crystal Growth 193:197–218
57. Wang X, Schultz AJ, Halpern Y (2002) Kinetics of methane hydrate formation from polycrystalline deuterated ice. J Phys Chem A 106:7304–7309

58. Staykova DK, Kuhs WF, Salamatin AN, Hansen T (2003) Formation of porous gas hydrates from ice powders: diffraction experiments and multistage model. J Phys Chem B 107:10299–10311
59. Shindo Y, Lund PC, Fujioka Y, Komiyama H (1993) Kinetics of formation of CO_2 hydrate. Energy Conver Manag 34:1073–1079
60. Shindo Y et al (1993) Kinetics and mechanism of the formation of CO_2 hydrate. Int J Chem Kinet 25(9):777–782
61. Shindo Y, Sakaki K, Fujioka Y, Komiyama H (1996) Kinetics of the formation of CO_2 hydrate on the surface of liquid CO_2 droplet in water. Energy Convers Manag 37:485–489
62. Lund PC, Shindo Y, Fujioka Y, Komiyama H (1994) Study of the pseudo-steady-state kinetics of CO_2 hydrate formation and stability. Int J Chem Kinet 26:289–297
63. Dalmazzone D, Hamed N, Dalmazzone C (2009) DSC measurements and modelling of the kinetics of methane hydrate formation in water-in-oil emulsion. Chem Eng Sci 64(9):2020–2026
64. Teng H, Yamasaki A, Shindo Y (1996) Stability of the hydrate layer formed on the surface of a CO_2 droplet in high-pressure, low-temperature water. Chem Eng Sci 51:4979–4986
65. Freer EM, Selim MS, Sloan ED Jr (2001) Methane hydrate film growth kinetics. Fluid Phase Equilib 185:65–75
66. Mu L, Li S, Ma QL, Zhang K, Sun CY, Chen GJ, … Yang LY (2014) Experimental and modeling investigation of kinetics of methane gas hydrate formation in water-in-oil emulsion. Fluid Phase Equilib 362:28–34
67. Rempel AW, Buffett BA (1997) Formation and accumulation of gas hydrate in porous media. J Geophys Res Solid Earth 102:10151–10164
68. Yin Z, Chong ZR, Tan HK, Linga P (2016) Review of gas hydrate dissociation kinetic models for energy recovery. J Nat Gas Sci Eng 35:1362–1387
69. Liu X, Flemings PB (2007) Dynamic multiphase flow model of hydrate formation in marine sediments. J Geophys Res Solid Earth, 112
70. Uddin M, Coombe D, Law D, Gunter B (2008) Numerical studies of gas hydrate formation and decomposition in a geological reservoir. J Energy Resour Technol 130:032501
71. Zerpa LE, Rao I, Aman ZM, Danielson TJ, Koh CA, Sloan ED, Sum AK (2013) Multiphase flow modeling of gas hydrates with a simple hydrodynamic slug flow model. Chem Eng Sci 99:298–304
72. Ribeiro CP Jr, Lage PL (2008) Modelling of hydrate formation kinetics: state-of-the-art and future directions. Chem Eng Sci 63:2007–2034
73. Yin Z, Khurana M, Tan HK, Linga P (2018) A review of gas hydrate growth kinetic models. Chem Eng J 342:9–29